N 69 13483

CR-72457
PWA-3516

QUIET ENGINE DEFINITION PROGRAM
FINAL REPORT

CASE FILE COPY

BY
JOHN H. LEWIS, III, PROGRAM MANAGER

VOLUME IV
TASK III

PREPARED FOR
NASA-LEWIS RESEARCH CENTER CLEVELAND, OHIO 44135
UNDER CONTRACT NAS3-10497

Pratt & Whitney Aircraft
DIVISION OF UNITED AIRCRAFT CORPORATION

NOTICE

This report was prepared as an account of Government sponsored work. Neither the United States, nor the National Aeronautics and Space Administration (NASA), nor any person acting on behalf of NASA:

A.) Makes any warranty or representation, expressed or implied, with respect to the accuracy, completeness, or usefulness of the information contained in this report, or that the use of any information, apparatus, method, or process disclosed in this report may not infringe privately owned rights; or

B.) Assumes any liabilities with respect to the use of or for damages resulting from the use of any information, apparatus, method or process disclosed in this report.

As used above, "person acting on behalf of NASA" includes any employee or contractor of NASA, or employee of such contractor, to the extent that such employee or contractor of NASA, or employee of such contractor prepares, disseminates, or provides access to any information pursuant to the employment or contract with NASA, or his employment with such contractor.

FINAL REPORT
ON THE
QUIET ENGINE DEFINITION PROGRAM
PWA-3516

by

John H. Lewis, III, Program Manager

VOLUME IV
TASK III

prepared for

NATIONAL AERONAUTICS AND SPACE ADMINISTRATION

October 4, 1968

CONTRACT NAS3-10497

Technical Management

NASA Lewis Research Center
Cleveland, Ohio
Propulsion Systems Acoustics Branch
J. J. Kramer
J. F. McBride

Pratt & Whitney Aircraft
DIVISION OF UNITED AIRCRAFT CORPORATION

EAST HARTFORD, CONNECTICUT

COPY NO.

PREFACE

The final Report for the Quiet Engine Definition Program has been prepared in five volumes. This volume describes the work carried out under Task III, which was a design study on the QE Quiet Engine cycle. A summary of the over-all program, discussions of Tasks I and II, and the performance of the QE-3 engine are given in the other four volumes, which are listed below:

Volume I	Summary
Volume II	Task I
Volume III	Task II
Volume V	QE-3 Performance

TABLE OF CONTENTS

LIST OF ILLUSTRATIONS

LIST OF ILLUSTRATIONS (Cont'd)

LIST OF ILLUSTRATIONS (Cont'd)

LIST OF ILLUSTRATIONS (Cont'd)

LIST OF ILLUSTRATIONS (Cont'd)

LIST OF ILLUSTRATIONS (Cont'd)

LIST OF ILLUSTRATIONS (Cont'd)

LIST OF TABLES

SECTION I
INTRODUCTION AND SUMMARY

It is the objective of the Quiet Engine Definition Program to define the characteristics of an engine whose noise is substantially below that of current large, subsonic transport aircraft powerplants. To accomplish this objective, definition of the Quiet Engine has evolved through a screening process in a series of three study tasks. At the outset of the program, study Task I covered a broad parametric range of cycle design variables, described in Volume II of this report. Then, from the Task I results a series of four potentially low noise candidate designs were selected for further study and evaluation in Task II, which is described in Volume III. While the attention in Task I was centered on the effects of cycle variables, Task II emphasized practicality of mechanical design while providing a more exact determination of engine noise for the selected candidate engines. Based on the Task II results, a final configuration was selected for refined design evaluation and definition in Task III, described in this volume.

As discussed more fully in Volume III, the candidate engines selected for Task II evaluation were characterized primarily by differences in design bypass ratio and overall mechanical arrangement. Candidate engines having 3.0, 5.0, and 8.0 design bypass ratios represented variations in spool arrangements, with special emphasis on two-stage rather than single-stage fans for the two lower bypass ratio engines. The overall results and conclusion from the Task II study which led to the selection of a final engine for Task III can be summarized as follows:

Result

Two-stage lightly loaded fans result in increased mechanical complexity and engine length and weight for no obvious noise advantage.

Conclusion

Design for a relatively highly loaded, single-stage fan

Result

Fan tip speed rather than bypass ratio has the more direct influence on overall engine noise

Conclusion

Design for low tip speed with a cycle selected to produce low jet velocity and low jet exhaust noise.

Result

Proper choice of the design cycle variables can result in a jet noise level well below the fan noise level to allow margin for nacelle acoustical treatment to suppress fan noise.

Conclusion

Select and modify the cycle design variables to ensure relatively low jet noise levels

Although the foregoing itemization tends to oversimplify a rather complex selection process, it does highlight some of the more salient factors leading to the final selection of the Quiet Engine characteristics and their initial specification by the NASA Project Manager. The selected characteristics specified by the NASA Project Manager which initiated the Task III effort were as follows:

• Nominal cycle bypass ratio	5.5
• Cruise design point turbine inlet temperature at 35,000 feet (10,069 meters), Mach 0.82	1750°F (1228°K)
• Standard day sea level take-off turbine inlet temperature	1950°F (1339°K)
• Primary jet exhaust noise level goal on takeoff at the 3-mile (4.73 km) point	90 PNdb
• Bypass portion fan pressure ratio (approximately)	1.5
• Configuration	two-rotor with single-stage fan on separate rotor
• Maximum design pressure ratio on one compressor rotor	12.5:1
• Overall cycle pressure ratio	to be determined by Task III studies within above constraints
• Maximum cruise rating thrust	4,900 pounds (21,800 N)

The overall Task III work effort to complete an engine design around these specified characteristics involved six main stages:

1. A "fine-tuning" study to define more precisely values for the design cycle variables which achieve an optimum arrangement within the constraints of maximum jet noise and maximum compressor-spool pressure ratio.

2. A fan integration study to determine fan design characteristics best suited to low noise and compatibility with the overall engine design.

3. A preliminary aerodynamic design analysis for each component.

4. Conceptual mechanical design leading to a preliminary engine structural arrangement.

5. Detailed aerodynamic design of the fan.

6. Detailed aeroelastic analysis and mechanical design of the fan.

These six main stages of effort represent the major work statement provisions and were completed in the listed sequence during the course of Task III. In addition, the work statement called for:

7. Determination of fan and engine noise minimization features.

8. Prediction of engine noise levels.

9. Tabulation of engine performance data.

10. Preparation of a design specification.

Broadly, undertaking these final items depended on the results of the overall mechanical and aerodynamic design effort, and they were individually completed towards the end of the Task.

The ten enumerated items encompass the entire Task III work statement provisions and, conveniently, serve as the basis for the arrangement of this volume into separate sections. Section II discusses the initial fine-tuning study results, Section III describes the fan integration study, Section IV describes the preliminary mechanical and components aerodynamic design analysis, Section V presents engine noise, Section VI contains a description of the more detailed aerodynamic, aeroelastic and mechanical design of the fan, while Section VII and the Appendix present an alternate design study and the engine specification respectively. The engine performance data tabulation is included separately in this report as Volume V.

The four candidate engines of Task II were identified by the designations QA, QB, QC, and QD. The final engine selected for the Task III refined design effort has been designated QE. Compared with the engines powering current large, subsonic transport aircraft, the QE-3 engine (the -3 signifies the third variation evolved during the course of the task) potentially is not only substantially quieter, but also has appreciably lower fuel consumption, and its weight and dimensions are expected to be within the requirements for practical application to future aircraft. Table I summarizes the performance and physical characteristics of the QE-3 design, which is illustrated in Figure 1.

TABLE I
SUMMARY OF QE-3 ENGINE CHARACTERISTICS

Performance

Design Bypass Ratio	-	5.4:1
Design Overall Pressure Ratio	-	18.9:1
Cruise* Thrust	-	4,900 pounds (21,800N)
Cruise* Thrust-Specific Fuel Consumption (Minimum)	-	0.62 hour^{-1}
Take-off Thrust	-	22,000 pounds (98,000N)

* 35,000 feet (10,069 meters) at Mach 0.82

Configuration Arrangement

Spool Arrangement		Two-spool, fan plus high-pressure compressor
No. Stages:		
Fan	-	1
High-Pressure Compressure	-	12
High-Pressure Turbine	-	2
Low-Pressure (fan driving) Turbine	-	5
Combustor	-	Annular

Physical Characteristics

Weight	-	4950 pounds (4, 517 Kg)
Max Diameter	-	70.8 inches (180 cm)
Overall Length	-	116 inches (295 cm)

Predicted Peak Flyover Noise (4 Engines)

Take-off (1, 000 feet* altitude):		
Total Noise	-	104.0 PNdb
Jet Exhaust Noise	-	93.0 PNdb
Landing Approach (325 feet* altitude, 4800 pounds** thrust):		
Total Noise	-	104.5 PNdb
Jet Exhaust Noise	-	84.0 PNdb

* 1000 feet = 305 meters
325 feet = 99 meters

** 4800 pounds = 21, 400N

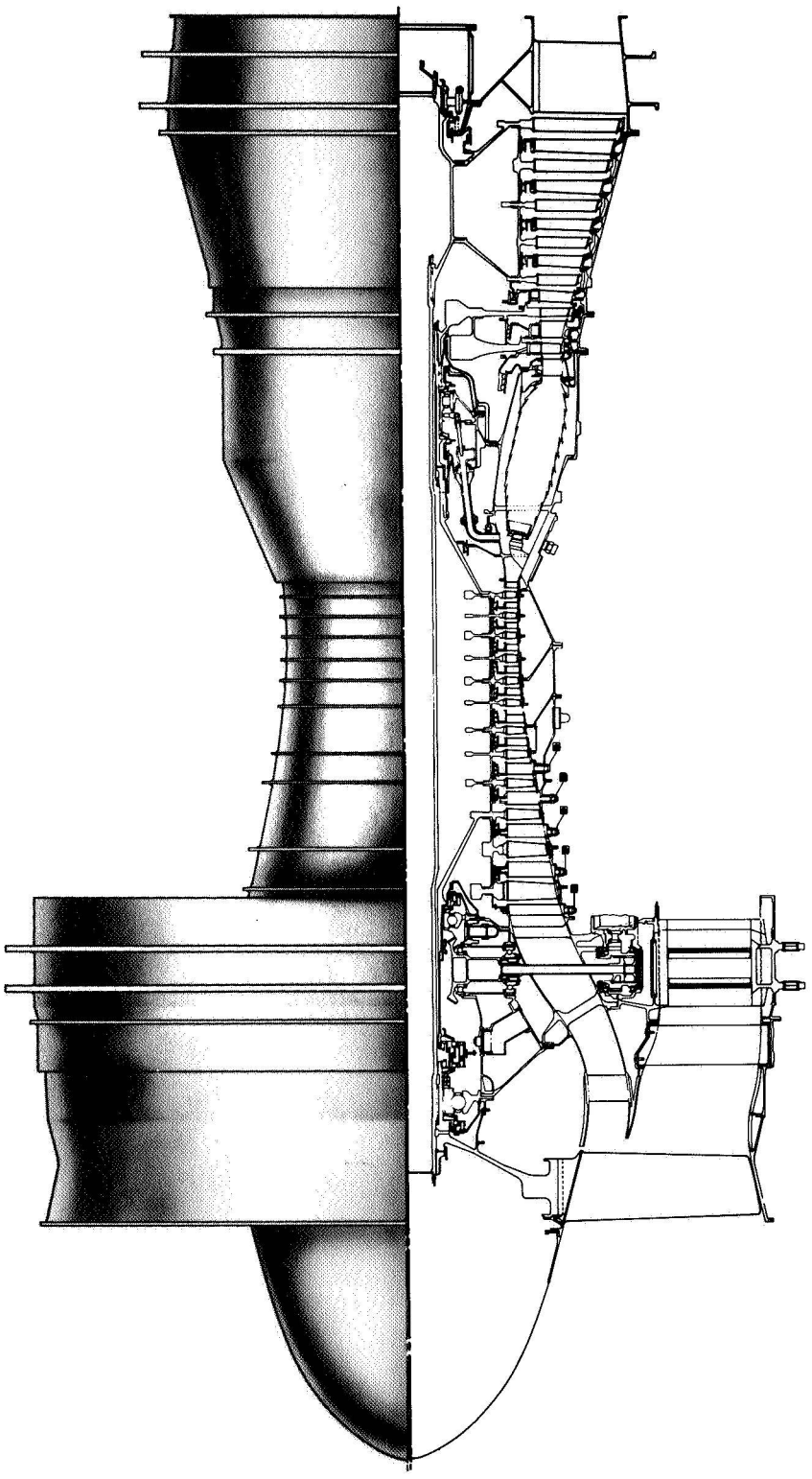

Figure 1 The QE-3 Engine

SECTION II
FINE-TUNING STUDY

Recognizing the iterative process essential to refining and optimizing an engine design, the NASA Project Manager's specification of the quiet engine nominal cycle characteristics to initiate Task III was accompanied by the direction in the very first work statement provision for the Contractor to evaluate variations around the specified cycle in order to achieve an optimum balance of performance, noise, and a well integrated design for the components. This evaluation, termed the "fine-tuning" study for short, chiefly involved a parametric analysis of noise and performance related to the primary cycle variables of bypass ratio and turbine inlet temperature, and a preliminary integration of the components into an overall design. Preliminary integration of the components relied on an initial establishment of the key design variables, which were subsequently verified or modified by actual analytical design of the components. Establishment of the key design variables permitted the selection of the number of stages for the compressor and turbines and the determination of an aerodynamic flow path for the entire engine which served as the basis for the mechanical design effort.

While the initial fine-tuning study focused attention on the primary variables of bypass ratio and turbine inlet temperature, there remained for consideration the third primary cycle variable, fan pressure ratio. Since more precise selection of fan pressure ratio depended heavily on rather detailed aerodynamic and mechanical design considerations, this choice was deferred until completion of the next stage of the Task III effort, the "fan integration" study, discussed in Section III of this volume. For the purposes of the initial fine-tuning evaluation, fan pressure ratio was fixed at 1.5, a level apparently consistent with aerodynamic capability both of a single fan stage and of a five-stage fan driving turbine. Subsequently, the fan integration study determined that a more ambitious fan pressure ratio level of 1.6 could be justified, and the results of the initial fine-tuning study were reviewed and utilized in a new evaluation and selection of nominal cycle design bypass ratio and turbine temperature levels consistent with the higher fan pressure ratio. Thus, in effect, the refinement and optimization of the engine design truly became an iterative process as anticipated.

To identify the various design cycle modifications to the basic Task III engine as it evolved through major iterative adjustments, the engine numerical designations were changed. The first cycle selected at the outset of the task was designated QE-1. When the fine tuning was completed by the selection of new bypass ratio and turbine inlet temperature levels, the designation was changed to QE-2. The background and basis for the QE-2 selection are de-

scribed in the following paragraphs.

Figures 2, 3, and 4 summarize the results of parametrically varying design turbine inlet temperature and bypass ratio about the originally selected nominal condition. Figures 2 and 3 reveal the significant result that holding a constant take-off jet noise level is tantamount to fixing the fan's diameter and the thrust per unit airflow at cruise, also indicative of engine size. The effect of nearly constant engine size with fixed jet noise is the cumulative effect of cycle performance and off-design engine matching factors, all taken into account in the parametric fine-tuning evaluation. Figure 4 shows that cruise thrust-specific fuel consumption and jet noise can be improved by increasing the bypass ratio or by decreasing the design turbine inlet temperature. However, by increasing the bypass ratio at constant design turbine inlet temperature, a greater reduction in fuel consumption can be obtained for a given noise reduction.

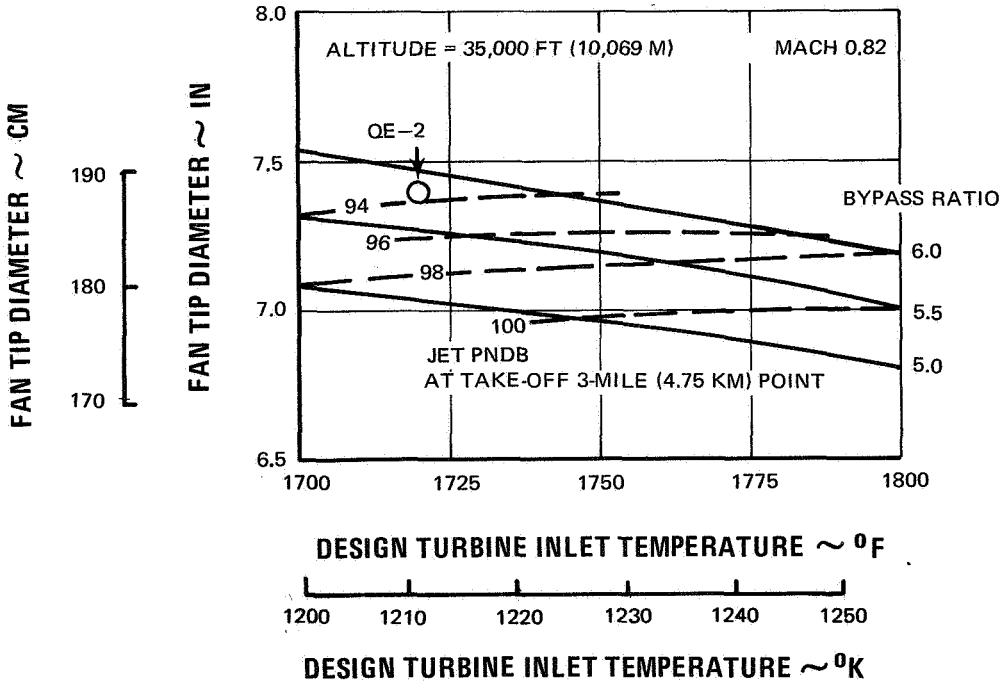

Figure 2 Fan Tip Diameter vs Turbine Inlet Temperature

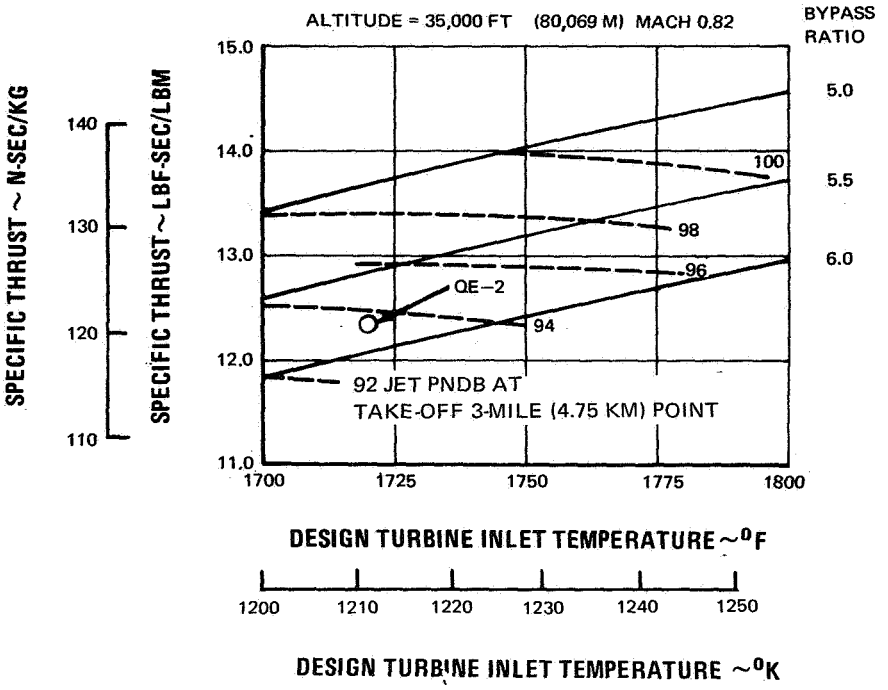

Figure 3 Specific Thrust vs Turbine Inlet Temperature

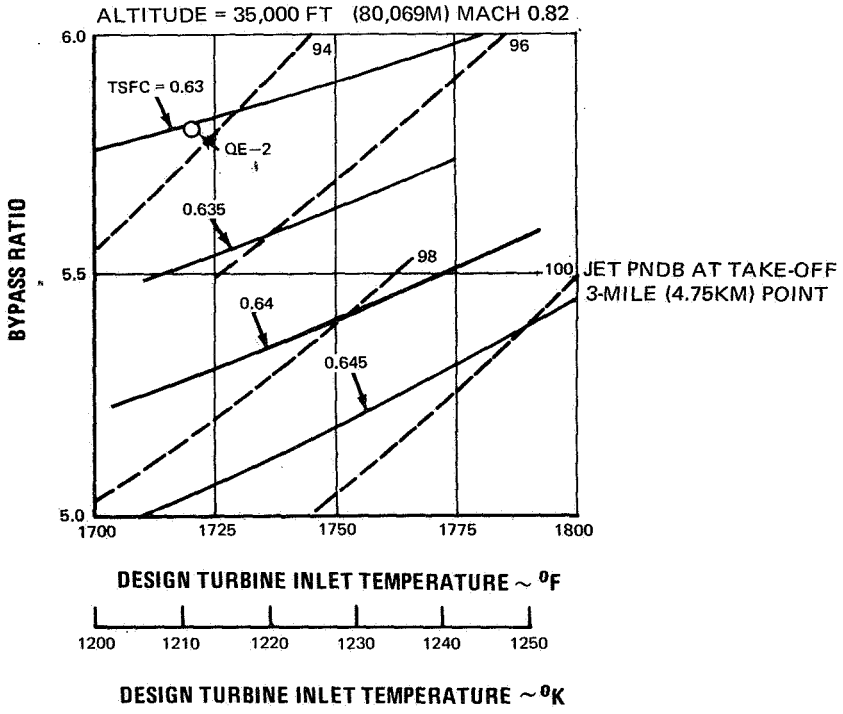

Figure 4 Bypass Ratio vs Turbine Inlet Temperature

To summarize and explain the study results:

- For constant bypass ratio and constant take-off turbine inlet temperature, increasing the design turbine inlet temperature decreases altitude at the three-mile (4.83-km) point, decreases take-off speed, and increases jet velocity. These changes result in increased jet noise and increased total noise. For jet noise, the increase is about 5 PNdb for each 100F° (55.6K°), but for total noise, the increase is only about 2 PNdb for each 100F° (55.6K°).

- For constant bypass ratio and constant design turbine inlet temperature, increasing the take-off turbine inlet temperature increases jet velocity, take-off tip speed, and altitude. The change in jet velocity is approximately balanced by the change in altitude, so there is little change in jet noise, but the altitude effect overpowers the increase in tip speed, so there is a reduction in total noise amounting to 2 PNdb for every 100F° (55.6K°).

As shown on all three figures, while the jet noise goal of 90 PNdb represented an extreme in engine physical size and performance compromise, there is sufficient sensitivity that modifying the goal to a level about 10 PNdb below the predicted fan noise of the engine was both reasonable and satisfactory. This recommendation was agreed to by the NASA Project Manager. The selected QE-2 cycle design point indicated on Figures 2 through 4 is at a bypass of 5.8, a design turbine inlet temperature of 1720°F (1211°K), and an overall pressure ratio of 18:1. Compared to the original QE-1, jet noise is 3.5 PNdb lower, thrust-specific fuel consumption is improved about 1 percent, and the diameter is only 2.5 percent greater.

SECTION III
FAN INTEGRATION STUDY

The design selection of the fan was considered to be the pivotal decision in establishing the Quiet Engine design configuration, because the fan is the primary source of engine noise. Accordingly, before undertaking the more refined aerodynamic and mechanical design of the engine, and following the fine-tuning study preliminary cycle selection, a comprehensive evaluation of key fan design parameters was completed. This evaluation was called the fan integration study to signify that the main intent of the evaluation was to select a fan design well integrated with the overall design of the engine. To achieve this integration, consideration was made of not only the effects of fan aerodynamics on engine cycle performance, but also on its influence on the weight and mechanical integrity of the engine front end as related to the overall engine design. With a fixed flow-path elevation for the engine, starting with the front of the compressor, variations in the aerodynamic flow path of the fan can influence the location and size of the transition sections connecting the fan to the rest of the engine, the fan case, and the shafting and bearing support sections. To properly account for the fan influence in these areas, the fan integration study involved separate evaluation of transition duct design, weights and mechanical design, and overall engine performance in addition to the basic fan aerodynamic analysis. Results of the studies were orally presented to the NASA Project Manager in the early part of Task III, and resulted in the selection of the QE-3 engine for further evaluation during the remainder of Task III.

In order to provide a starting point for the fan integration study, an over-all engine layout was prepared as soon as preliminary information was available for the selected QE-2 engine design. Preparation of the layout was based on a bypass ratio of 5.8, a hub-to-tip ratio of 0.45, and an aspect ratio of 3.58, to be consistent with the 1.5 fan pressure ratio. The layout is shown in Figure 5. A rough stiff-bearing analysis showed that it would be feasible to mount the engine on four bearings, so this feature was incorporated in the layout. The first layout was important because it permitted a more detailed study of the fan and main engine ducting to provide a meaningful approximation of the weights involved. Four additional layouts showing the effects of varying hub-to-tip ratio and aspect ratio on the fan configuration were also prepared. They are shown in Figures 6 through 9.

The fan integration study was essentially composed of four separate parts: fan aerodynamics, transition-duct design, engine weight, and engine performance.

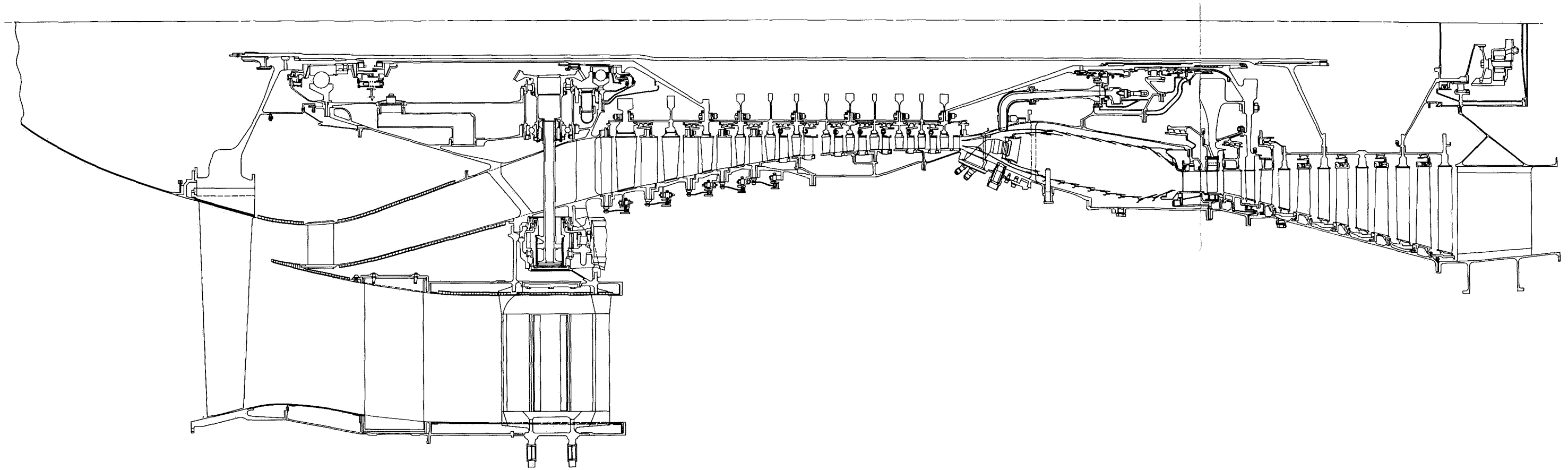

Figure 5 QE-2 Layout

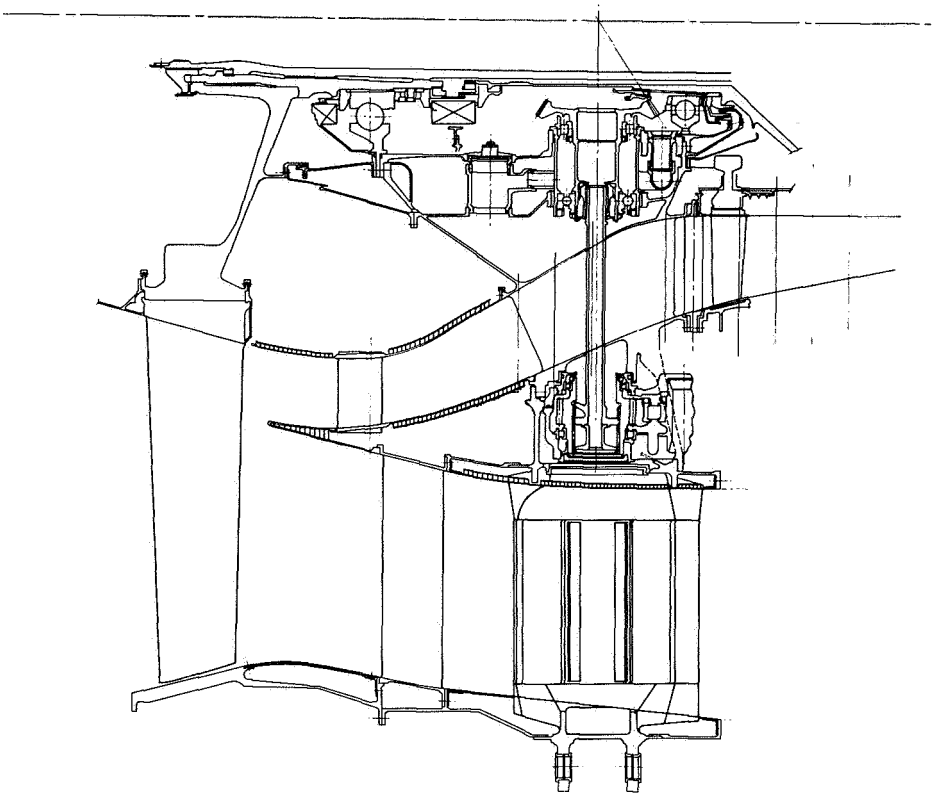

Figure 6 Study Fan with a Hub-to-Tip Ratio of 0.45 and an Aspect Ratio of 3.15

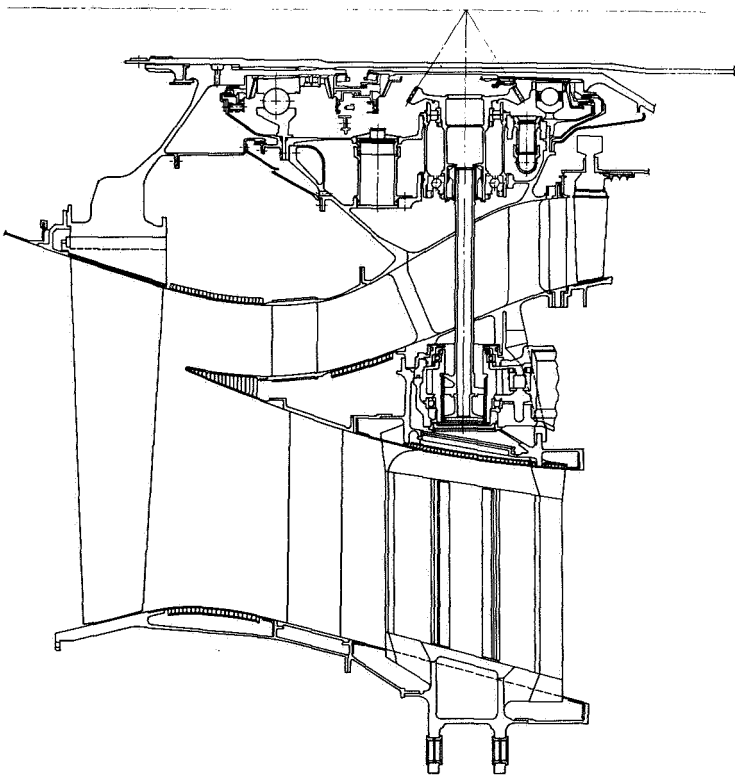

Figure 7 Study Fan with a Hub-to-Tip Ratio of 0.40

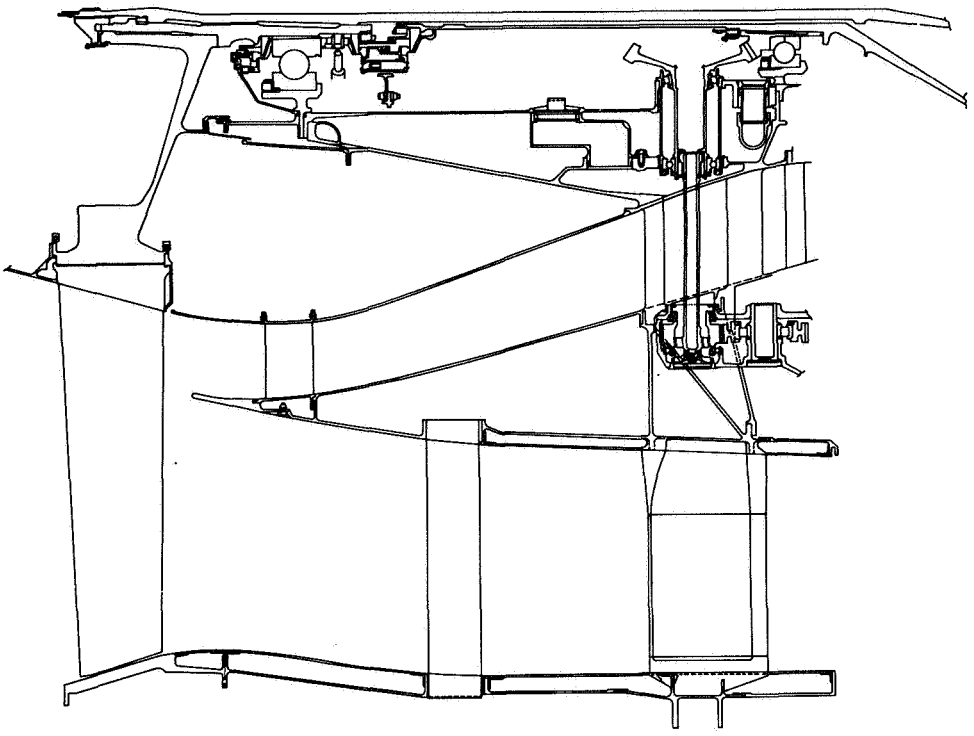

Figure 8 Study Fan with a Hub-to-Tip Ratio of 0.45 and an Aspect Ratio of 3.84

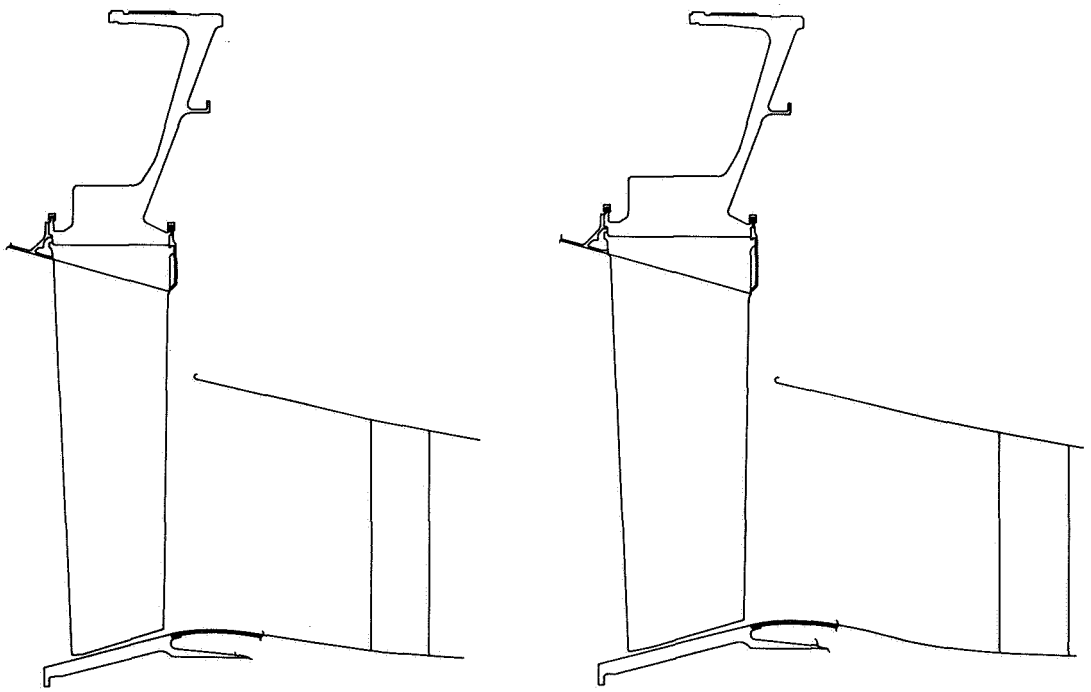

Figure 9 Fan Blades with Aspect Ratios of 2.68 (Left) and 3.3 (Right)

A. FAN AERODYNAMICS

The fan aerodynamics analysis consisted primarily of an evaluation of fan aspect ratio and hub-to-tip ratio to determine the effect of their variation on the performance of the fan. It was found that the duct pressure ratio could be increased if the fan aspect ratio (based on the tip chord) were decreased independently of hub-to-tip ratio, and that the engine pressure ratio could be increased if the hub-to-tip ratio were increased independently of aspect ratio.

An off-design analysis with varying aspect-ratio was performed at the take-off point, the condition where the fan is most susceptible to surge from duct back pressure. It was found that the limitation of fan loading at the tip gave the same surge margin as that of the JT9D at this condition, and that some reduction in loading on the duct exit guide vanes was required at low fan aspect ratios.

In varying hub-to-tip ratio, off-design analysis was performed at the flight-idle point, the condition where the fan is most susceptible to surge from engine back pressure. It was found that the limiting loading was at the root of the first stator, and that about 22 percent bleed would be required to make this loading acceptable.

1. Analytical Method

a. Off-Design Requirements

To determine the off-design requirements, the contractor first set up the design point on a streamline program, which included the effects of the flow splitter, to determine the blade row exit air angles and losses. This design point was used with the appropriate speed, flow, and bypass ratio for the off-design running. No iteration was introduced to correct losses or deviations caused by changes in Mach number and incidence from their design-point values. While these changes have some effect on the location of speed lines and efficiency islands on the compressor map, they have little effect on surge margin. The NASA D (Diffusion) factor was used as a measure of loading throughout the study.

For the fan duct section, the operating line for sea-level static conditions is the closest to the surge line. Therefore, if there is sufficient duct surge margin at the sea-level take-off condition, there will be sufficient margin at lower speeds. For the engine gas generator portion of the fan section, the altitude operating line is closest to the surge line, and the flight-idle condition is critical. Both this condition and the design point were examined for loading.

b. Determination of Loading Levels

Loading levels were determined by independently varying the duct and engine back pressures from the chosen off-design condition. This was done by reducing either the duct or the engine flow. Duct back pressure has only a slight effect on the engine portion of the fan and practically no effect on the first stator in the gas generator, but it has a pronounced effect on the duct portion of the fan and the duct exit guide vane (exit stator). The major influence of the engine back pressure is on the loading of the first stator. The effect of a reduction in engine flow on the loading of the fan is diluted because of the high bypass ratio of the design, but there are noticable effects on both the fan and the duct exit guide vane (stator).

c. Loading Limits

Loading limits were determined for the fan tip, the fan peak loading, the first stator, and the duct exit guide vane. It has been empirically determined that if the loading in the fan rotor tip (90 percent span) exceeds a critical value, the fan will surge. The tip loading limit is, to a lesser extent, affected by changes include these parameters in the analysis.

The fan peak loading was taken to be the largest value of D factor which occurred anywhere along the fan blade. Values of D factor as high as 0.665 have been attained in testing the JT9D fan, but a slightly more conservative value of 0.65 was used for this study.

High loadings on the first stator and the duct exit guide vane do not necessarily cause the fan to surge, but they do indicate that the performance of the fan would suffer from high losses. Experience with the JT9D has indicated that at 10-percent span, a value of 0.65 for the D factor is acceptable. Ten-percent span was used rather than the root to avoid the effects of wall boundary layers, and is hereafter referred to as the root. Since both the first stator and the duct exit guide vane have their maximum loading at the root, a D-factor limit of 0.65 was used for both rows.

d. Flowpath Analysis

Tip aspect ratios of 2.2, 2.7, and 3.15 were studied at a hub-to-tip ratio of 0.45 for the aspect-ratio study. Hub-to-tip ratios of 0.4, 0.45, and 0.5 were studied at a tip aspect ratio of 3.15 for the hub-to-tip ratio study. For each combination of aspect ratio and hub-to-tip ratio, design-point duct and engine pressure ratios were selected in such a way that loading limits would not be exceeded.

Throughout the aspect-ratio study, the flowpath from the splitter to the high-pressure compressor and the fan-root flowpath were kept constant. All fan designs had the same tip slope, inlet specific flow, and tip speed. This combination of parameters resulted in an increase in rotor convergence and a slight decrease in hub-to-tip ratio with a decrease in aspect ratio.

In the study of hub-to-tip ratios, the fan tip slope, tip speed, convergence, and aspect ratio were kept constant. This combination of parameters resulted in an increasing root slope with decreasing hub-to-tip ratio. The radius of curvature of the inner wall from the fan trailing edge to the intermediate case ducting was held constant throughout the study, and the flow splitter was positioned to maintain the same first stator exit Mach number.

For both the studies of hub-to-tip ratio and aspect ratio, the gap-to-chord ratios were set at about 0.42 at the root of all blade rows. The first stator and the duct exit guide vane were assumed to have a constant chord. The fan tip gap-to-chord ratio was set at about 0.735, and a linear chord variation with span was used. The ratio of the fan's tip chord to root chord is shown as a function of hub-to-tip ratio in Figure 10.

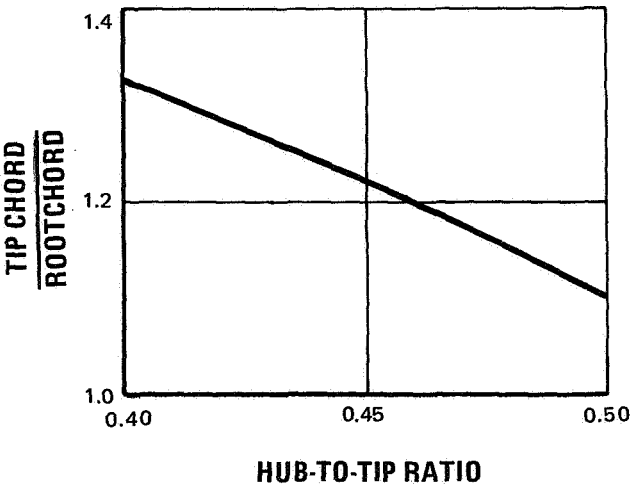

Figure 10 Effect of Hub-to-Tip Ratio on Ratio of Tip Chord to Root Chord

2. Results

a. Study of Hub-to-Tip Ratio

The primary effect of hub-to-tip ratio is on the root pressure ratio capability, with the principal limitation being the root loading of the first stator. Figure 11 shows the relationship between engine pressure ratio and hub-to-tip ratio.

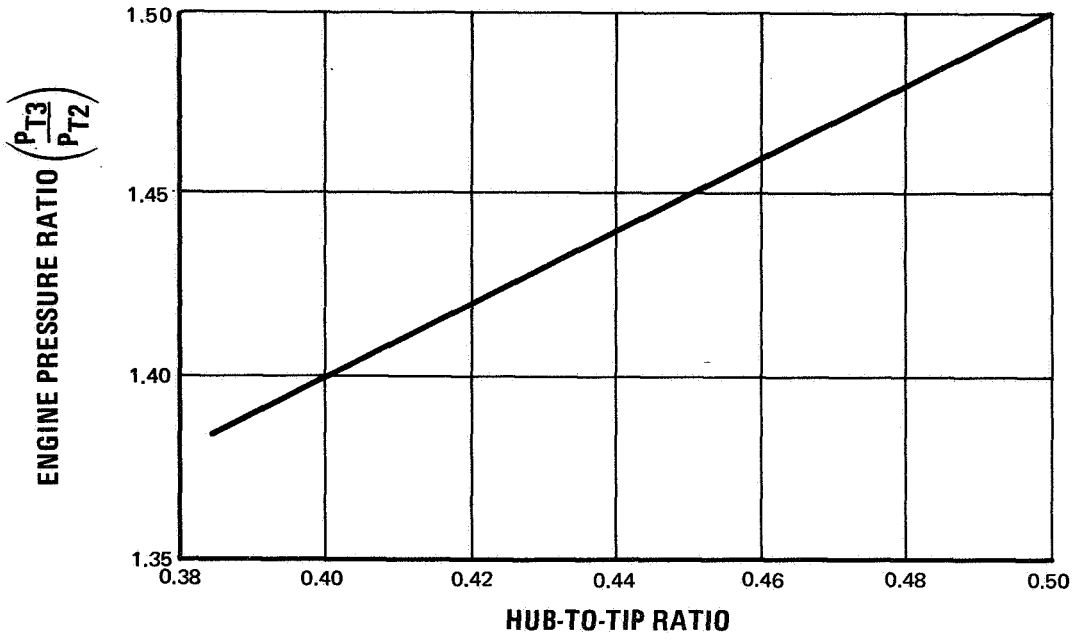

Figure 11 Effect of Hub-to-Tip Ratio on Engine Pressure Ratio for Equivalent Loading

b. Study of Aspect Ratio

The primary effect of aspect ratio is on the duct pressure ratio capability, with the principal limitation being the fan tip loading. Figure 12 shows the relationship between duct pressure ratio and fan tip aspect ratio.

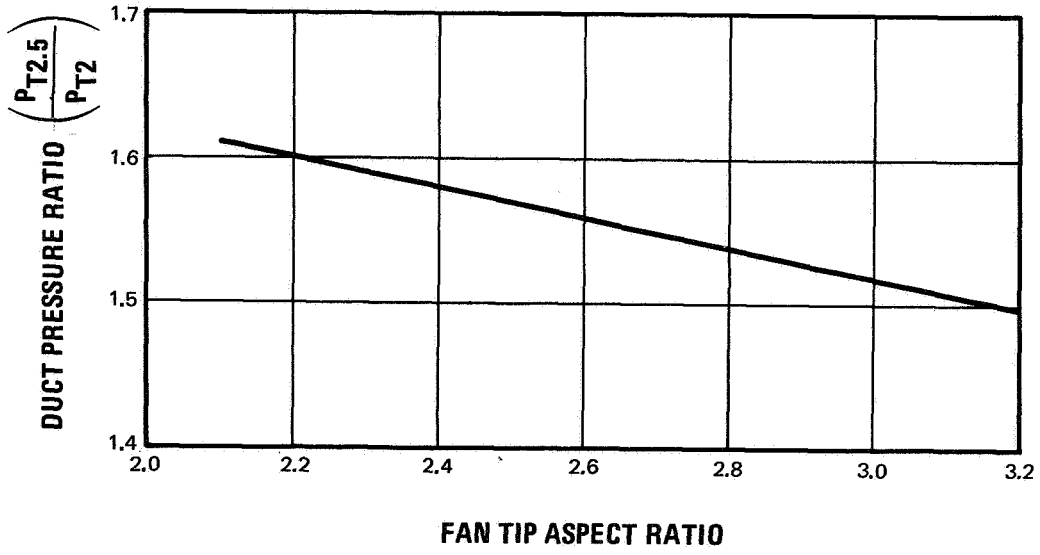

Figure 12 Duct Pressure Ratio as a Function of Fan Tip Aspect Ratio

c. Off-Design Requirements

The figures presented in this section give D factor as a function of a parameter called "percent surge margin". Percent surge margin is defined as:

$$\text{Percent Surge Margin} = \left[\frac{(W\sqrt{\theta/\delta})_{\text{op line}}}{W\sqrt{\theta/\delta}_{\text{surge}}} \times \frac{P_{r\ \text{surge}}}{P_{r\ \text{op line}}} - 1 \right] \times 100$$

Percent surge margin is essentially the ratio of exit corrected flow on the operating line to exit corrected flow at the point where surge occurs on the speed line in question minus 1.0. If the point in question is on the surge line, it will have 0 surge margin. To find the predicted surge margin for a given operating point, it is necessary to examine the curves for all of the critical locations to determine where the loading line first crosses its limiting value.

Since all the fans in the hub-to-tip ratio study had essentially the same duct configuration, only the effects of engine back pressure were examined. Plots of loading as a function of percent surge margin were prepared for the fan peak loading, fan tip, first stator root, and the duct exit guide vane at both the design point and the flight-idle condition. The limiting factor was found to be the loading on the first stator root at flight idle, where the surge line is actually below the operating line. As shown in Figure 13, there is negative surge margin at the intersection of the calculated first stator loading line and

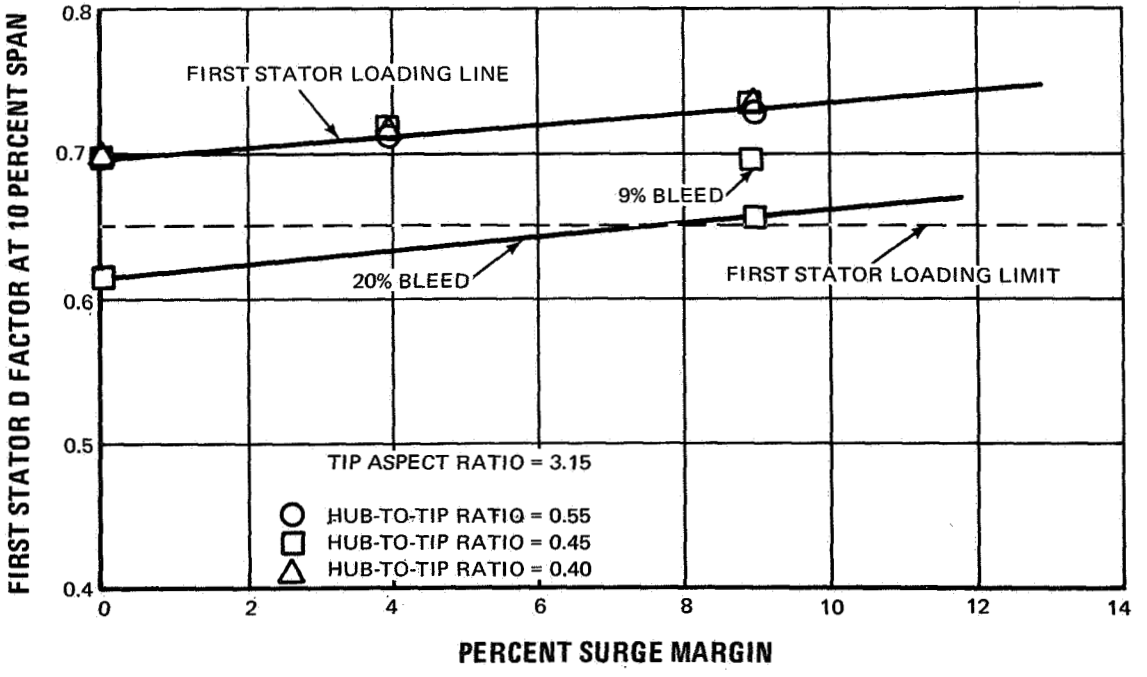

Figure 13 QE-2 Flight Idle Speed Line for a Tip Aspect Ratio of 3.15

the first stator loading limit line. It is concluded that some sort of surge protection device will be required for the first stator. This will probably take the form of a bleed, but some other device such as variable geometry could be used. Figure 13 also shows that about 22 percent bleed would be sufficient to get the required surge margin of 10 percent.

Since all of the fans in the aspect-ratio study had essentially the same engine section configuration, only the effects of duct back pressure were examined. Plots of loading as a function of percent surge margin were prepared for the fan peak loading, fan tip, first stator root, and duct exit guide vane at both the design point and the take-off speed line. The limiting factor was found to be the loading on the fan tip at take-off, where about 6.5 percent surge margin is available, as shown in Figure 14. This margin was considered to be satisfactory, since the JT9D is presently running with approximately that surge margin.

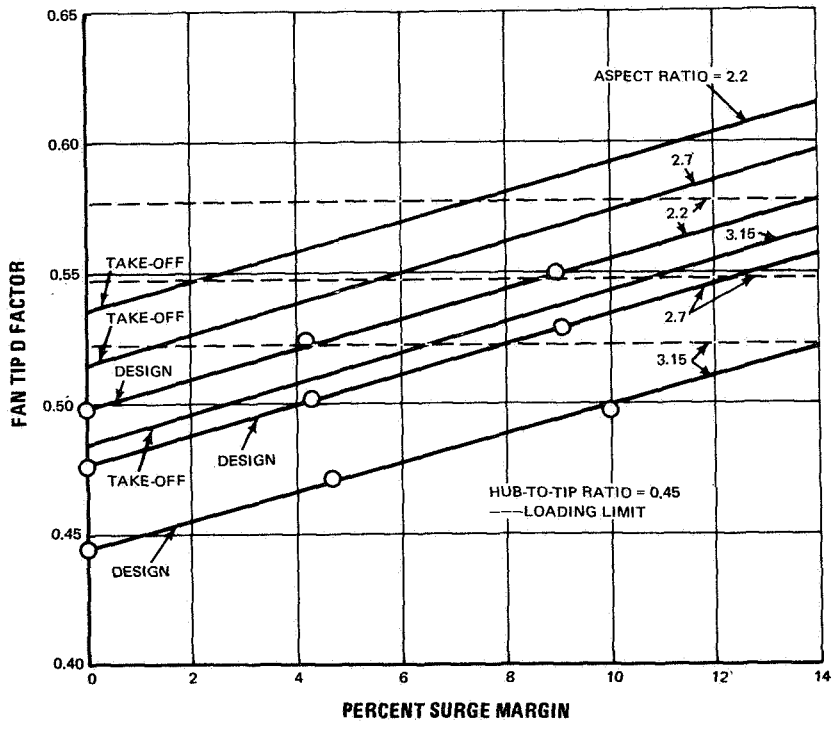

Figure 14 Fan Tip Loading at a Hub-to-Tip Ratio of 0.45

With a fan aspect ratio of 2.2, however, there is a loading problem at the root of the duct exit guide vane. This problem can be solved, however, by increasing the exit Mach number. All of the flowpaths for the study of aspect ratios were designed for a duct exit guide vane exit Mach number of 0.5, but increasing the exit Mach number to 0.55 will keep the loading on the vane within acceptable limits.

B. TRANSITION DUCTS

As a part of the fan integration study, the contractor prepared preliminary flowpaths for the compressor transition duct to determine a least length. This preliminary design work included configurations designed for fans with an aspect ratio of 3.75, and hub-to-tip ratios of 0.4, 0.45, and 0.5. A general arbitrary technique was used in sketching the first three configurations, which are shown in Figures 15, 16 and 17. The design selected for analysis was the one shown in Figure 17 because of the three, it had the largest offset. The analysis made use of the compressor streamline computer program to describe the flow characteristics, and used the modified Reshotko-Tucker boundary-layer computer program to determine the likelihood of flow separation.

The first analysis was performed on the configuration shown in Figure 17, using Inner Contour Number 1 and Outer Contour Number 1. The analysis showed that there would be separated flow at Point A, but it was felt that this duct length would perform satisfactorily with minor modifications to the wall contours. At this point, alternate inner and outer contours were tried. When combined with the original contours, the new ones yielded a total of four configurations. The outer wall showed no evidence of separated flow in any of the configurations. The tabulation below shows the analytical results for the inner wall.

Case	Inner Contour	Outer Contour	Possibility of Separated Flow
A	1	1	yes
B	1	2	marginal
C	2	1	yes
D	2	2	no

Figure 18 shows the distribution of flow speeds along the inner wall for the four configurations analyzed. Since the flatness of the speed curve is related to the probability of separated flow, these curves corroborate the results of the original computer analysis.

Although the configurations shown in Figures 15 and 16 were not analyzed, it is felt that their duct lengths are reasonable and would perform satisfactorily with minor changes to the wall contours.

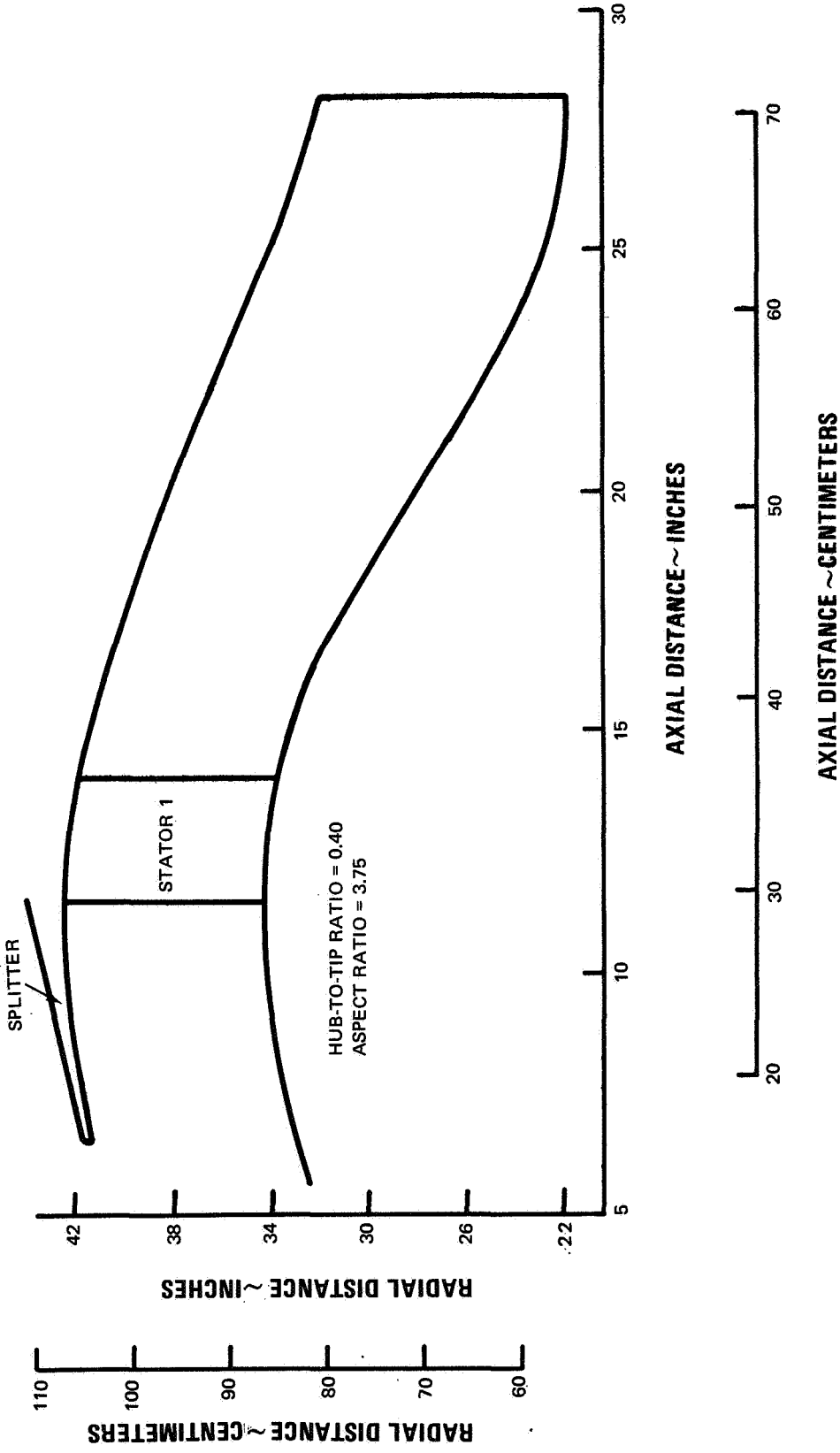

Figure 15 QE-2 Transition Duct Designed for a Fan Hub-to-Tip Ratio of 0.40 and a Fan Aspect Ratio of 3.75

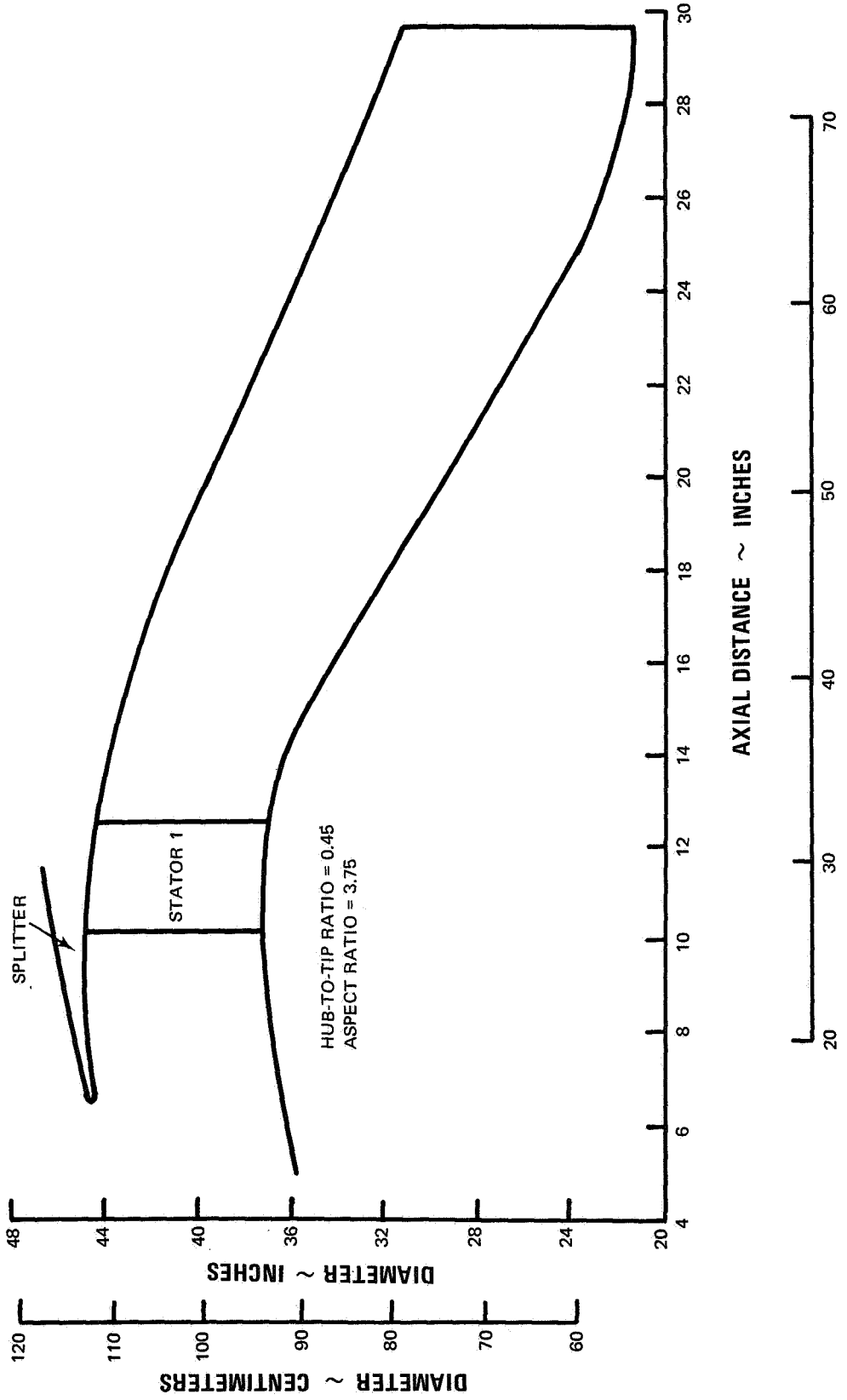

Figure 16 QE-2 Transition Duct Designed for a Fan Hub-to-Tip Ratio of 0.45 and a Fan Aspect Ratio of 3.75

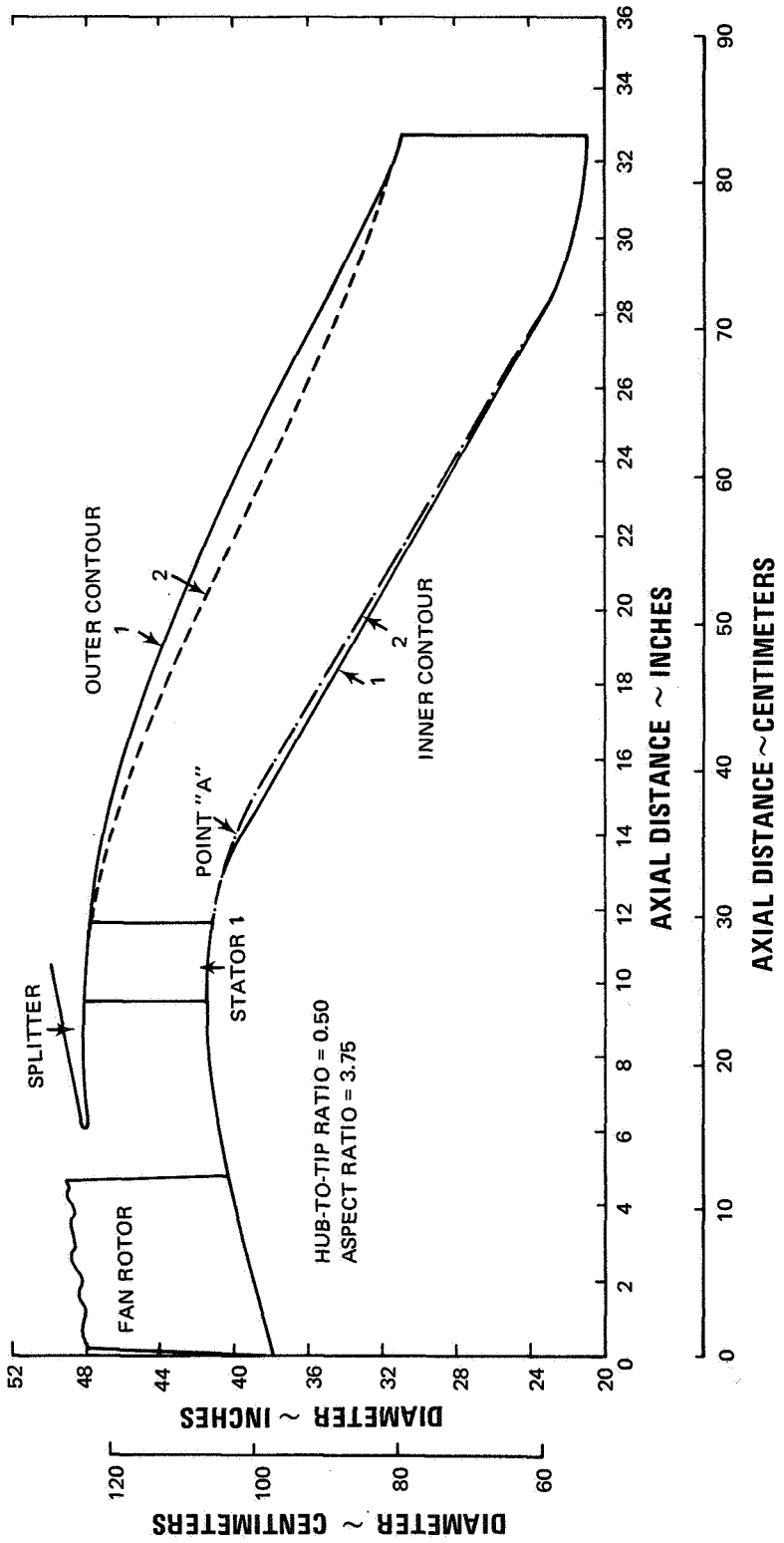

Figure 17 QE-2 Transition Duct Designed for a Fan Hub-to-Tip Ratio of 5.0 and a Fan Aspect Ratio of 3.75

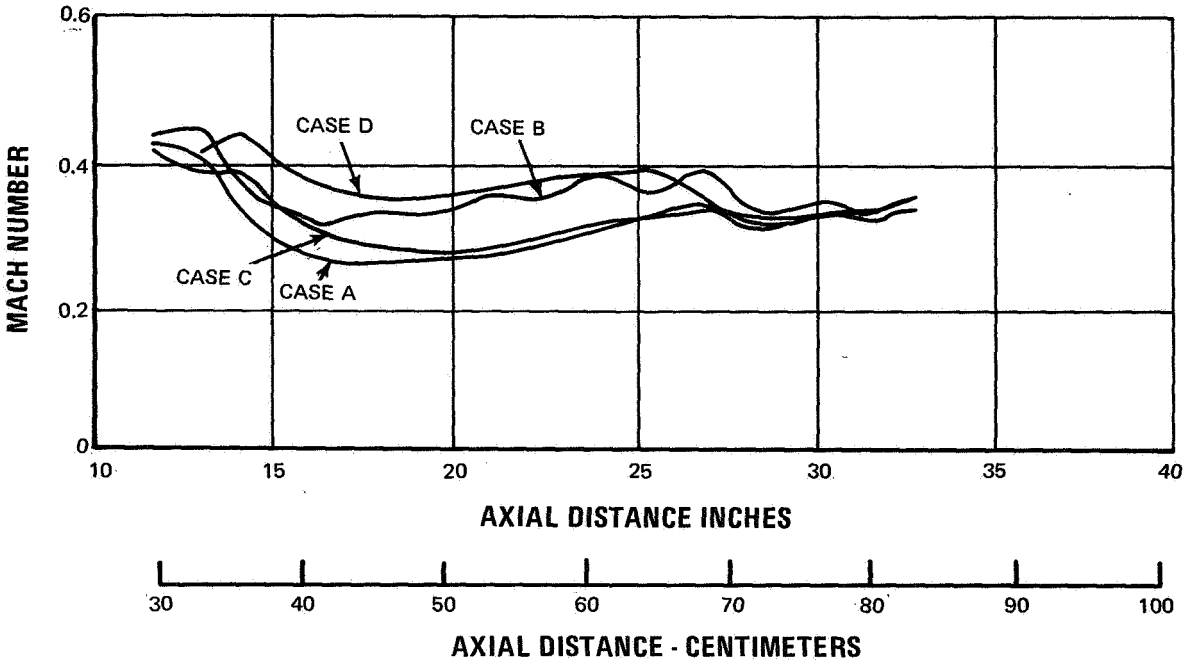

Figure 18 Flow Velocities along the Inner Wall of the QE-2 Transition Duct

C. ENGINE WEIGHT

As the third part of the fan integration study, the contractor has evaluated the effects of fan aspect ratio and hub-to-tip ratio on engine weight. For this evaluation, root aspect ratios of 2.68, 3.30, and 3.85 were selected. As shown in Figure 19, the results of the aspect-ratio study showed that a fan with an aspect ratio of 2.68 would be about 220 pounds (99.5 kilograms) heavier than one with an aspect ratio of 3.85.

Two sections are affected by a change in aspect ratio: the blade and disk assembly and the containment case. Changes in the fan support structure caused by changes in the fan overhung moment were not evaluated in this study, but these effects should not affect the results appreciably.

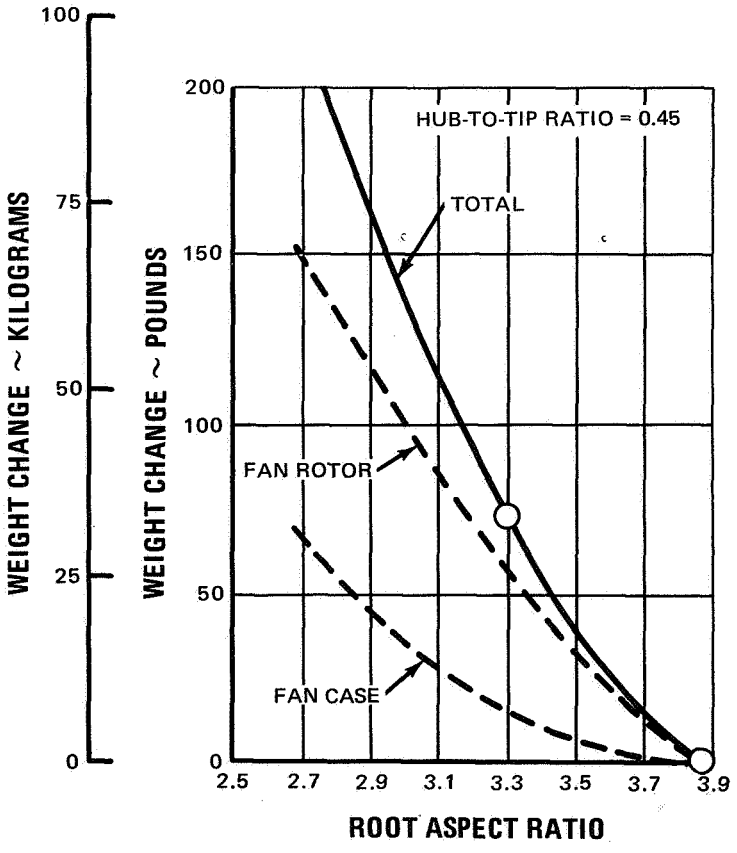

Figure 19 The Effect of the Fan Aspect Ratio on Fan Weight

Fan hub-to-tip ratios of 0.40, 0.45, and 0.50 were evaluated for a constant tip aspect ratio of 3.15. As shown in Figure 20, the fan with a hub-to-tip ratio of 0.50 was found to be about 225 pounds (102 kilograms) heavier than one with a ratio of 0.40. Because each hub-to-tip ratio implies a unique fan-root pressure ratio and a unique flow through the high-pressure compressor, it was necessary in this study to evaluate size changes through the engine. Fans with low hub-to-tip ratios have lighter rotors and cases because of the reduced flowpath diameters, and have shorter transition ducts to the high-pressure compressor is higher for the low hub-to-tip ratios, which results in a larger and heavier high-pressure compressor, diffuser-burner, and turbine. The reduced weight in the fan rotor, case, and transition sections is much greater than the weight additions in the high-pressure spool.

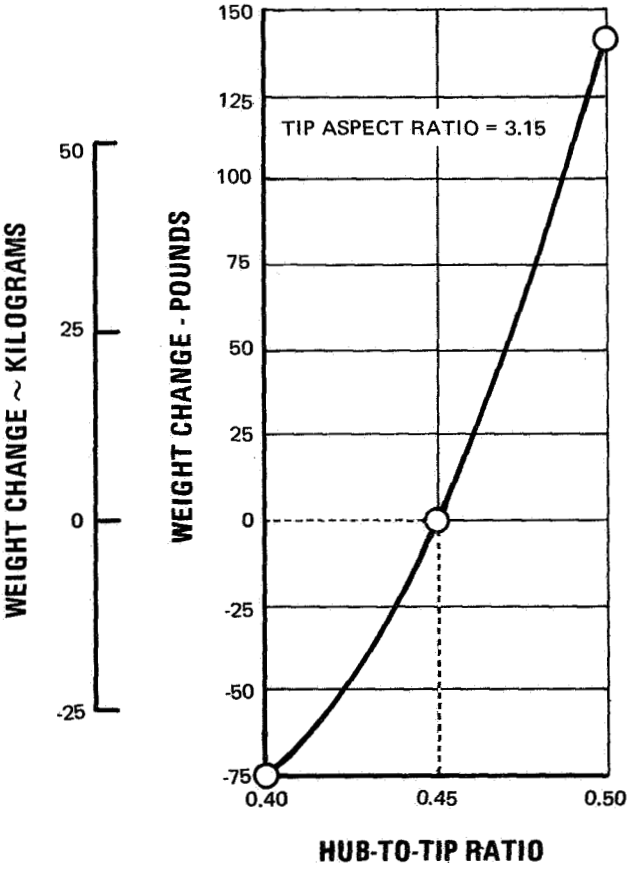

Figure 20 The Effect of Fan Hub-to-Tip Ratio on Engine Weight

D. ENGINE PERFORMANCE

The performance study served a dual purpose. First, it investigated, parametrically, the cycle performance effects of varying fan pressure ratio. Second, because cycle performance is a key factor in the fan selection, it served to synthesize the mechanical design and weights evaluation into an overall parametric study, leading to the final selection of the QE-3 engine configuration.

1. Assumptions

In order to determine the effects of hub-to-tip ratio and aspect ratio on engine performance, certain assumptions had to be made concerning other fan and engine parameters. For the study of hub-to-tip ratio, the following design point assumptions were made:

- Tip speed of 1120 ft/sec (342 m/sec)
- Fan tip aspect ratio of 3.15
- Fan tip pressure ratio of 1.5
- Bypass ratio of 5.8
- Constant flow per unit fan frontal area
- High-pressure compressor pressure ratio of 12.5

For the aspect-ratio study, the following design point assumptions were made:

- Tip speed of 1120 ft/sec (342 m/sec)
- Fan hub-to-tip ratio of 0.45
- Fan root pressure ratio of 1.45
- Over-all pressure ratio of 18.1
- Low-pressure turbine efficiency of 0.907
- Varying fan tip pressure with tip aspect ratio (see Figure 21)

2. Effects of Hub-to-tip Ratio

The effects of hub-to-tip ratio on engine diameter and length are illustrated in Figures 22 through 24. Hub-to-tip ratio has a particularly strong effect on the length of the transition duct, as discussed in Section B.

Figures 25 and 26 and Table II summarize the effect of hub-to-tip ratio on cycle parameters. Increasing the hub-to-tip ratio of the fan increases the fan root pressure ratio and the over-all pressure ratio. Increasing the over-all pressure ratio results in a loss in specific thrust at cruise. Since all engines are sized for constant cruise thrust, an increase in total corrected design airflow results. In addition, an increase in fan hub-to-tip ratio at constant tip speed gives a lower low-pressure spool rotational speed. The resulting loss in the low-pressure turbine's velocity ratio reduces its efficiency. This loss adds further to the airflow scale effect with over-all pressure ratio.

Figure 26 shows the combined effect of over-all pressure ratio and low-pressure turbine efficiency on thrust specific fule consumption at the design point. For constant low-pressure turbine efficiency, increasing the fan's hub-to-tip ratio from 0.4 to 0.5 improves thrust specific fuel consumption by about one percent. When the variation in low-pressure turbine efficiency is accounted for, thrust specific fuel consumption is nearly constant with fan hub-to-tip ratio.

The study of hub-to-tip ratio has led to the conclusion that low hub-to-tip ratios are desirable. When turbine effects are accounted for, there is little if any performance advantage associated with the higher ratios, while there is an obvious weight penalty. However, a lower limit on hub-to-tip ratio may be required in order to prevent an excessive spanwise pressure gradient.

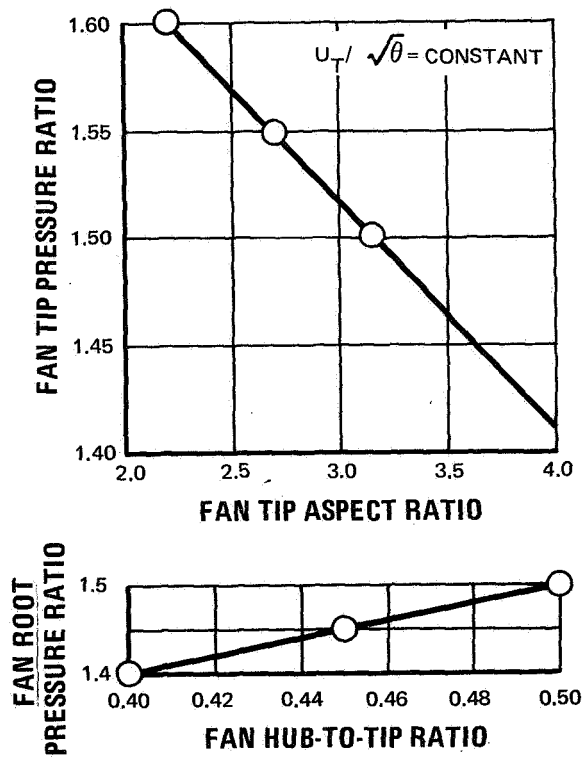

Figure 21 Fan Tip Pressure Ratio Assumptions for Constant Corrected Tip Speed

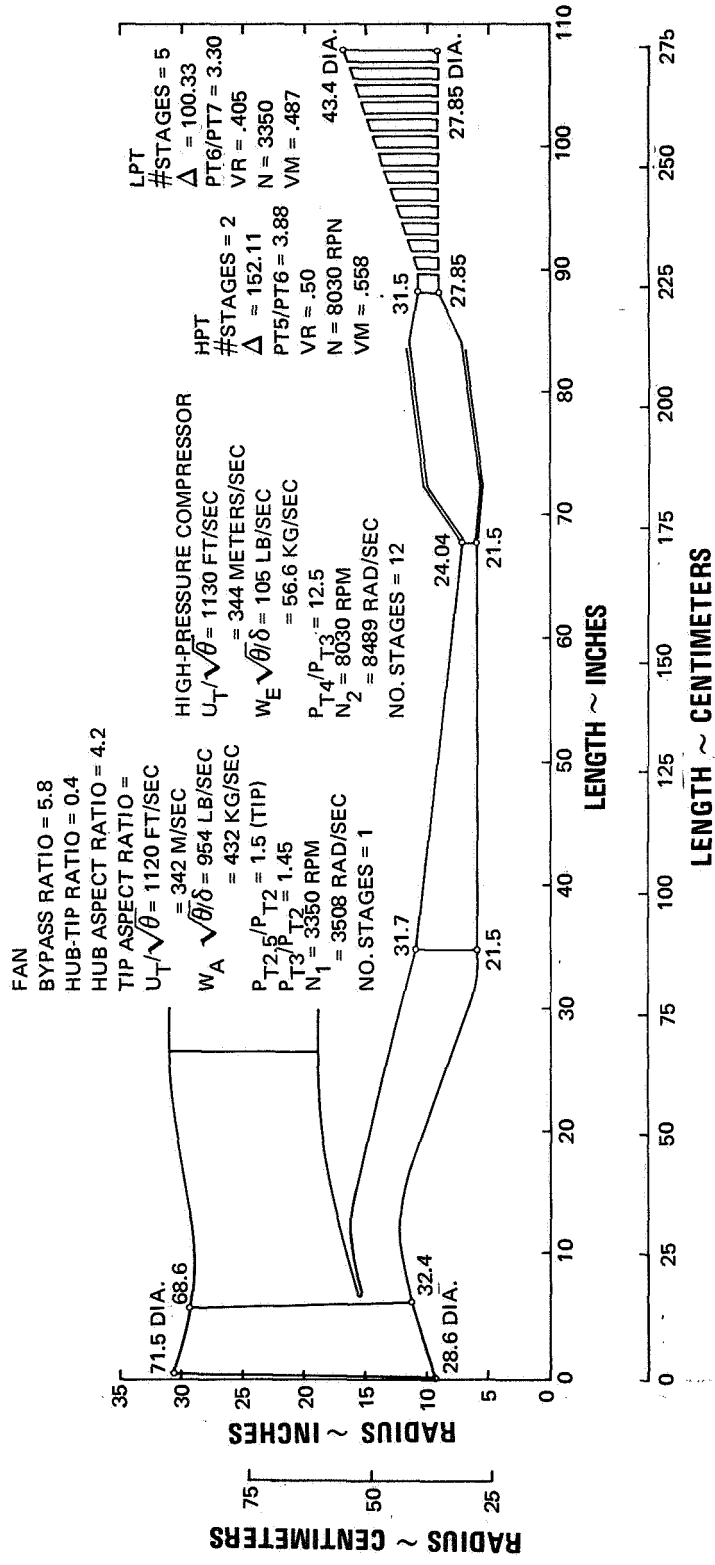

Figure 22 QE-2 Flowpath for an Aspect Ratio of 3.15 and a Hub-to-Tip Ratio of 0.40

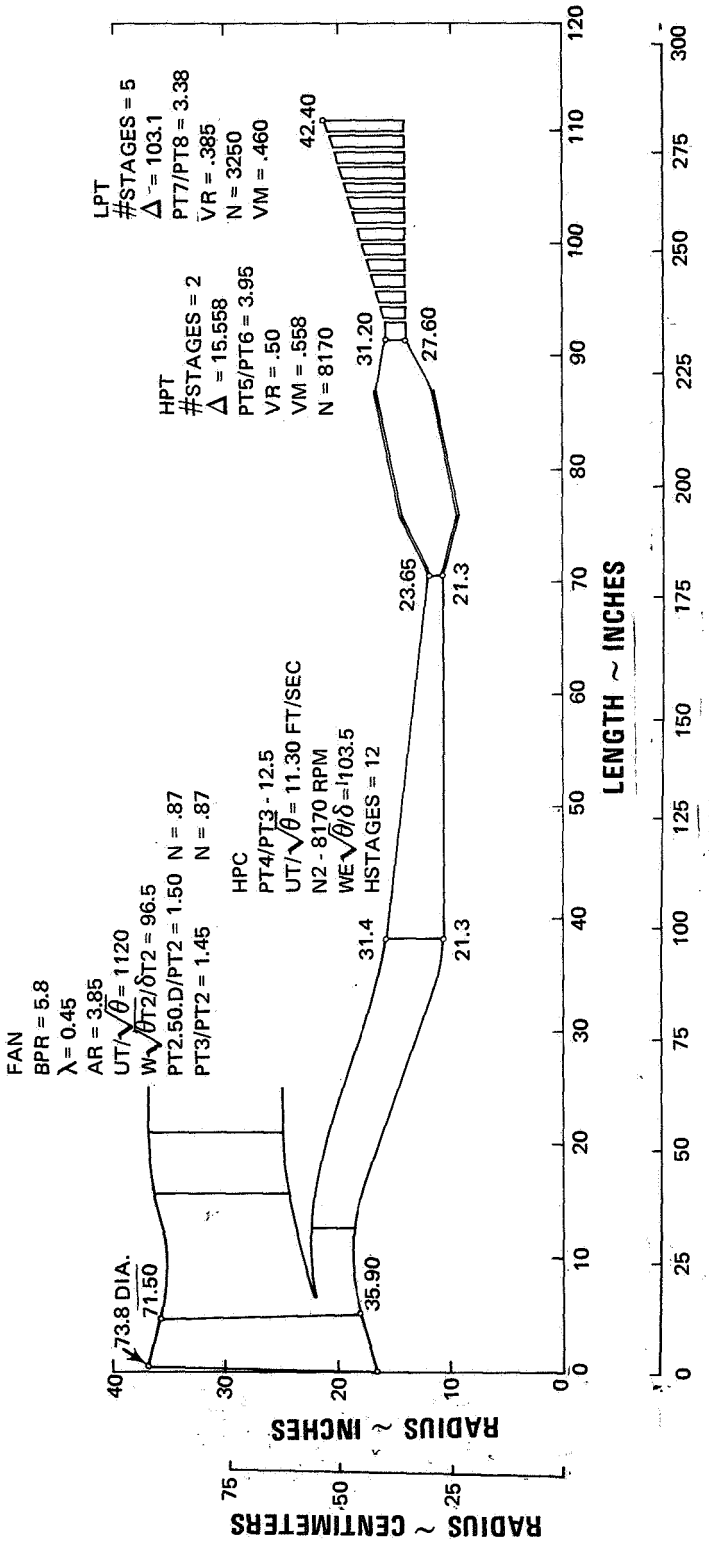

Figure 23 QE-2 Flowpath for an Aspect Ratio of 3.15 and a Hub-to-Tip Ratio of 0.45

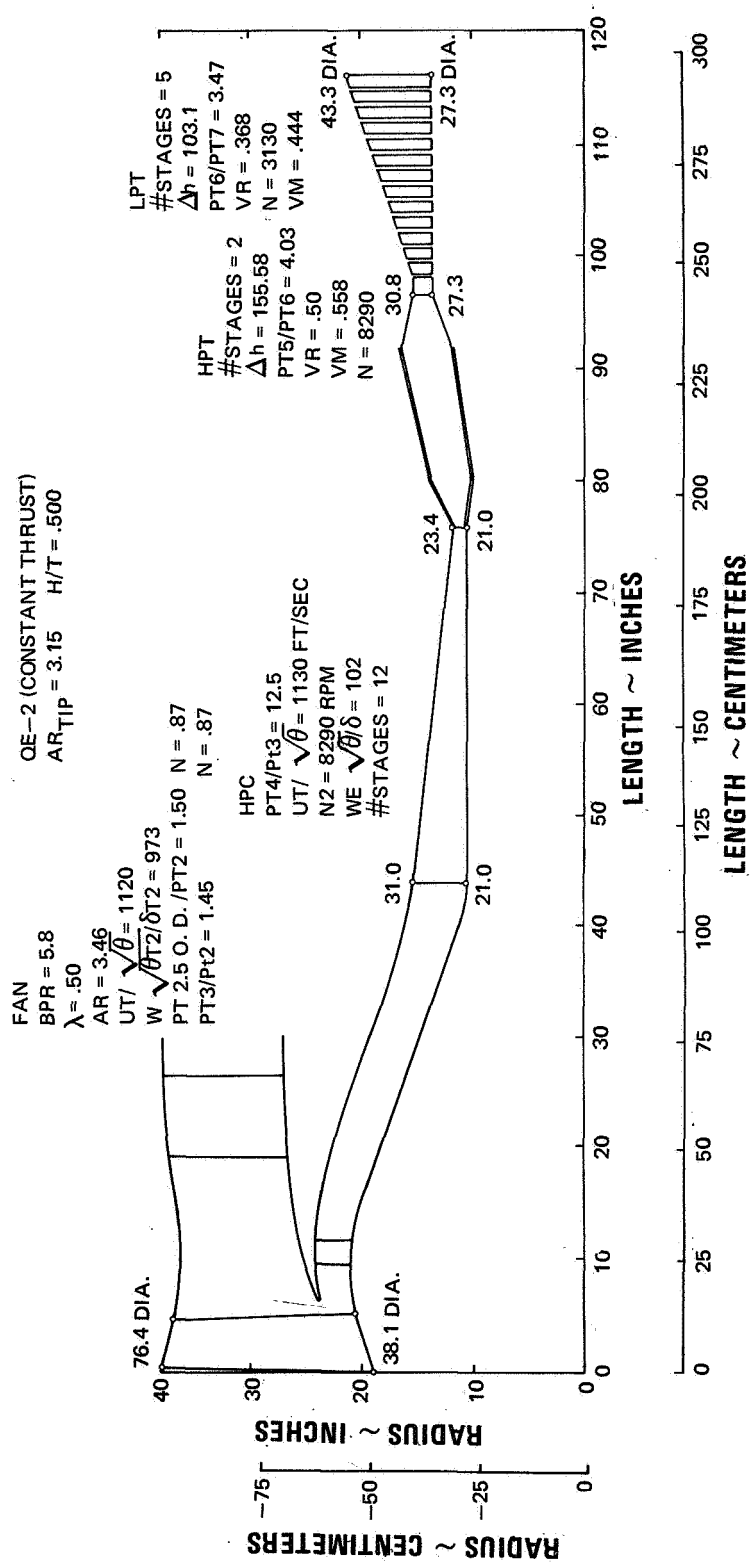

Figure 24 QE-2 Flowpath for an Aspect Ratio of 3.15 and a Hub-to-Tip Ratio of 0.50

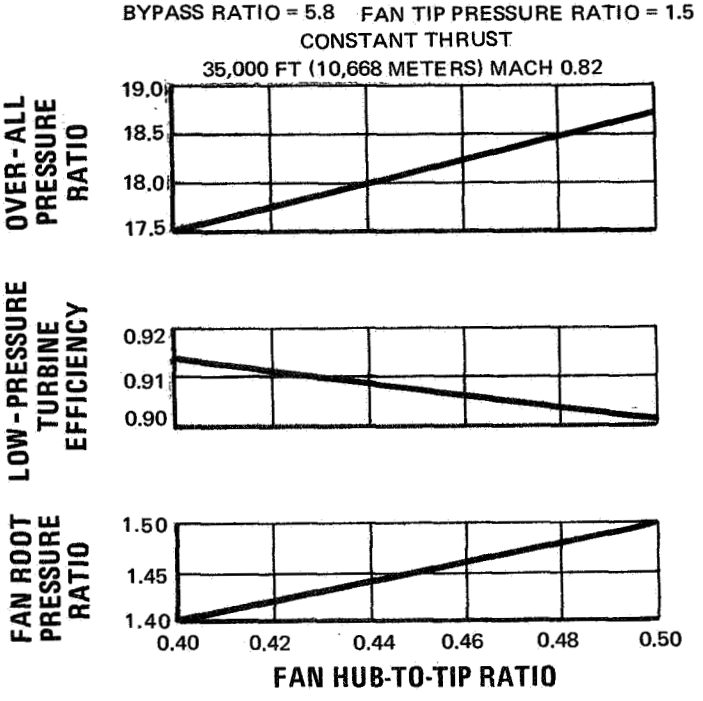

Figure 25 Effect of Hub-to-Tip Ratio on Fan Root Pressure Ratio, Low-Pressure Turbine Efficiency, and Over-all Pressure Ratio

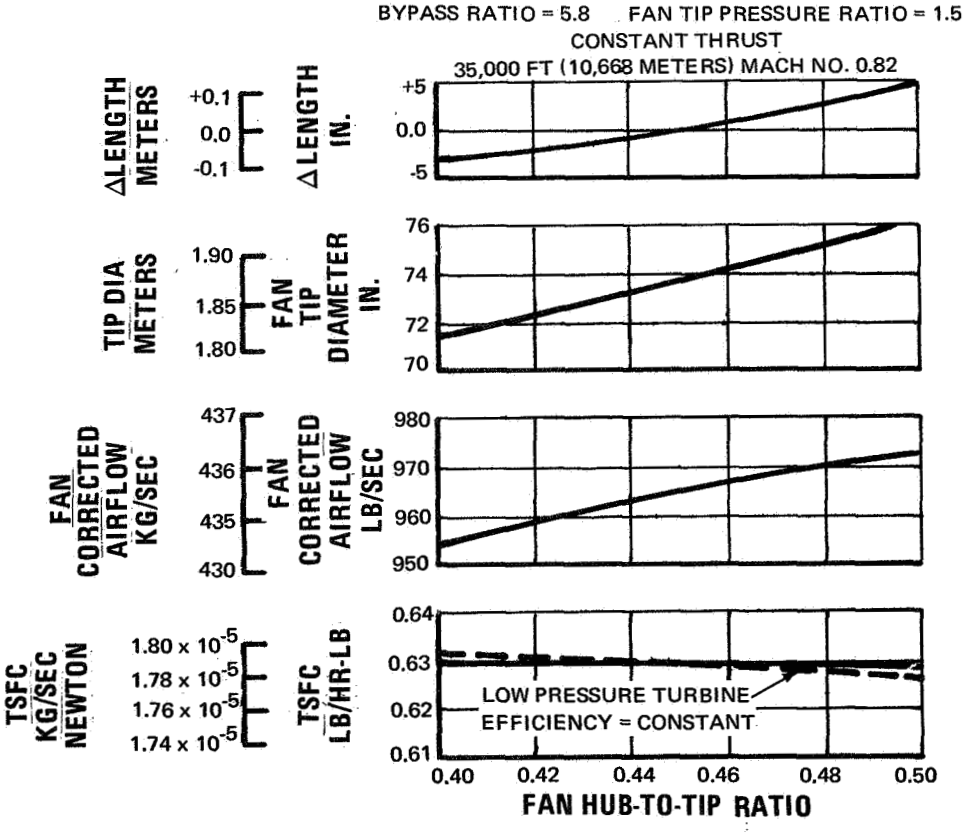

Figure 26 Effect of Hub-to-Tip Ratio on TSFC, Fan Corrected Airflow, Tip Diameter, and Length

TABLE II
EFFECT OF HUB-TO-TIP RATIO ON CYCLE PARAMETERS

Bypass Ratio = 5.8 Fan Tip Pressure Ratio = 1.5

Fan Hub-to-Tip Ratio	0.40	0.45	0.50
Fan Root Aspect Ratio	4.20	3.84	3.47
Fan Root Pressure Ratio	1.40	1.45	1.50
Over-all Pressure Ratio	17.5	18.1	18.7
Low-Pressure Turbine Mean Velocity Ratio	0.49	0.46	0.44
Low-Pressure Turbine Efficiency	0.914	0.907	0.901
Uninstalled TSFC (hr^{-1})	0.630	0.630	0.629
Total Corrected Airflow (lb_m/sec)	954	965	973
Total Corrected Airflow (kg/sec)	432	438	442
Fan Tip Diameter (in)	71.5	73.8	76.4
Fan Tip Diameter (cm)	182	187	194

3. Effects of Aspect Ratio

This study incorporated variations in bypass ratio and design turbine inlet temperature in order to best accommodate the changes in fan tip pressure ratio afforded by varying aspect ratio. All engines were scaled to the same thrust at the cruise design point. Variations in fan corrected airflow and tip diameter which were investigated are shown in Figure 27. In general, changes in the fan tip pressure ratio and design turbine inlet temperature do not result in substantial airflow changes at the design point.

Variations in thrust specific fuel consumption and specific thrust are presented in Figure 28. The desirability of the highest fan tip pressure ratio (1.6) as the bypass ratio decreases from 5.8 to 5.0 is immediately apparent. At a bypass ratio of 5.8, in general, the fan tip pressure ratio of 1.6 is a little higher than optimum. As a base point, the Quiet Engine configuration which had been selected prior to the fan integration study is circled on the curves. This design was the QE-2, which had a bypass ratio of 5.8, a design turbine inlet temperature of 1720°F (1040°K), and an over-all pressure ratio of 1.5.

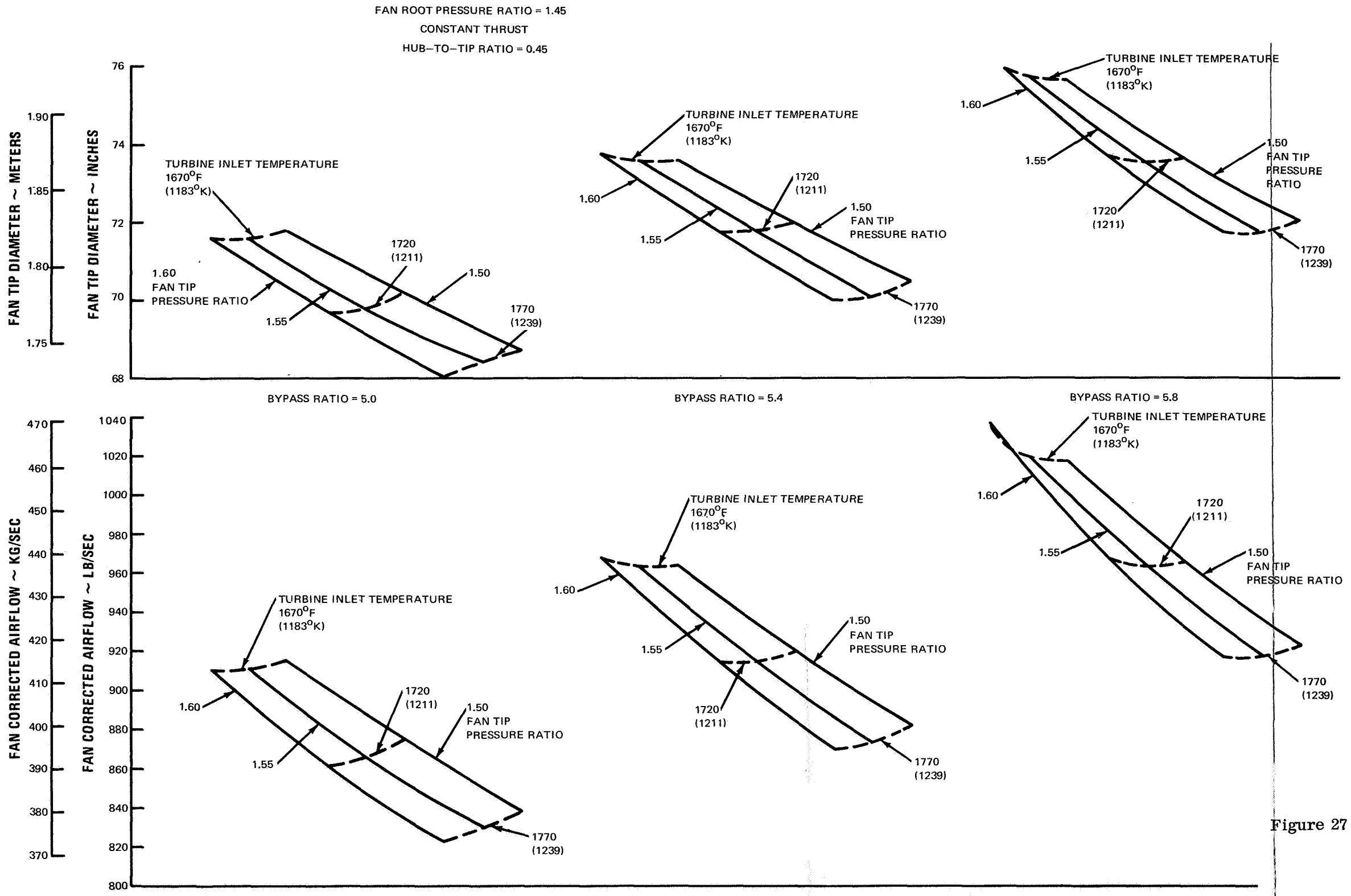

Figure 27 Effects of Fan Pressure Ratio and Turbine Inlet Temperature on Fan Airflow and Fan Tip Diameter

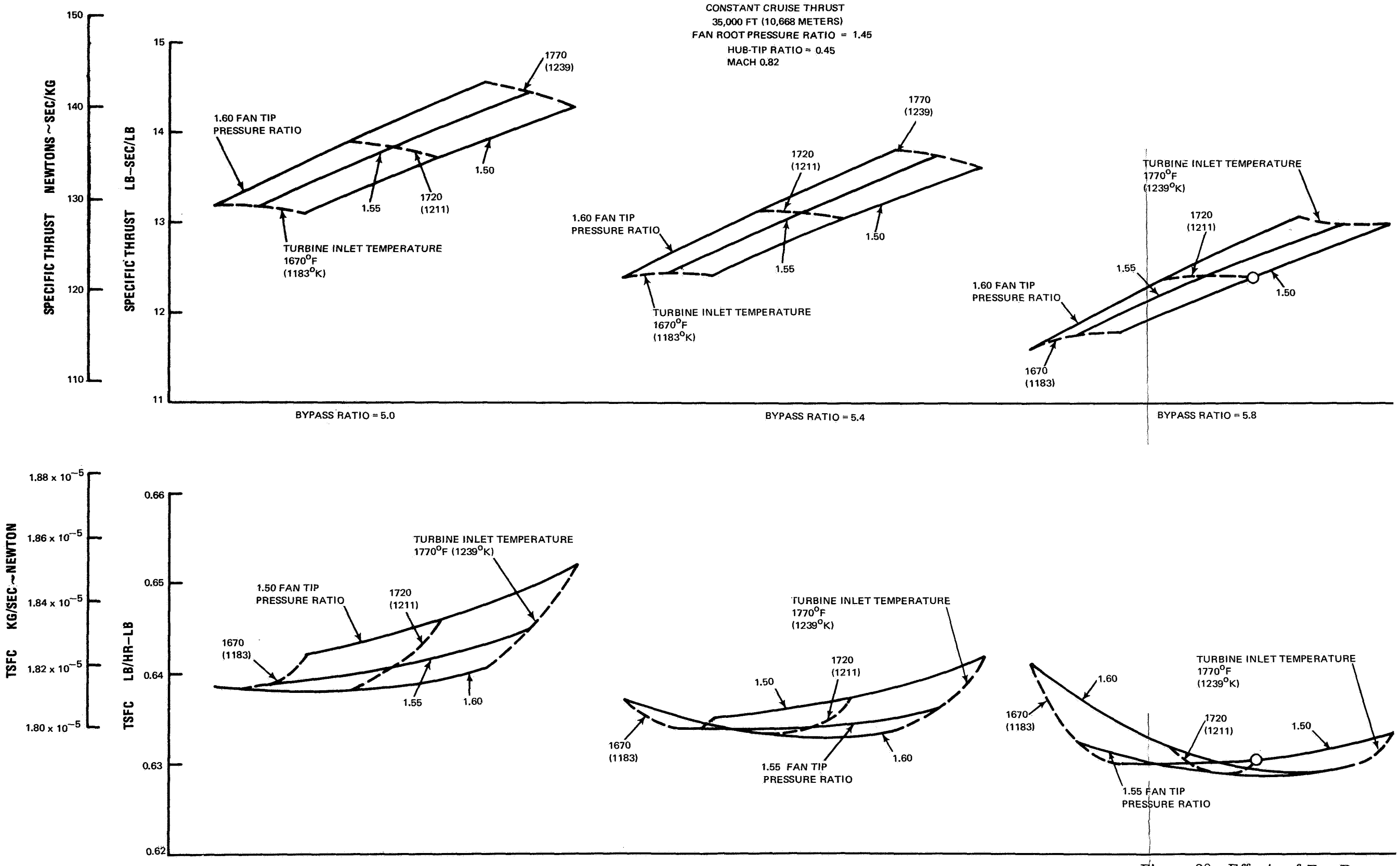

Figure 28 Effects of Fan Pressure Ratio and Turbine Inlet Temperature on TSFC and Specific Thrust

Figure 29 presents the take-off jet noise and total noise at the three-mile (4.82-kilometer) point. For a fixed turbine inlet temperature of 2000°F (1230°K) at take-off, an increase in design turbine inlet temperature results in a reduced tip speed at take-off. However, the reduced take-off thrust associated with the higher design temperature results in a lower altitude at the three-mile (4.82-kilometer) point. The resultant effect on total noise is a slight increase with increased design turbine inlet temperature. The net effect is slight, since the two effects tend to cancel each other. However, there is agreement with previous studies which have shown that operating the engine at higher take-off temperatures and higher tip speeds for a given design temperature results in some reduction in total noise at the three-mile (4.82-kilometer) point.

Jet noise at the three-mile (4.82-kilometer) point also increases with increasing design turbine inlet temperature for the fixed take-off temperature. The increased noise is caused by the increased jet velocity at take-off. The decrease in altitude at the three-mile (4.82-kilometer) point further accentuates the increase in jet noise with increasing design temperature.

The variation in the rim velocity ratio of the low-pressure turbine is presented in Figure 30. For purposes of comparison and to narrow down the range of interest, a jet noise level of 94 PNdb has been adopted as an upper limit. Table III compares selected engines from the previous carpet plots. Engine A is the QE-2, the base engine. Engine B has a bypass ratio reduced to 5.4 and a fan tip pressure ratio increased to 1.55 from the base levels, so as to maintain both jet and total noise at a nearly constant level. If the fan pressure ratio is further increased to 1.6, as in Engine C, about a 2 db reduction in jet noise results, at the cost of a rather substantial increase in weight caused by the reduction in aspect ratio. Engine D is the same as Engine C, except that design turbine inlet temperature is 50°F (27.8°K) higher. This change results in a substantial reduction in total airflow and engine weight, and jet noise is increased to level of the base engine. Engine E has its bypass ratio reduced to 5.0 and its design turbine inlet temperature at the base engine level. Jet and total noise are approximately the same as that of the base engine. Engine F is a variation of the base engine which has both increased fan pressure ratio and increased turbine inlet temperature.

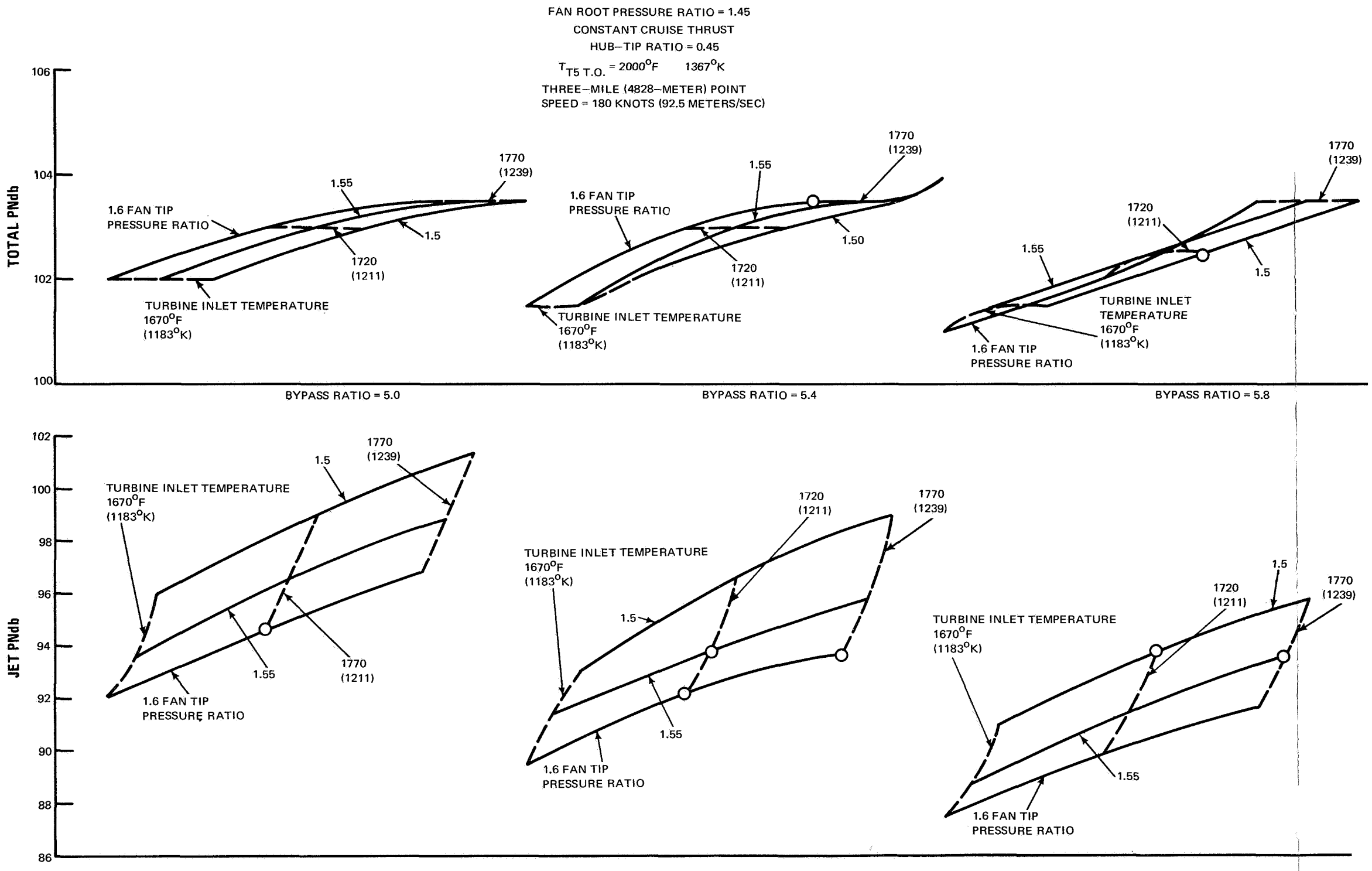

Figure 29 Effects of Fan Pressure Ratio and Turbine Inlet Temperature on Jet and Total Noise

TABLE III
COMPARISON OF SELECTED ENGINES

Engine	A (QE-2)	B	C	D (QE-3)	E	F
Bypass Ratio	5.8	5.4	5.4	5.4	5.0	5.8
Over-all Pressure Ratio	18.1	18.1	18.1	18.1	18.1	18.1
Fan Tip Pressure Ratio	1.50	1.55	1.60	1.60	1.60	1.55
Design Turbine Inlet Temperature (F)	1720	1720	1720	1770	1720	1770
Design Turbine Inlet Temperature (K)	1210	1210	1210	1240	1210	1240
Take-off Turbine Inlet Temperature (F)	1950	1950	1950	2000	1950	2000
Take-off Turbine Inlet Temperature (K)	1345	1345	1345	1368	1345	1368
Total Corrected Flow (lb_m/sec)	966	914	914	870	862	918
Total Corrected Flow (kg/sec)	438	414	414	394	391	417
Thrust Specific Fuel Consumption (hr^{-1})	0.6305	0.6340	0.6335	0.6330	0.6380	0.6290
Fan Tip Diameter (in)	73.7	71.8	71.8	70.0	69.7	71.8
Fan Tip Diameter (cm)	187.5	182.5	182.5	178.0	177.0	182.5
Fan Tip Aspect Ratio	3.15	2.7	2.2	2.2	2.2	2.7
Fan Hub-to-Tip Ratio	0.45	0.45	0.45	0.45	0.45	0.45
Low-Pressure Turbine Rim Velocity Ratio	0.388	0.398	0.386	0.386	0.410	0.373
Engine Weight (lb_m)	5300	5345	5490	5240	5430	5120
Engine Weight (kg)	2410	2430	2490	2340	2370	2320
Jet Noise (PNdb)*	93.7	93.9	92.2	93.6	94.5	93.7
Total Noise (PNdb)*	103.4	103.9	103.9	103.5	103.9	103.5

* At take-off 3-mile (4.75 km) point

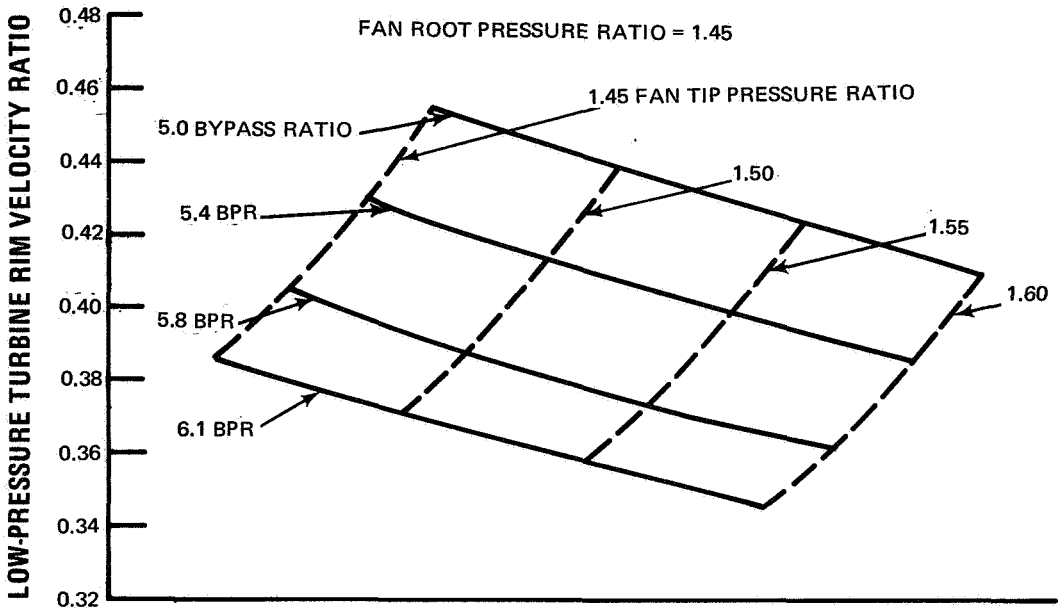

Figure 30 Effects of Bypass Ratio and Fan Tip Pressure Ratio on Low-Pressure Turbine Rim Velocity Ratio

The results of the aspect-ratio study have led to the following conclusions:

1. Reducing bypass ratio does not necessarily reduce bare engine weight. For constant turbine inlet temperature, weight generally increases with decreasing bypass ratio because the effect of aspect ratio on weight over-rides the effect of the reduction in airflow. When nacelle weight is added to bare engine weight, however, it is likely that the higher bypass ratio will show little or no weight advantage.

2. In general, the configurations investigated show little difference in thrust specific fuel consumption. Engines with lower bypass ratios do show a slight penalty in uninstalled thrust specific fuel consumption, which will be reduced or eliminated when the installation effects are accounted for.

3. Reducing bypass ratio with respect to the base engine results in decreased diameter, which will permit reduced nacelle weight and drag.

4. Increasing design turbine inlet temperature with respect to the base engine results in decreased diameter and decreased engine weight.

5. It is possible to reduce bypass ratio and increase design turbine inlet temperature while maintaining constant jet and total noise, if the fan tip pressure ratio is increased from 1.5 to 1.6.

From the conclusions above, Engine D of Table III was selected by the NASA Project Manager as the configuration for further study under Task III with the concurrence of the Contractor and was designated the QE-3. It is shown schematically in Figure 31. A fan hub-to-tip ratio of 0.45 was selected for the QE-3 as the lowest which was consistent with an acceptable spanwise pressure gradient. The aspect ratio selection involved considerations which went beyond those directly explored in the integration study. This was particularly true in that there was no strong choice indicated by the study results. These considerations included:

1. Design Flexibility - The relatively low aspect ratio associated with a 1.6 tip pressure ratio demands the greatest effort to achieve a lightweight, practical design. Any future modification to higher aspect ratio would be inherently feasible in the QE-3 design.

2. Mid-Span Shroud - A mid-span shroud is necessary for mechanical vibration stability in higher aspect ratio blades. Elimination of the mid-span shroud through the use of a lower aspect ratio design could provide potential benefit in aerodynamic performance, noise, and fabrication complexity. As the QE-3 design subsequently developed, however, a single shroud was required for stability. This was compensated for to some extent by the reduction of the airfoil thickness which may improve noise and aerodynamic performance.

3. Noise - Irrespective of the presence of the shroud, the direct effects of aspect ratio on fan noise production remain unknown. The true value of the integration study will be evident as background during the future course of the Quiet Engine program at such time as the necessary experimental evidence becomes available.

4. Composites - The low aspect ratio airfoil is readily adaptable to the future application of composite materials.

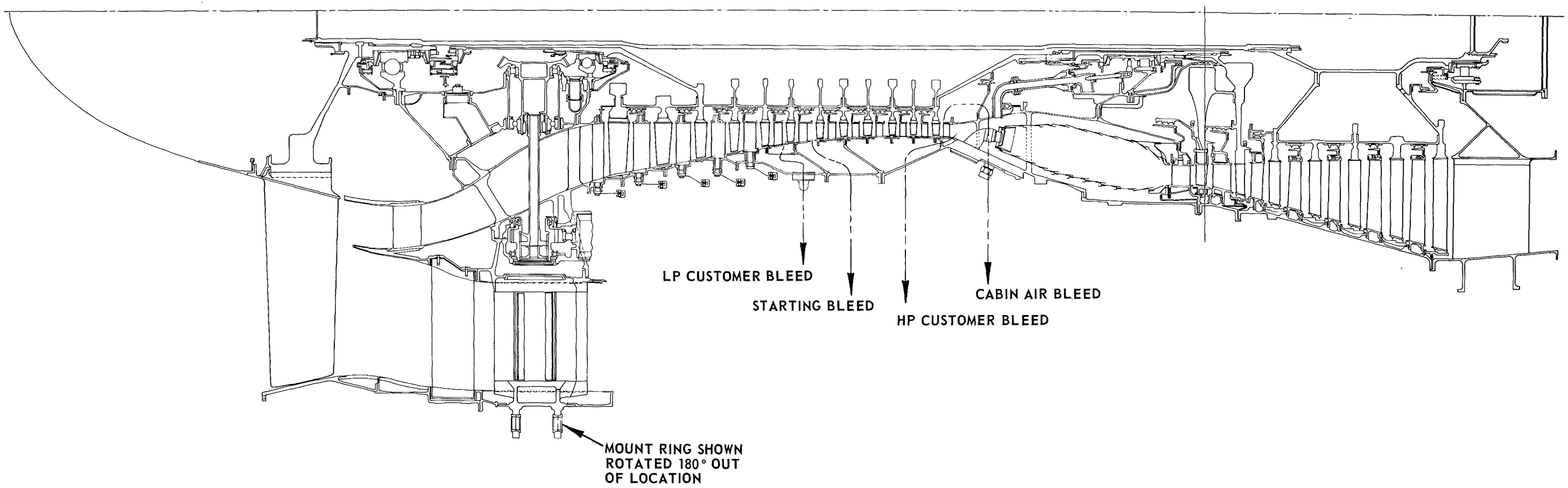

Figure 31 QE-3 Layout

SECTION IV

QE-3 ENGINE DESIGN

A. GENERAL DESCRIPTION

The QE-3 engine is a twin-spool axial-flow turbofan rated for 4900 pounds (21,800N) of cruise thrust at 35,000 feet (10,680 meters) on a standard day. Its thrust-specific fuel consumption at the same flight condition is 0.631 hours $^{-1}$. The mechanical arrangement, bearing locations, and structural cases of the engine are shown in Figure 31. The major components of the engine are listed below:

- Single-stage high-performance fan
- Twelve-stage high-pressure compressor
- Annular combustor
- Two-stage high-pressure turbine
- Five-stage low-pressure turbine

Fundamental to Pratt & Whitney Aircraft's design philosophy in recent years has been a concerted effort to reduce the number of critical rotating and static parts in an engine. In accordance with this philosophy, the QE-3 was designed with four bearings and three major bearing support structures. In addition to these design features, the QE-3 incorporates all known practical features to reduce engine noise. These features include the use of a single-stage fan, no inlet guide vanes, low fan tip speeds, fan rotor to exit guide vane axial spacing, blade and vane number combinations as near optimum as possible, acoustical treatment of the fan case aft of the rotor, acoustical treatment of the ducting leading to the high-pressure compressor, and low jet exhaust velocities. The aerodynamic and mechanical design features of the QE-3 are discussed in the remaining paragraphs of this section.

B. COMPONENTS

1. Fan

The single-stage fan develops at design a pressure ratio of 1.6 in the fan bypass portion. The fan was subjected to a more rigorous design evaluation than the other components. Discussion of its design features is treated separately in more detail in Section VI of this volume.

2. High-Pressure Compressor

The QE-3 high-pressure compressor is based upon up-to-date Pratt & Whitney Aircraft compressor design philosophy and test experience. With 12 stages, the QE-3 compressor produces a pressure ratio of 12.3 at its aerodynamic design point (100 percent speed and airflow). As shown in Figure 32, it is supported at the third and last stages with the first two stages cantilevered. The inlet guide vane and first four stators of the compressor have variable geometry. Air for various engine and airframe functions is extracted at appropriate locations along the outer case.

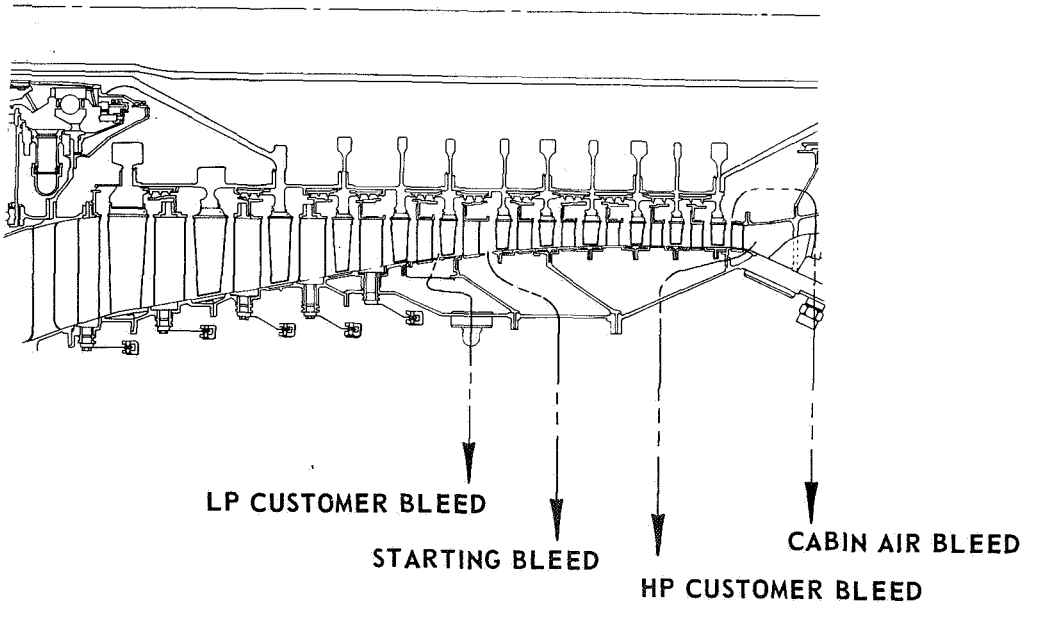

Figure 32 QE-3 High-Pressure Compressor

The point selected for the cruise design condition (discussed in Section IV D of this volume) is slightly in the overspeed region on the compressor performance map, so that the design cycle is achieved at a high-pressure compressor pressure ratio of 13.0.

3. Burner

The combustor section of the QE-3 engine consists of a liquid-fuel downstream-injection annular burner and an annular diffuser. With an over-all length of 20 inches (50.8 cm), the combustion section is designed to provide the required hot day take-off turbine inlet temperature of 2028°F, (1385°K) and the required temperature rise of 1179°F (655°K) with good durability. The burner is also designed so that minimal development will provide a low level of engine exhaust smoke, a uniform circumferential temperature pattern to the turbine, a radial temperature profile consistent with turbine structural requirements, and adequate altitude ignition capability.

As shown in Figure 33, the burner consists of four basic sections: the diffuser and combustion chamber cases, the combustion chamber assembly, the fuel system, and the ignition system. The diffuser cases are contoured to provide efficient diffusion of the compressor discharge air prior to entry into the annular combustion chamber. The inner and outer diffuser cases are connected radially by ten aerodynamically shaped sheet metal struts. The outer diffuser case also provides support for the fuel nozzle assemblies. The material for the diffuser and combustion chamber cases is Inconel 718, which was chosen for its high strength at elevated temperatures.

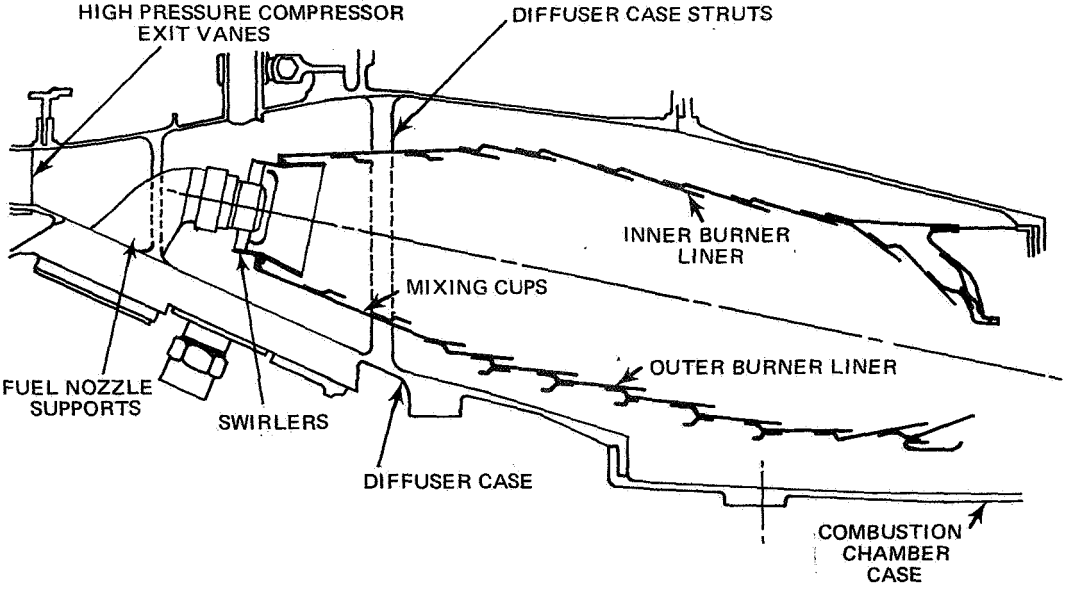

Figure 33 QE-3 Burner

The Hastelloy X combustion chamber assembly is composed of a cup front end and outer liner assembly and an inner liner. An axial flow swirler is supported at the front end by ten radial pins located behind the diffuser struts. The rear end is supported by a slip fit on the front support of the turbine inlet guide vanes. The inner liner is supported by a slip fit in the front and is bolted at the rear to the inner support of the turbine inlet guide vanes. The liners are of louvered construction, and Z-shaped circumferential stiffeners are provided on the outer liner to increase its buckling strength. Where slip fits are used, the contacting surfaces are coated with a chromium carbide plasma spray.

The fuel system is composed of 20 dual-orifice nozzles which are supplied by primary and secondary fuel manifolds. The manifolds are located outside the case to prevent fouling caused by thermal decomposition. With the dual-orifice pressure-atomizing nozzles, only small pressure variations are required in the fuel supply to achieve good atomization over the wide range of fuel flows required to ensure the reliability of the ignition system, two four-joule spark ignitors are provided in the combustion chamber. They are located nine degrees (0.157 radian) above the horizontal centerline in the transition region between the swirl cups and the combustion chamber.

During the design of the QE-3 burner, particular attention was paid to smoke emission, and the turbine inlet temperature pattern. Preliminary design and performance data for the burner are presented in Table IV for the burner design point, sea-level take-off with an ambient temperature of 84°F (302°K).

The turbine inlet temperature profile is controlled largely by the flow of air through the burner. Air enters the mixing cups through the swirlers, combustion holes in each cup, and through cooling louvers. The shroud air is injected into the annular portion of the combustion chamber through combustion holes in the inner and outer liners and cooling holes in the forward face of the cooling louvers.

The air fed to the primary zone of the combustion chamber, in addition to providing the major portion of the combustion air, creates a recirculation zone to achieve piloting and flame stability. The air added downstream of this region through the flush holes dilutes and mixes with the combustion products to provide the required turbine inlet temperature profile and pattern. The mixing in both the primary and dilution zones determines the uniformity of the turbine inlet temperature pattern. This system has proven capable of achieving a nearly ideal radial temperature profile, as shown in Figure 34.

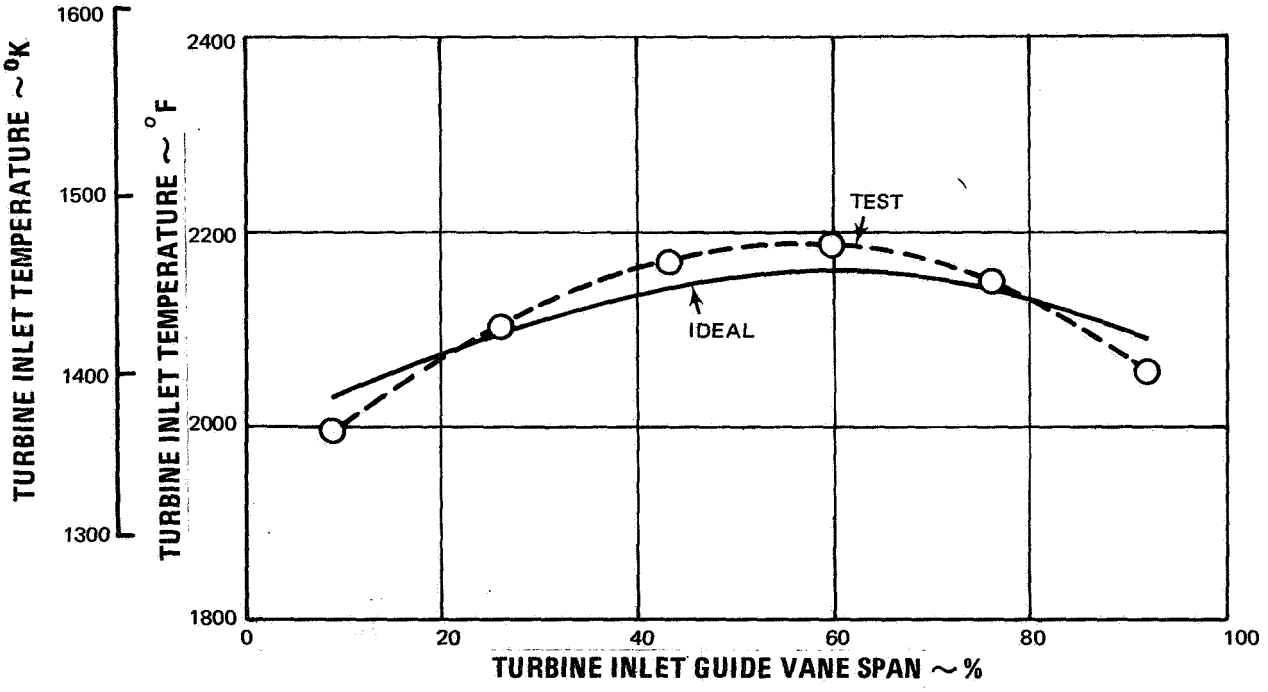

Figure 34 Radial Temperature Profile

TABLE IV
PRELIMINARY DESIGN AND PERFORMANCE DATA
FOR THE QE-3 BURNER

	U.S. Units	International Units
Conditions		
Engine airflow	120.4 lb/sec	54.6 kg/sec
Combustion chamber airflow	111.9 lb/sec	50.7 kg/sec
Compressor discharge pressure	249.8 psia	172 N/cm^2
Compressor discharge temperature	849 °F	727 °K
Turbine inlet temperature	2028 °F	1385 °K
Design		
Total length	20.0 in	50.8 cm
Length from fuel nozzle to turbine inlet	15.6 in	39.6 cm
Maximum radial height	4.2 in	10.4 cm
Characteristic length (length/radial height)	3.72	3.72
Length from compressor exit to fuel nozzle	4.8 in	12.4 cm
Compressor exit area	78.8 in^2	508 cm^2
Combustor maximum flow area	352 in^2	2270 cm^2
Diffuser area ratio	2.04	2.04
Number of fuel nozzles	20	20
Aerodynamics and Performance		
Compressor discharge Mach number	0.240	0.240
Cold liner velocity	90 ft/sec	27.4 m/sec
Shroud velocity at diffuser exit	210 ft/sec	64.0 m/sec
Temperature rise	1179 F°	655 K°
Combustor efficiency	1.00	1.00
Exit temperature pattern factor	0.2	0.2
Diffuser pressure loss	2.1 %	2.1 %
Combustion chamber pressure loss	2.6 %	2.6 %
Total burner pressure loss	4.7 %	4.7 %
Percent of combustion chamber flow used for liner cooling	42 %	42 %
Combustor heat release rate	3.6×10^6 Btu/hr-ft^3-atm	367 J/sec-m-N

4. Turbines

The QE-3 engine has a two-stage high-pressure turbine and a five-stage low-pressure turbine. Both turbines are shown in Figure 35. The number of stages and diameters were selected to achieve good efficiency without excessive weight, cost, or complexity. The turbine design reflects up-to-date aerodynamic design philosophy and experience. Significant design parameters for the turbines are shown in Table V.

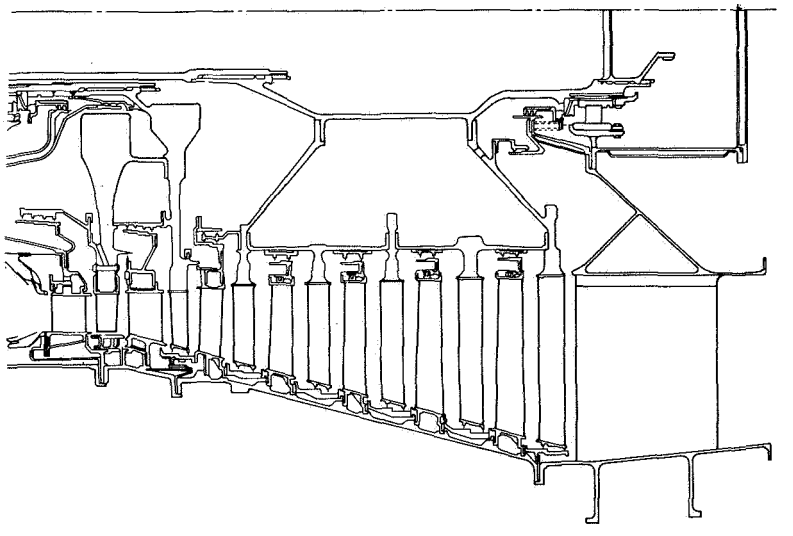

Figure 35 QE-3 Turbines

Both high- and low-pressure turbines utilize controlled-vortex flow patterns to provide maximum efficiencies. This concept, which has been well proven in rig and engine testing, enables the designer to control the work extraction and reaction at different radial locations. To further achieve high levels of efficiency, tip clearance control is employed on all seven rotors.

Predictions of off-design performance are provided in Figures 36 through 39. Figures 36 and 37 show efficiency as a function of velocity ratio and pressure ratio. Figures 38 and 39 show flow capacity as a function of pressure ratio and corrected speed.

TABLE V
AERODYNAMIC DESIGN PARAMETERS FOR THE QE-3 TURBINES

High-Pressure Turbines	
Number of stages	2
Rim velocity ratio	0.513
Mean velocity ratio	0.559
Average stage pressure ratio	2.019
Average stage work (Btu/lb)	78.71
Average stage work (J/g)	272
Work/Inlet Temperature average stage (Btu/lb-°R)	0.0358
Work/Inlet Temperature average stage (J/g-°K)	0.223
First blade hub-to-tip ratio	0.875
Mean blade discharge relative Mach number	0.720
Cooled efficiency	0.899
Turbine inlet temperature (°F)	1740
Turbine inlet temperature (°K)	1220
Low-Pressure Turbine	
Number of stages	5
Rim velocity ratio	0.371
Mean velocity ratio	0.453
Average stage work (Btu/lb)	21.15
Average stage work (J/g)	73.0
Work/ Inlet Temperature average stage (Btu/lb-°R)	0.0133
Work/Inlet Temperature average stage (J/g-°K)	0.0828
Cooled efficiency	0.916

The design parameters for the QE-3 are generally within the range of previous experience. Each of the most significant parameters is discussed separately in the following paragraphs.

a. Velocity Ratio

The velocity ratio relates the stage work to the available wheel speed of the blading as shown in the equation below:

$$\text{Velocity ratio} = \frac{V}{\sqrt{2 \frac{}{g} j \Delta h}}$$

where V = wheel speed
g = acceleration of gravity
j = Joule's constant
h = Stage work

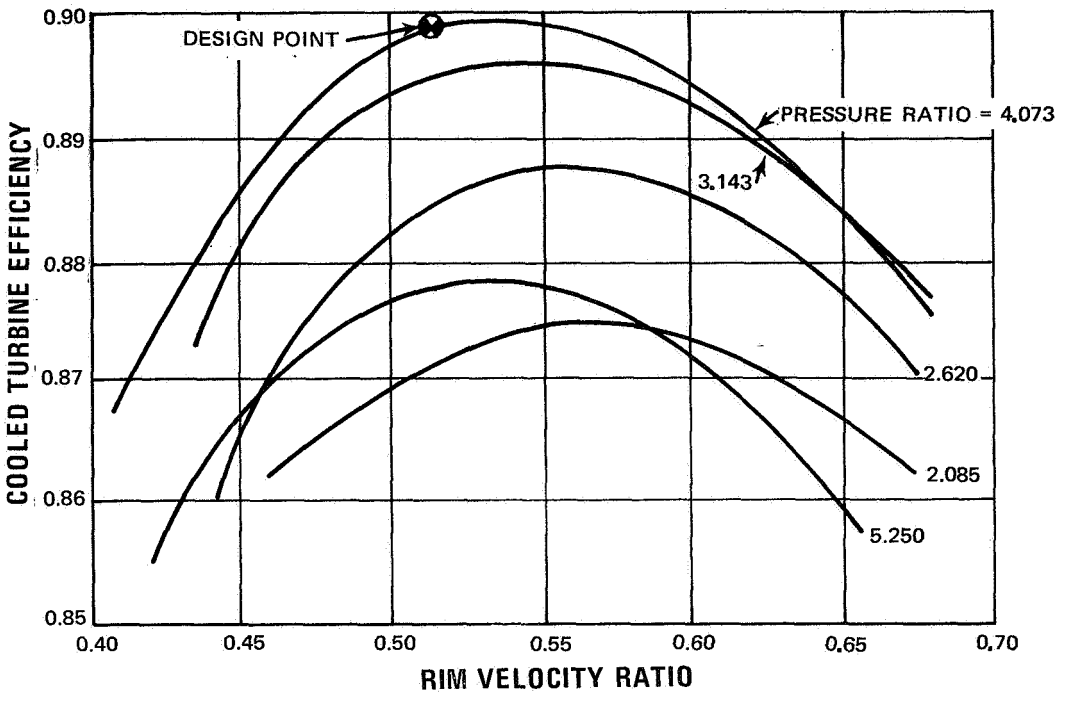

Figure 36 High-Pressure Turbine Efficiency as a Function of Rim Velocity

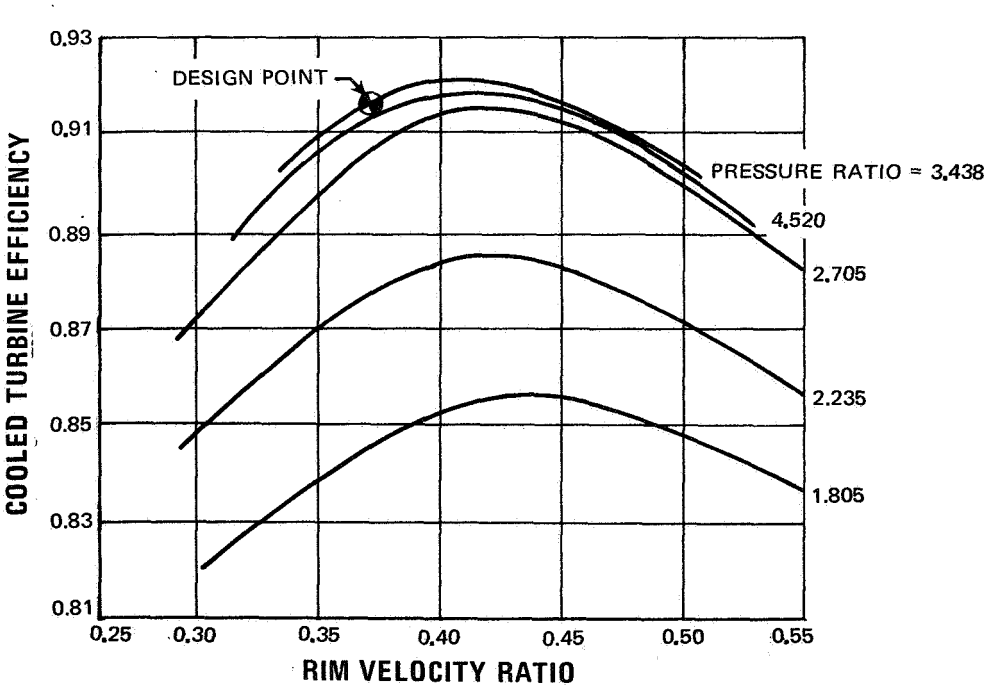

Figure 37 Low-Pressure Turbine Efficiency as a Function of Rim Velocity Ratio

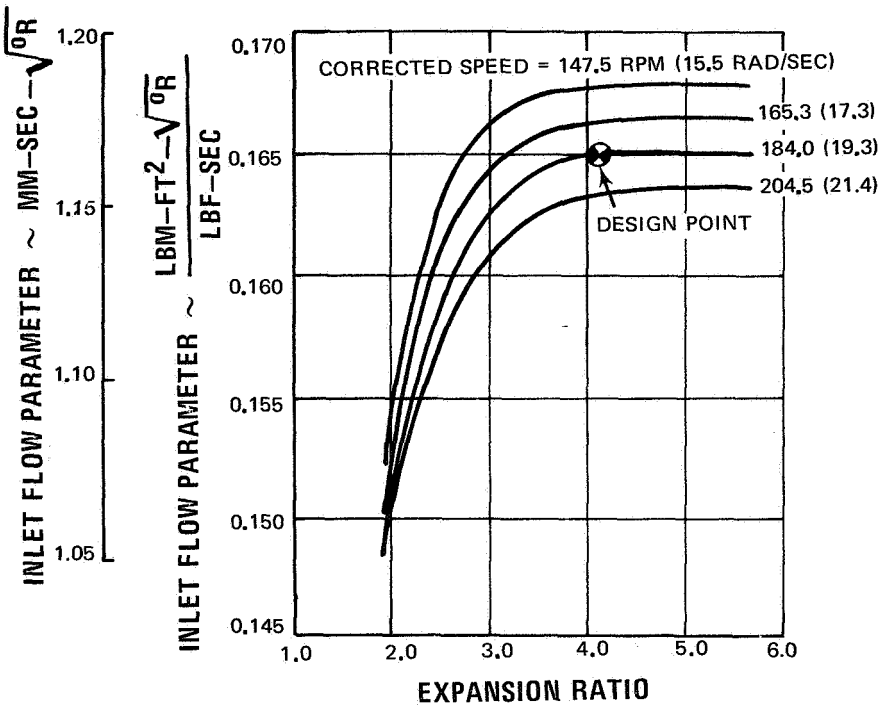

Figure 38 High-Pressure Turbine Flow Capacity as a Function of Expansion Ratio

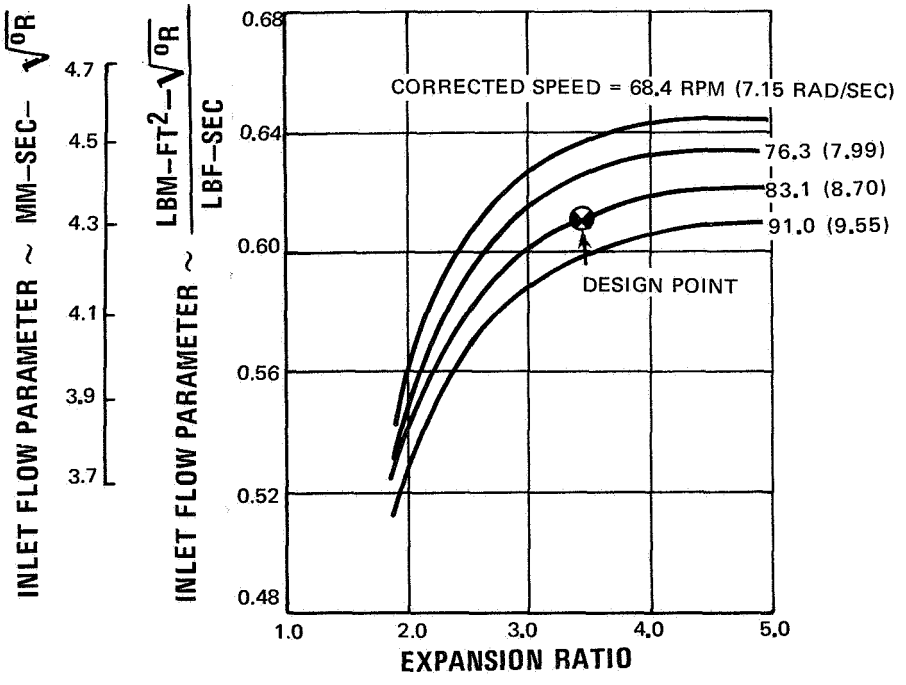

Figure 39 Low-Pressure Turbine Flow Capacity as a Function of Expansion Ratio

Although mean velocity ratio is the most significant parameter for over-all performance considerations, rim velocity ratio is also important. It represents the aerodynamic characteristics at the root of the blading, where the airfoil is most difficult to design. The velocity ratio was selected to provide the best compromise between efficiency and weight. The QE-3 high-pressure turbine has a mean velocity ratio of 0.559, while its rim velocity ratio is 0.513. The low-pressure turbine has a mean velocity ratio of 0.453, and its rim velocity ratio is 0.371.

The velocity ratios of the low-pressure turbine fall near the low end of the experience spectrum because of the low rotational speed resulting from the fan requirements. Velocity ratios for the high-pressure turbine are near the high end of the experience band in order to utilize a fixed rotational speed by providing the largest possible diameter (and hence wheel speed).

b. Turbine Work Parameter

The QE-3 high-pressure turbine is required to produce a work level of 157.4 Btu/lb (545 J/g) at a turbine inlet temperature of 1740°F (1220°K). The resulting turbine work parameter is 0.0358 Btu/lb-°R (0.223 J/g-°K). The low-pressure turbine work requirement of 105.7 Btu/lb (365 J/g) results in a turbine work parameter of 0.0133 Btu/lb-°R (0.0828 J/g-°K). The work parameter for the high-pressure turbine is near the low end of existing experience. Although the work parameter for the low-pressure turbine is somewhat below the existing level of experience, it is not expected that this will present any problem.

c. Pressure Ratio

The QE-3 high-pressure turbine has a pressure ratio of 4.073. The pressure ratio was determined almost entirely from the engine cycle selection and, to a certain extent, from the component efficiencies. The average stage pressure ratio is 2.019, which is consistent with existing experience.

The low-pressure turbine has a pressure ratio of 3.438, giving an average stage pressure ratio of 1.28 for the five stages. This again is somewhat lower than existing experience, and is associated with the low work parameter.

d. Vane and Blade Exit Mach Numbers

Airfoil exit Mach numbers are determined by the stage pressure ratio, velocity ratio, and reaction. Because of the low stage loading for the QE-3 turbine, the airfoil exit Mach numbers are relatively low. Although the values for the high-

pressure turbine are somewhat lower than other Pratt & Whitney Aircraft high-pressure turbines, there is much experience at lower airfoil Mach numbers in existing low-pressure turbines.

e. Axial Mach Number

The selection of axial Mach number determines the length of the turbine airfoils. Short blade lengths and high axial Mach numbers can be expected to produce light turbines because of reduced airfoil weight, reduced centrifugal loads on the disks, lower blade stresses, and the resulting compact turbine envelope. However, when the airfoil lengths are reduced to the point where axial Mach numbers become excessively high or airfoil aspect ratios become too low, turbine efficiency is decreased. The exit axial Mach number selected for the QE-3 turbine is within current experience on existing turbines.

f. Hub-to-Tip Ratio

Hub-to-tip ratio is a significant design parameter for high-pressure turbines. When the hub-to-tip ratio becomes high, the ratio of blade tip clearance to blade height is large, resulting in excessive leakage. The hub-to-tip ratio of the first blade is 0.87. Although this is high, it is well within the limits of existing experience.

g. Solidity

The load coefficients for the QE-3 turbine were selected to be consistent with current Pratt & Whitney Aircraft practice. The resulting solidities are shown in Table VI.

TABLE VI
QE-3 TURBINE AIRFOIL AVERAGE SOLIDITIES

Stage	Vane Solidity	Blade Solidity
1	0.94	0.81
2	1.03	0.945
3	1.52	1.25
4	1.22	1.25
5	1.42	1.15
6	1.44	1.21
7	1.29	1.21

h. Aspect Ratio

For the QE-3 turbine, airfoils with short chords and high aspect ratios were selected to minimize weight and length. Table VII is a summary of blade and vane aspect ratios for all turbine stages.

TABLE VII
QE-3 TURBINE AIRFOIL ASPECT RATIOS

Stage	Vane Aspect Ratio	Blade Aspect Ratio
1	1.39	1.72
2	1.45	3.39
3	2.58	3.91
4	3.68	4.52
5	4.96	5.17
6	4.67	5.35
7	5.30	6.27

C. MECHANICAL DESIGN

The preliminary mechanical design of the QE-3 engine has concentrated on those areas which have been shown by previous experience to be the primary determinants of a sound engine design. Component analysis has been performed in close coordination with the mechanical design to contribute to the completion of this portion of Task III. This analysis has included rotor critical speeds, bearing and seal analyses, the secondary air system of thrust balance and cooling air, and the vibration characteristics of rotors and blades. All of these factors are discussed in this section, as well as structural arrangement, weights, and maintainability.

1. Structural Arrangement

a. Low-Speed Rotor

The low-speed rotor of the QE-3 consists of a single-stage overhung fan, a shaft and a five-stage low-pressure turbine. Mechanical design of the fan is discussed separately in Section VI of this volume.

The low-pressure turbine has been subjected to a more rigorous analysis than had been originally planned in order to fully evaluate the effect of low rotational speed. The maximum speed of the low-speed rotor is 3597 rpm (378 rad/sec), which makes it possible to use lightweight disks. The lightweight disks are to be assembled using short bolts, rather than long tie-bolts. All of the disks in the low-speed rotor will be made of PWA 1003 (Incoloy) material and will have a 30-percent burst margin. This design gives an allowable average tangential stress of 63,900 psi, (44,100 N/cm^2). A weight reduction of 30 pounds (13.6 kilograms) was achieved by the use of a drum-like construction without inheriting the associated problems of cantilevered vanes, efficiency loss, tangential slots, and split stators. The critical speed of the system was analyzed at two conditions. The stiff-bearing analysis assemed bearing supports with spring rates of 1.0×10^9 lb/in (1.75×10^9 N/cm), while the soft-bearing analysis used spring rates of 2.0×10^6 lb/in (3.51×10^6 N/cm), which more closely simulate actual engine hardware.

The stiff-bearing critical speed of the low-speed rotor occurred at 4678 rpm (491 rad/sec), which represents a margin of approximately 28 percent over the maximum speed of 3615 rpm (380 rad/sec). The soft-bearing critical speed occurred at 3929 rpm (413 rad/sec), providing a margin of 5 percent above the maximum rotor speed. Figures 40 and 41 illustrate the rotor mode shapes as they occur at the first frequency for both stiff and soft bearing supports. Maximum shaft deflections under flight maneuver conditions are minimized so as to provide adequate running clearances on the order of 0.200 inch (0.508 cm).

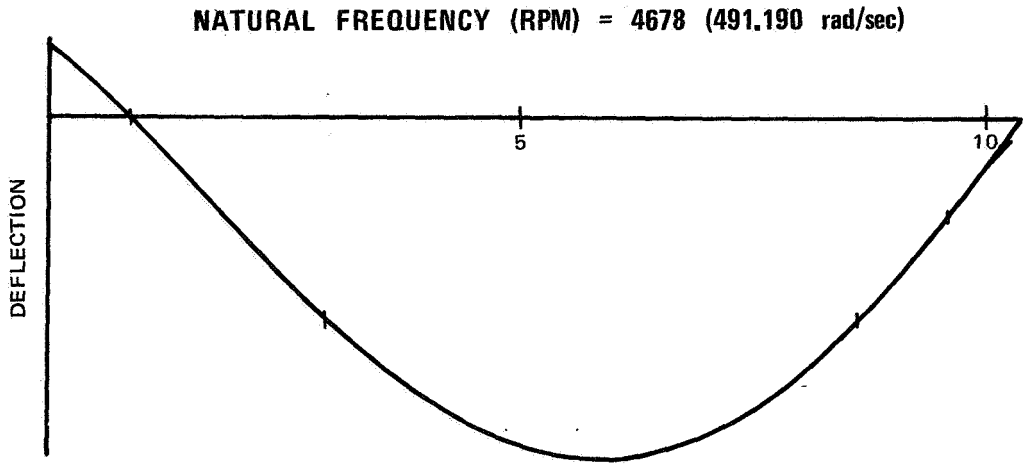

Figure 40 First Critical Mode of the Low-Speed Rotor as Determined by a Stiff-Bearing Analysis

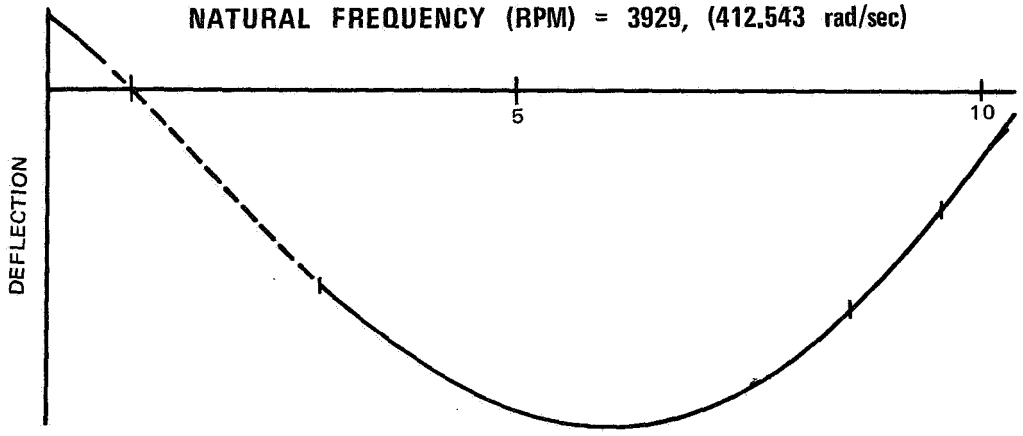

Figure 41 First Critical Mode of the Low-Speed Rotor as Determined by a Soft-Bearing Analysis

b. High-Speed Rotor

The high-speed rotor consists of the high-pressure compressor, the related shafting, and the high-pressure turbine. Like the low-pressure turbine, it is assembled with short bolts rather thanwith long tie bolts. The first two stages of the high-pressure compressor are cantilevered in this design: the number 2 bearing supports the rotor at the third compressor stage. The inlet guide vane and the first four stators of the high-pressure compressor are variable to prevent stall. Air for various engine and airframe functions is extracted at appropriate locations along the outer cases of the compressor.

The two-stage high-pressure turbine was designed for a maximum speed of 9678 rpm (1010 rad/sec) and a burst margin of 30 percent. The disks will be made of PWA 1007, (Waspaloy). The burst margin of 30 percent gives an allowable average tangential stress of 71,000 psi (48,990 N/cm^2). The rotor rim speed is 1023 ft/sec (312 m/sec) at the design point. The turbine inlet guide vanes, first-stage blades, and first-stage vanes are air cooled. The turbine inlet temperature is 1770°F (1240°K) at the aerodynamic design point and 2140°F (1440°K) at sea-level take-off on a hot day. The high-speed rotor system (which consists of the high-pressure compressor and the high-pressure turbine) demonstrated a stiff-bearing critical speed of 14,900 rpm (1560 rad/sec) for a margin of 58 percent over the maximum rotor speed of 9455 rpm (993 rad/sec). Figure 42 shows the rotor mode shape of the stiff-bearing support system at the first critical speed.

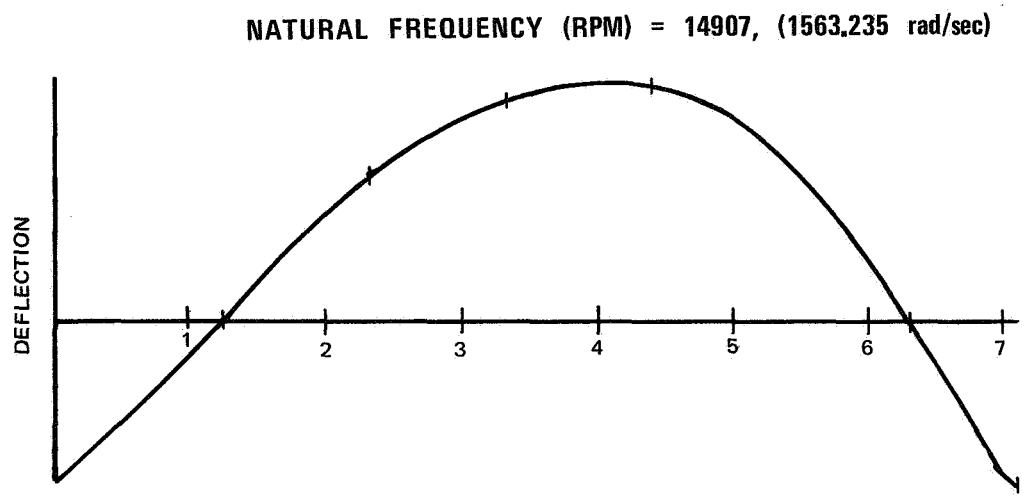

Figure 42 First Critical Bending Mode of the High-Speed Rotor as Determined by a Stiff-Bearing Analysis

In the soft bearing critical-speed analysis, the first critical speed encountered is a rigid-body mode which occurs at 7234 rpm (760 rad/sec), approximately 24 percent below the maximum rotor speed. This mode is shown in Figure 43. The next critical speed produces a shaft bending mode, as illustrated in Figure 44. This mode occurs at 12,227 rpm (1280 rad/sec), and represents a value approximately 29 percent greater than the maximum rotor speed.

As designed, the high-speed rotor system is required to run through the rigid-body mode to a level below the shaft-bending mode. This condition presents no problem, as it is a common practice in engine operation. The critical speeds

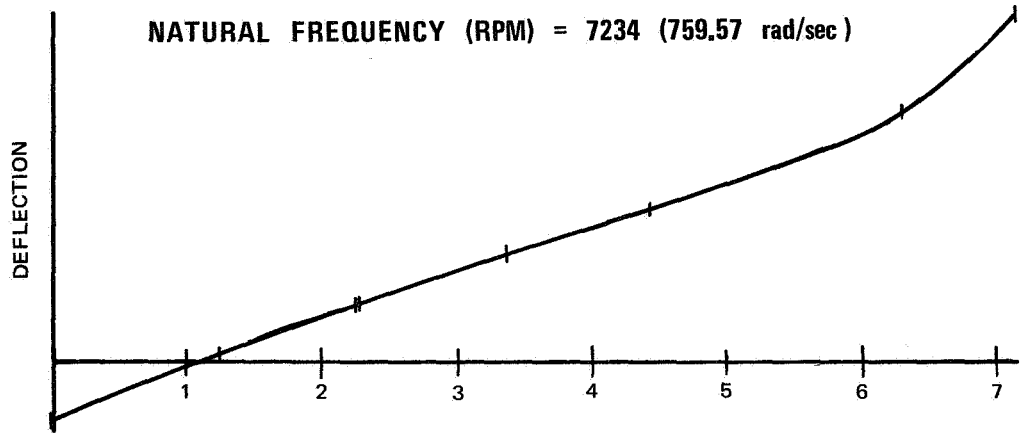

Figure 43 Rigid-Bode Mode of the High-Speed Rotor as Determined by a Soft-Bearing Analysis

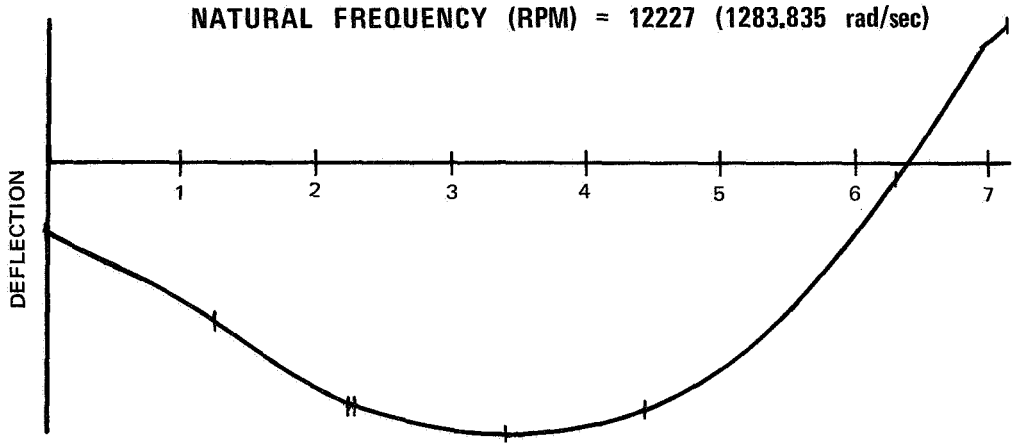

Figure 44 Second Critical Bending Mode of the High-Speed Rotor as Determined by a Soft-Bearing Analysis

and margins represent values consistent with present-day technology. Shaft diameters were sized to meet critical speed requirements and to provide adequate torsional shear capability.

c. Support Structure

The front bearing support structure, the intermediate case is a main structural segment of the engine. This case, which is constructed of titanium alloy, takes all the thrust-bearing loads of the two rotors.

Many engine services are transmitted through the intermediate case struts, including the combined power take-off for engine and airframe accessories and the starter gear train. A right-angle bevel gear set meshing at the forward end of the high-pressure compressor makes up the power take-off. The accessory gearbox location is internal rather than external, allowing for a smaller engine envelope. Structural struts extending across the fan duct carry the engine loads to a mount ring on the fan duct exterior. The location of the mount point and accessory gearbox envelope are discussed in the Appendix.

The rear engine mount is located on the rear case, which also supports the Number 4 bearing and the inner exhaust cone. The rear case is a low-risk item because of its simple design and the fact that the inner exhaust cone keeps the hot exhaust gases from coming in contact with it. Oil lines for the Number 4 bearing are fed through the rear case, keeping them from the high-temperature environment of the turbine as much as possible.

d. Diffuser Section

The diffuser section of the engine accomplishes many aerodynamic and mechanical functions in as simple a manner as possible. Aerodynamically, it serves to straighten the direction of airflow and to reduce the velocity of the high-pressure compressor's discharge air to a velocity suited for the combustion process. It also divides the air into three separate channels: one to cool the inner burner liner, one to cool the outer liner, and one which goes directly into the front of the combustion chamber. Aircraft bleed air is bled from the diffuser section at two points. Both points are high-pressure air, but one is primary or "clean" air, while the other is secondary air.

Mechanically, the diffuser case has many functions to perform. First, it is a main structural outer engine case which must be capable of withstanding engine thrust and maneuver loadings. Second, it supports and supplies service lines to the Number 3 bearing compartment. Third, it provides support for the front end of the combustion chamber. Fourth, it supports the fuel nozzles.

Inconel 718 is the material used for the diffuser case. It was selected for its high-temperature properties. Inner wall buckling is limited due to pressure and blade-loss criteria. The outer case maximum yield is limited because of pressure, thrust loading, and maneuver loading.

An annular burner was used in the combustion section of the QE-3 because of its low weight, high efficiency, and small size. At the front of the combustion chamber are located 20 fuel nozzles. Bolted to pads on the diffuser case, they can be replaced individually without having to unbolt any main engine case flange. Borescope bosses are provided in the diffuser case for inspection of the nozzles. To allow the nozzles to be replaced easily, the combustion chamber case can be telescoped forward over the diffuser case.

The outer combustion chamber liner, having high pressure on its outside, is buckling limited. Therefore, Z-shaped circumferential stiffeners are welded to the liner. The inner liner is yield limited because its high-pressure region is on the inside. The liners and the diffusing section of the combustion chamber are made of Hastelloy X nickel alloy. The excellent oxidation resistance of this material at temperatures up to 2000°F (1370°K) has made it a highly satisfactory material for combustion chamber components in many engines.

The mixture of fuel and air is ignited by two four-joule igniter plugs located 9 degrees (0.157 radian) above the horizontal centerline. Their locations was determined by the need for accessability for maintenance.

2. Internal Cooling System

In many regions of the QE-3 engine, cooling must be provided to prevent metal temperatures and thermal gradients from exceeding acceptable levels. The cooling system for this engine is similar to previously tested designs. Internal cavity-pressure and temperature measurements from similar arrangements have substantiated the design and prediction methods employed. The QE-3 system was designed to provide:

- Minimum cooling requirements to minimize cycle performance losses
- Reliability with minimum adverse effect in case of seal clearance variations
- System pressures that are compatible with rotor thrust load requirements.

A steady-state-temperature map of the engine for the three design conditions is provided in Figure 45a through h. The routing of the cooling airflow is shown in Figure 46 along with the flow rates and pressures for the maximum short-time operating condition. The pressures and airflow rates shown are representative of all high-power operation at near the design pressure-ratio. The sources for the various cooling airflows are the high-pressure compressor inlet, the sixth-stage compressor, the seventh-stage compressor, the high-pressure compressor discharge, and the burner secondary. The following table lists the quantities of air extracted from these sources for cooling:

High-Pressure Compressor Inlet	0.17% Wae
Sixth-Stage Compressor	0.12
Seventh-Stage Compressor	0.60
High-Pressure Compressor Discharge	3.66
Burner Secondary	3.30
Total Cycle Bleed	7.85% Wae

Of this total, 0.02 percent is used primarily for carbon-seal pressurization, 0.50 percent for the thermally controlled turbine-blade-tip seals, and 4.50 percent for cooling turbine vanes and blades. The balance of 2.83 percent is used primarily for cooling structural components.

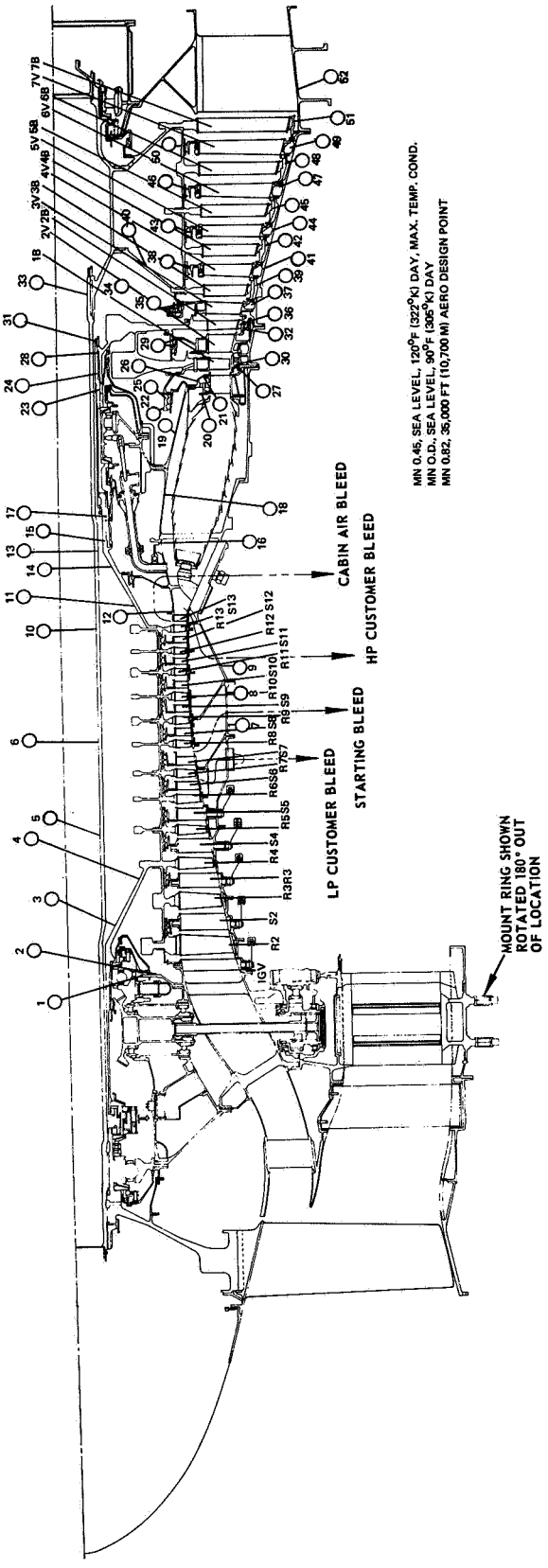

Figure 45 Steady-State Temperature Map of the QE-3

GAS-PATH AND LINER TEMPERATURES

Mn 0.45, Sea Level, 120°F (322°K), Max. Temp. Cond.

Location	Temperature		Location	Temperature	
	°F	°K		°F	°K
1	263	402	27	1118	876
2	269	405	28	838	721
3	446	503	29	1100	866
4	451	506	30	1660	1177
5	508	538	31	878	744
6	711	651	32	1158	897
7	548	560	33	817	709
8	739	666	34	901	756
9	961	789	35	981	798
10	792	696	36	1330	995
11	1029	826	37	1178	907
12	1028	825	38	1256	955
13	817	709	39	1343	1000
14	991	806	40	901	756
15	916	764	41	1088	859
16	1010	816	42	1250	952
17	1003	810	43	1136	886
18	1022	823	44	1007	814
19	1067	849	45	1154	897
20	1043	835	46	1100	866
21	1558	1130	47	924	769
22	1048	833	48	1117	875
23	918	765	49	966	791
24	996	808	50	1008	815
25	1087	858	51	1061	844
26	1238	943	52	870	739

Figure 45 (a)

GAS-PATH AND LINER TEMPERATURES

Mn 0.0, Sea Level, 90°F (305°K) Day

Location	Temperature		Location	Temperature	
	°F	°K		°F	°K
1	202	368	27	1066	770
2	201	368	28	-	-
3	388	471	29	1044	834
4	399	478	30	1636	1161
5	457	510	31	-	-
6	626	604	32	1121	879
7	484	524	33	-	-
8	669	627	34	844	722
9	911	761	35	851	728
10	735	664	36	1316	988
11	974	796	37	1029	828
12	990	805	38	-	-
13	-	-	39	1333	996
14	943	780	40	844	722
15	864	736	41	1067	849
16	958	786	42	1226	936
17	950	784	43	-	-
18	975	796	44	982	802
19	1030	827	45	1132	884
20	1346	1005	46	-	-
21	1526	1103	47	897	755
22	985	803	48	1082	858
23	-	-	49	938	775
24	-	-	50	-	-
25	1031	829	51	1035	830
26	1194	918	52	815	708

Figure 45 (b)

GAS-PATH AND LINER TEMPERATURES

Mn 0.82, 35,000 Ft (16,700 M), Aero Design Point

Location	Temperature °F	Temperature °K	Location	Temperature °F	Temperature °K
1	68	294	27	837	721
2	64	292	28	-	-
3	231	384	29	806	704
4	249	394	30	1331	995
5	297	421	31	-	-
6	446	503	32	880	745
7	332	439	33	-	-
8	492	528	34	640	611
9	712	650	35	707	648
10	547	561	36	1047	836
11	750	672	37	932	773
12	760	678	38	1045	836
13	-	-	39	1090	861
14	724	658	40	640	611
15	662	622	41	835	719
16	749	672	42	993	807
17	737	665	43	888	747
18	772	685	44	759	615
19	825	714	45	904	757
20	1080	855	46	815	707
21	1239	944	47	678	633
22	760	855	48	951	783
23	1239	944	49	813	707
24	-	-	50	720	657
25	797	698	51	811	612
26	947	781	52	706	595

Figure 45 (c)

COMPRESSOR GAS-PATH AND DISK TEMPERATURES

Mn 0.45, Sea Level, 120°F (322°K), Max. Temp. Cond.

	R1		IGV		R2	
	°F	°K	°F	°K	°F	°K
Root	174	352	215	474	230	384
Mean	171	350	199	366	221	378
Tip	183	357	201	367	230	384
Rotor L.R.	-	-	-	-	260	399
Bore	-	-	-	-	226	380
Average	-	-	-	-	249	390

	R4		S4		R6	
	°F	°K	°F	°K	°F	°K
Root	379	466	419	488	533	552
Mean	332	437	364	457	457	509
Tip	357	454	393	474	496	531
Rotor L.R.	415	486	-	-	576	576
Bore	405	481	-	-	582	579
Average	420	489	-	-	580	578

	S6		R7		S7	
	°F	°K	°F	°K	°F	°K
Root	580	578	622	601	661	623
Mean	489	527	530	549	552	562
Tip	532	550	569	572	606	593
Rotor L.R.	-	-	646	614	-	-
Bore	-	-	674	641	-	-
Average	-	-	674	641	-	-

Figure 45 (d)

COMPRESSOR GAS-PATH AND DISK TEMPERATURES

Mn 0.45, Sea Level, 120°F (322°K), Max. Temp. Cond. (Cont.)

	R9		S9		R11	
	°F	°K	°F	°K	°F	°K
Root	783	691	819	710	931	773
Mean	646	614	674	629	762	679
Tip	716	654	751	672	859	732
Rotor L.R.	813	708	-	-	963	791
Bore	797	699	-	-	851	729
Average	803	703	-	-	876	741
	S11		R13		S13	
	°F	°K	°F	°K	°F	°K
Root	973	797	1059	844	1100	866
Mean	787	692	865	736	887	748
Tip	893	752	991	806	1025	825
Rotor L.R.	-	-	1091	861	-	-
Bore	-	-	901	756	-	-
Average	-	-	956	785	-	-

Figure 45 (d cont'd)

COMPRESSOR GAS-PATH AND DISK TEMPERATURES

Aero Design Point

	R1		IGV		R2	
	°F	°K	°F	°K	°F	°K
Root	18	266	57	286	70	294
Mean	15	264	43	279	62	289
Tip	27	271	45	280	70	294
Rotor L.R.	--	--	--	--	96	308
Bore	--	--	--	--	65	291
Average	--	--	--	--	87	303

	R4		S4		R6	
	°F	°K	°F	°K	°F	°K
Root	200	367	234	386	333	440
Mean	159	344	186	358	267	403
Tip	180	355	212	373	301	423
Rotor L.R.	230	384	--	--	370	461
Bore	215	375	--	--	365	458
Average	230	384	--	--	368	459

	S6		R7		S7	
	°F	°K	°F	°K	°F	°K
Root	374	463	441	501	444	502
Mean	295	419	323	435	350	450
Tip	333	440	365	458	397	476
Rotor L.R.	--	--	431	495	--	--
Bore	--	--	441	501	--	--
Average	--	--	441	501	--	--

Figure 45 (e

COMPRESSOR GAS-PATH AND DISK TEMPERATURES

Aero Design Point (Cont.)

	R9		S9		R11	
	°F	°K	°F	°K	°F	°K
Root	550	561	582	579	678	643
Mean	431	495	455	506	532	550
Tip	492	523	522	545	625	603
Rotor L.R.	577	575	--	--	706	647
Bore	556	564	--	--	600	589
Average	564	569	--	--	624	609

	S11		R13		S13	
	°F	°K	°F	°K	°F	°K
Root	707	648	790	694	825	714
Mean	553	564	620	600	640	611
Tip	645	614	731	663	760	677
Rotor L.R.	--	--	818	709	--	--
Bore	--	--	654	619	--	--
Average	--	--	710	650	--	--

Figure 45 (e' cont'd)

Figure 45 (f)

TURBINE GAS-PATH AND DISK TEMPERATURES

Mn 0.45, Sea Level, 120°F (322°K)

Stage		Vane			Blade			Disk		
		Root	Mean	Tip	Root	Mean	Tip	Rim	Bore	Average
1	°F	COOLED VANE			COOLED BLADE			1226	1060	1086
	°K							939	844	859
2	°F	COOLED VANE			1354	1459	1409	1281	975	1048
	°K				1009	1063	1038	967	796	838
3	°F	1272	1367	1307	1392	1397	1347	1340	911	1168
	°K	965	1013	985	1029	1031	1003	1000	762	904
4	°F	1192	1277	1237	1202	1299	1252	1392	1196	1279
	°K	920	966	944	924	976	951	1029	919	965
5	°F	1112	1189	1152	1112	1205	1162	1140	916	1025
	°K	874	914	895	872	925	900	889	763	826
6	°F	1033	1102	1172	1022	1112	1070	1030	1045	1038
	°K	829	868	907	823	872	849	827	836	833
7	°F	954	1017	992	934	1017	977	1032	911	972
	°K	784	820	809	774	820	798	828	760	795

TURBINE GAS-PATH AND DISK TEMPERATURES

Sea Level Take Off, 90°F (305°K)

Stage		Vane			Blade			Disk		
		Root	Mean	Tip	Root	Mean	Tip	Rim	Bore	Average
1	°F	COOLED VANE			COOLED BLADE			1177	1010	1036
	°K							909	817	831
2	°F	COOLED VANE			1343	1448	1398	1262	922	1000
	°K				1002	1060	1032	957	768	811
3	°F	1264	1361	1301	1281	1386	1336	1320	854	1087
	°K	958	1011	979	968	1028	999	990	730	859
4	°F	1181	1271	1231	1191	1291	1241	1360	--	--
	°K	912	962	939	917	974	945	1011	--	--
5	°F	1098	1181	1141	1101	1196	1146	1130	--	--
	°K	866	912	888	867	920	892	883	--	--
6	°F	1013	1094	1161	1006	1051	1096	1020	--	--
	°K	818	814	902	815	846	864	822	--	--
7	°F	931	1006	979	916	1004	959	1023	854	939
	°K	771	815	800	765	812	787	824	729	776

Figure 45 (g)

Figure 45 (h)

TURBINE GAS-PATH AND DISK TEMPERATURES

Aero Design Point

Stage		Vane			Blade			Disk		
		Root	Mean	Tip	Root	Mean	Tip	Rim	Bore	Average
1	°F	COOLED VANE			COOLED BLADE			919	721	751
	°K							766	656	672
2	°F	COOLED VANE			1120	1229	1167	983	703	771
	°K				878	938	904	802	646	681
3	°F	1068	1168	1104	1140	1122	1082	1119	640	895
	°K	849	904	867	891	880	856	877	611	753
4	°F	979	1073	1021	951	1043	999	1145	967	1056
	°K	798	856	824	784	846	810	892	791	844
5	°F	893	983	939	866	962	916	927	655	791
	°K	752	803	777	736	790	764	769	620	694
6	°F	807	889	852	779	863	832	837	768	803
	°K	704	749	729	688	735	718	720	682	702
7	°F	722	800	765	690	785	744	732	650	691
	°K	601	701	680	639	692	669	662	617	640

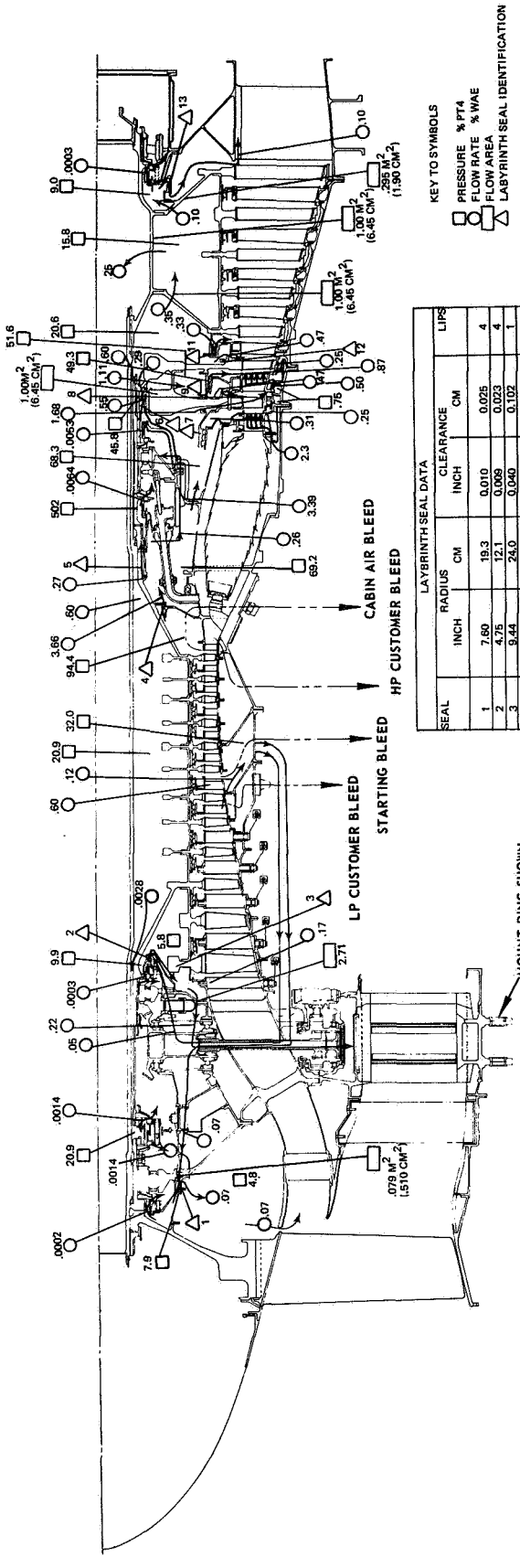

SEAL	RADIUS INCH	RADIUS CM	CLEARANCE INCH	CLEARANCE CM	LIPS
1	7.60	19.3	0.010	0.025	4
2	4.75	12.1	0.009	0.023	4
3	9.44	24.0	0.040	0.102	1
4	5.67	14.4	0.084	0.213	2
5	4.75	12.0	0.010	0.025	4
6	4.75	12.0	0.010	0.025	4
7	10.00	25.4	0.009	0.023	4
8	11.92	30.3	0.176	0.045	1
9	11.44	29.0	0.019	0.048	4
10	12.44	31.6	0.130	0.330	1
11	10.80	27.4	0.033	0.084	2
12	11.40	29.0	0.030	0.076	2
13	6.95	17.7	0.011	0.028	2

Figure 46 Cooling Airflow in the QE-3

a. Cooling Requirements

The fan, compressor, diffuser, and turbine-exhaust cases do not require cooling as their environmental temperatures are well below material limitations. The inner and the outer burner cases receive radiation from the hot burner-liners and are convectively cooled by the compressor discharge air which surrounds the liners and scrubs the cases. The burner outer case radiates some heat to the engine accessory compartment and, therefore, operates at a slightly lower temperature than the inner case. The inner and outer burner liners are film cooled with compressor discharge air injected along the liner wall through cooling louvers. The forward portion of the turbine case is convectively cooled by the burner secondary air which is supplied to cool the first-stage and second-stage turbine rubstrips and the second-stage turbine vanes. The rear portion of the turbine case is uncooled except for the heat radiated to the engine accessory compartment.

The first-stage and second-stage turbine nozzle vanes are cooled with burner secondary air. No cooling provisions are needed for the remaining nozzle stages because the main engine gas-path temperatures are below the temperature limits of the materials.

Since environmental temperatures in the fan region are relatively low, the fan rotor is designed to withstand the local gas-path temperatures without cooling. Circulation of sixth-stage bleed air, used to pressurize the carbon seals in the number one-two bearing compartment, increases the transient thermal response of the disk bores and minimizes heating in the cavity.

The disk rim and spacer portion of the high-pressure compressor rotor are designed to withstand the local relative adiabatic recovery temperature at the root section of the main gas-path. These recovery temperatures are eight to ten percent above the local average gas-stream temperatures due to the boundary layer effects. The bore and web regions of the rotor are cooled by air bleed from the seventh-stage. This air provides adequate bore transient thermal response to achieve long low-cyclic-fatigue life on the disk.

The rim, web, and bore regions of the first-stage of the high-pressure turbine disk and the front face of the second-stage disk are cooled by high-pressure compressor discharge air. The rear face of the second-stage turbine disk is cooled by a mixture of seventh-stage compressor bleed-air and high-pressure compressor discharge bleed-air supplied from the intershaft passage. This cooling system provides satisfactory steady-state and transient thermal gradients in the turbine disks. The first-stage turbine blades are also cooled by high-pressure compressor discharge air supplied by means of holes drilled through the disk rim. The second-stage turbine blades are uncooled.

The web and bore regions of the low-pressure turbine disk are cooled by a mixture of seventh-stage bleed air and high-pressure compressor discharge bleed air supplied through the intershaft passage. This air provides the necessary thermal transient response. The gas-path temperatures are low enough in this region that uncooled turbine blades are used.

b. Cooling System Flow Paths

Air is bled from the outside of the gas path after the sixth compressor-stage and used to pressurize the number-one and number-two bearing compartment seals for oil containment at low power conditions. This air also serves to vent the bore of the second-stage and third-stage disks. Venting is required to eliminate thermal heating of the disk bores resulting from the viscous shearing of the trapped air between the stationary and rotating structures. To prevent this air from flowing radially into the compressor gas-path and causing flow distortion, a small quantity of air is bled from the gas path in this region and vented to ambient along with the pressurization air.

Air is bled from just aft of the seventh-stage compressor stator and metered into the region of the high-pressure-compressor drum where it flows over the bores of the eighth-stage through thirteenth-stage rotor disks. This flow cools the bores of the disks and minimizes the radial thermal gradients in the disks during transient operation. A small portion of the seventh-stage bleed-air flows forward between the shafts and pressurizes the intershaft carbon-seals in the forward bearing compartment. The remaining air passes rearward between the high-pressure and low-pressure turbine shafts into the turbine section where it mixes with number-three bearing compartment carbon-seal pressurization air (high-pressure compressor discharge air). The air is then used to cool the low-pressure turbine disks and to pressurize the number-four carbon-seal.

Air is bled from the inside of the gas path at the high-pressure compressor discharge to cool the high-pressure turbine. This flow is throttled through a loose two-lip staggered lab-seal to approximately seventy percent of its original pressure and is used for turbine-blade cooling. A small amount of the high-pressure compressor discharge air leaks past the number-three bearing compartment front buffer seal and is vented through shunt pipes to mix with a small quantity of air that leaks through the rear buffer seal. This air is then vented through holes in the high-pressure turbine hub where it mixes with the seventh-stage bleed-air. The remainder of the cooling air from the high-pressure compressor flows through large holes in the number-three bearing support and serves primarily to cool the various high-pressure turbine components. A close clearance four-lip labyrinth-seal on the front face of the first-stage turbine disk maintains the cavity pressure required to supply cooling air for the first-stage

turbine blades. The leakage past this seal is utilized for cooling the front face of the first-stage turbine disk. The rear face of this disk and the front face of the second-stage disk are cooled by air metered through holes in the one-two turbine-spacer.

Burner secondary air from the outer burner section is used to cool the high-pressure turbine case, the first-stage and second-stage turbine vanes, and the thermally controlled blade-tip seals.

c. Cooling System Reliability

Deterioration of any of the primary thrust-balance and cooling-system seals will alter internal pressures and cooling flow rates. The effects of pressure variations on bearing thrust loads are discussed in the next section; the effects on cooling are discussed in the remainder of this section.

The high-pressure turbine front-seal is a close-clearance seal that is used to maintain pressure in the blade supply cavity. The small quantity of leakage through this seal is adequate to cool the front face of the first-stage turbine disk. Since this leakage is only a small part of the total flow through the blade supply cavity and since the cavity is directly coupled to the compressor discharge, variations in the clearance of this seal will not significantly affect the blade cooling air supply pressure.

The low-pressure turbine front-seal is a back-to-back labyrinth seal which provides positive cooling for the rear of the second-stage turbine disk rim during transient operation. This seal is designed to provide the required cooling airflow split between the rear of the second-stage disk and the front of the third-stage disk at full-power, steady-state operation. Any changes in the relative positions of the seal elements during transient operation will reduce the flow of cooling air to the front of the third-stage disk and force more cooling air to flow over the rear of the second-stage disk where the cooling problem is more acute.

The high-pressure compressor rear-seal is a relatively loose seal used to provide cooling air pressure for the structure of the high-pressure turbine. Small variations in this seal due to tolerances or normal engine-wear will only insignificantly change cooling flow.

d. Rotor Thrust Balance System

The rotor thrust loads, transmitted to the static structure through the thrust bearings, are the summation of the axial aerodynamic loads acting on the compressor and turbine components. These loads vary with altitude, flight speed,

power setting, and engine matching characteristics. Since the thrust loads have a strong influence on bearing performance, the rotors must be properly thrust balanced to obtain long bearing-life.

The axial gas-path loads which are due to the axial momentum and pressure forces acting on the compressor and turbine blades are a function of the aerodynamic design of these components and cannot readily be altered. Consequently, the internal compartments at either end of the compressor and turbine constitute the primary areas available for controlling the net axial loading on each rotor. Adjustment of the compartment pressures and seal diameters provides the means for obtaining a satisfactory thrust balance.

The QE-3 thrust balance system was designed to provide satisfactory bearing loads over the full operating envelope from sea-level-take-off to high altitude 35,000 ft (10,700 m) Mach 0.82 cruise power flight conditions. The system was designed to accommodate deviations in the nominal turbine-nozzle areas from two percent closed to five percent open to allow for normal production trim and deterioration. The thrust balance system was also designed to minimize seal leakage and to be totally compatible with the engine's cooling system requirements.

The thrust balance system which satisfies these design requirements is shown schematically in Figure 47. Engine compartment pressures are shown as percentages of compressor discharge pressure (P_{T4}) and are representative for all high-power operating conditions.

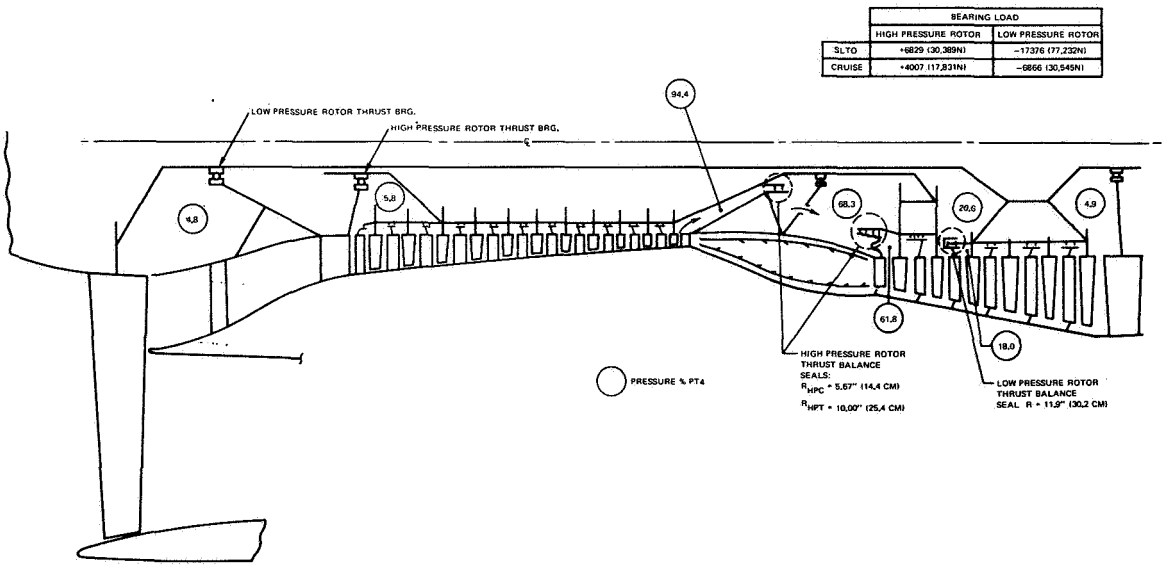

Figure 47 Thrust-Balancing Scheme for the QE-3

The high-pressure rotor system was balanced to provide a forward thrust load at all operating conditions. The thrust balance is achieved by subjecting the front face of the high-pressure compressor and the rear face of the high-pressure turbine to local gas-path static pressures and adjusting the forces acting on the front face of the turbine disk and the rear face of the high-pressure compressor. The desired thrust-balance bias is provided by a close clearance, four-lip, front high-pressure turbine stepped labyrinth-seal which is positioned at a mean radius of 10.00 inches (25.4 cm) and a two-lip, wide-clearance, rear high-pressure compressor stepped labyrinth-seal which is positioned at a mean radius of 5.67 inches (14.4 cm).

This simple thrust balance system is possible because the turbine diameter is considerably larger than the compressor diameter (note the canted burner) which, unlike more conventional in-line engine designs, naturally balances these components. Consequently, there is no need to pressurize the cavity in front of the high-pressure compressor which would produce radial outflow to the gas-path with attendant losses in high-pressure compressor efficiency. Similarly, the interrotor cavity between the high-pressure and low-pressure turbines is also biased to the local gas-path pressure by using a single-lip, large-clearance seal at the rear of the second-stage turbine disk. This seal serves only to prevent the recirculation of hot gases into the inner turbine cavity. If pressurization was required in this cavity, it would be necessary to bleed the cooling air from a higher-pressure stage in the compressor which would raise the cooling air temperature and impose both structural and performance penalties. Conversely, lower pressures would produce radial inflow of hot turbine-gases into the inner cavity which would be totally unacceptable.

The rear-compressor and front-turbine cavities are interconnected by a large open area through the number-three bearing support, and are biased through a loose two-lip labyrinth-seal to the gas-path static pressure behind the fifteenth-stage compressor blade. High-pressure (about 70% P_{T4}) is thus provided to satisfy the cooling requirements for the first-stage turbine blades. The customer airflow requirements are satisfied by bleed holes in the diffuser struts. The large diameter, high-pressure-turbine front-seal option was exercised because the turbine disk area outboard of the seal, which is subjected to the local gas-path pressure at the exit of the first-stage turbine nozzles, is minimized. Since this pressure varies significantly with the nozzle area chosen for a particular engine match, the resulting change in net thrust loading is minimized.

The high-pressure rotor thrust loads imposed on the number-two bearing are shown in Figure 48 as a function of the effective flow area (A5) of the first-stage turbine nozzle for the maximum-load and long-time-cruise flight conditions. Note that the minimum load occurs at the 35,000 ft (10,700 m), Mach 0.82 cruise power condition with a five percent open A5-nozzle area (maximum 2% trim and

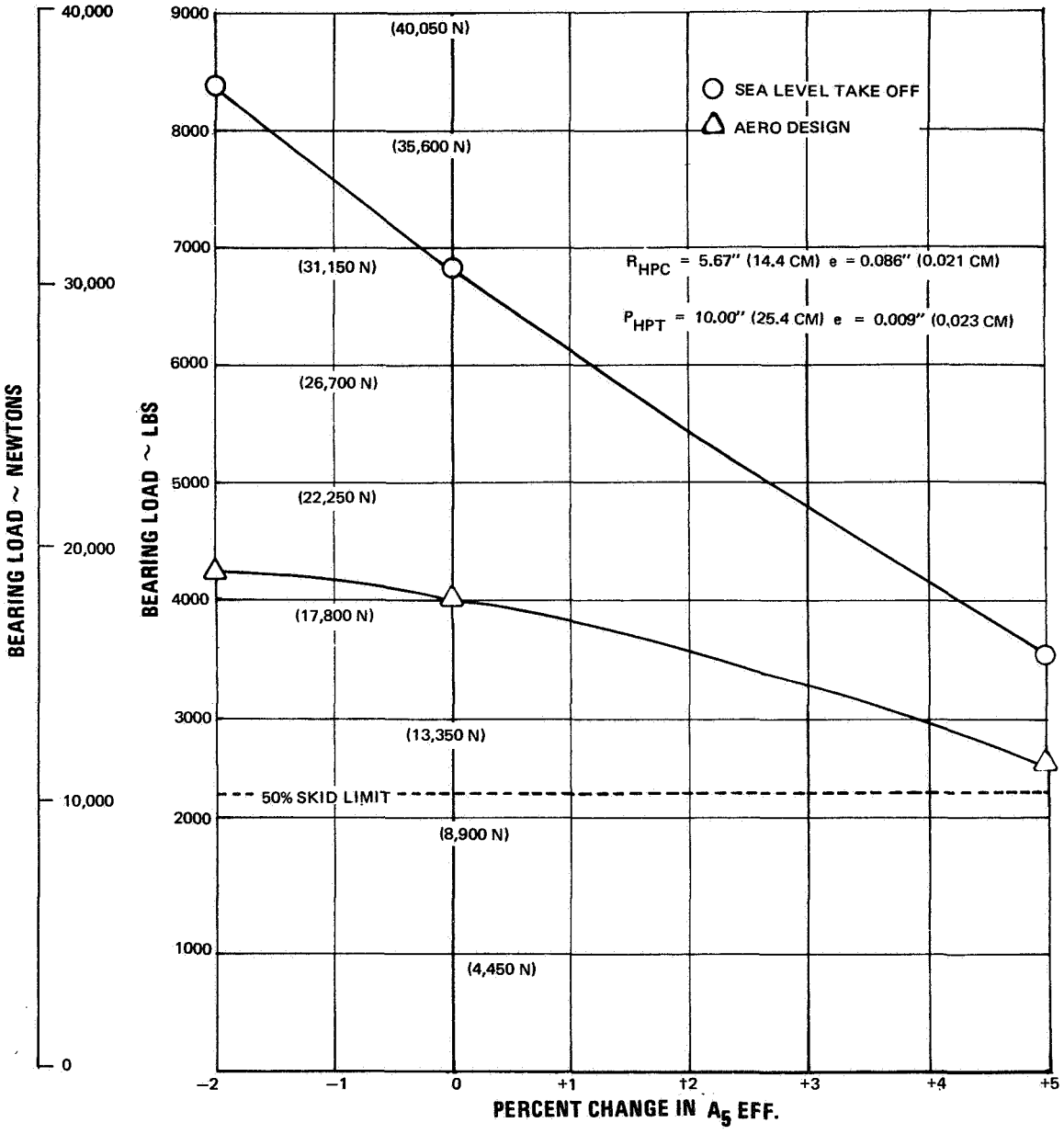

Figure 48 Thrust Loads on the QE-3 Number 2 Bearing

3% estimated deterioration). This point sets the required front turbine-seal radius of 10.00 inches (25.4 cm) and rear compressor seal radius of 5.67 inches (14.4 cm) to exceed the bearing 50 percent incipient skidding limit of 2150 lbs (9567 N). The bearing incipient skid is a theoretically determined value which is defined for a given speed as the minimum load required to keep the bearing from skidding. The fact that a bearing is not skidding implies that the rolling elements are rolling properly and that the bearing component speeds are predictable from geometric and dynamic considerations. Test determinations indicate that in actual practice, bearings in the QE-3 size range do not skid or slip and do not suffer skid damage until loads are substantially less than 50 percent of the theoretical load value, so the 50 percent incipient skidding limit was used in designing the bearings. The maximum anticipated flight-engine-load will occur at the sea-level-take-off condition with a two percent closed nozzle area.

The low-pressure rotor system was designed to have a rearward thrust load at all operating conditions. The thrust balance is obtained by subjecting the rear face of both the fan and low-pressure turbine to local gas-path static pressures and adjusting the forces acting on the front face of the first-stage disk of the low-pressure turbine. Since there is no static inlet case, there is no means of adjusting the pressure forces acting on the front face of the fan rotor. A close-clearance, four-lip, back-to-back, stepped labyrinth-seal which is positioned at a mean radius of 11.9 inch (30.2 cm) provides adequate thrust-balance bias.

For essentially the same reasons as described for the high-pressure rotor system, the low-pressure rotor tends to be normally balanced (zero net loading). Fortunately, positioning the single controlling seal on the front face of the first-stage disk of the low-pressure turbine at a large radius produces ample rearward thrust loading to be safely above the number-one bearing skid requirements while at the same time minimizes the bending stresses in the first-stage vane of the low-pressure turbine which carries the seal land.

A rearward thrust load is particularly advantageous on the low-pressure rotor to avoid thrust reversals following a throttle chop from cruise to flight idle power. When this occurs, the tailpipe pressure, which acts directly on the rear face of the low-pressure turbine, decays more rapidly than any other pressure in the engine and causes a sharp increase in rearward loading. The magnitude of this change would be sufficient to reverse a forward directed thrust balance system. A second prolonged-period of skidding operation would also occur when the aircraft decelerates to low flight-speed and ram pressure is reduced significantly to allow the rotor to shift back toward the forward loaded direction.

The low-pressure rotor thrust loads imposed on the number-one bearing are shown in Figure 49 as a function of the turbine nozzle effective flow area (A5) for maximum load and long-time-cruise flight conditions. Note that the minimum load of 6492 lbs (28,889 N) occurs at the 35,000 ft (10,700 m), Mach 0.82, cruise condition and is considerably higher than the predicted 100 percent incipient skid limit of 1000 lbs (4450 N). Since the corresponding maximum load of 17,376 lbs (77,232 N) occurring at the sea-level-take-off condition is moderate and the bearing life exceeds design requirements, the seal was retained at 11.90 inch (30.2 cm) radius to favor reduced bending stresses on the first-stage vane of the low-pressure turbine.

3. Bearings and Seals

When shaft sizes and speeds had been established, the bearing and seal types were selected and the feasibility of the designs was established. The bearing and seal designs chosen for the QE-3 represent current commercial practice: the DN values are within accepted criteria, and the seal conditions of rubbing speed, air pressure drop, and air temperature are within standard design ranges. The design standards used in the QE-3 bearings were derived from the criteria listed below:

- Ball thrust bearings have split inner races.
- Cooling oil for the mainshaft bearings flows under the races.
- Lubricating oil for ball thrust bearings comes through radial slots in the inner race.
- Roller bearings are mist lubricated.
- Mainshaft bearing cages will be made of fully machined AMS 6414 steel.
- The minimum bearing B-10 life* is 10,000 hours.
- In setting the thrust balance range, the mean effective thrust was assumed to be equal to 0.55 times the maximum allowable thrust.
- The Number 1 bearing static capacity was required to be at least one fifth of the radial imbalance caused by the loss of 10 percent of the fan blades.

*The B-10 life of a bearing is that time period which 90 percent of the bearings will survive at a given load and speed before the first evidence of fatigue.

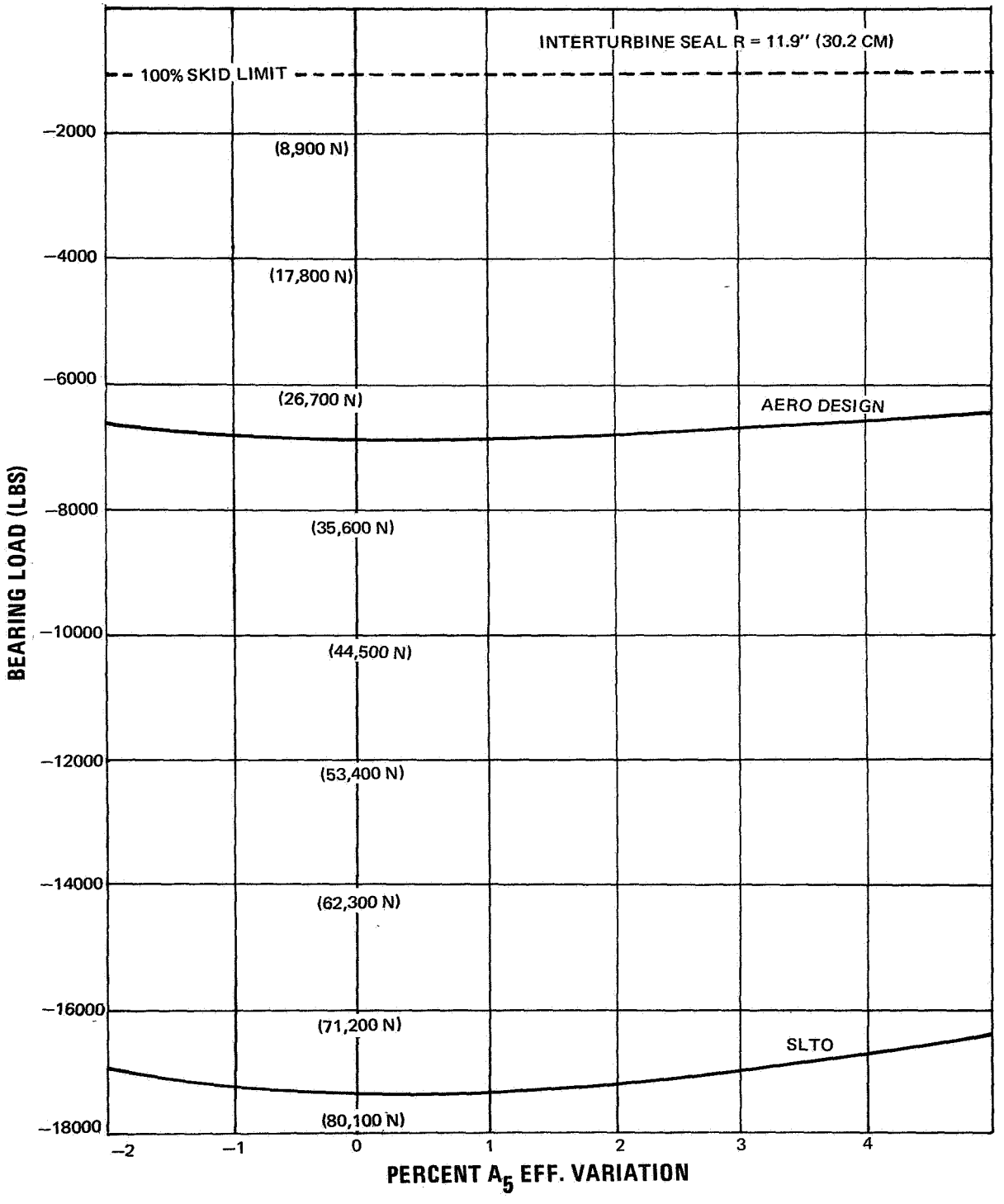

Figure 49 Thrust Loads on the QE-3 Number 1 Bearing

- The minimum thrust load on the bearings will be at least equal to the skid damage load, which has been empirically determined to be greater than 50 percent of the incipient skid load.

- Mainshaft bearing raceways and balls will be made of M50 material. This implies a multiplying factor of 10 for ball bearings and 5 for roller bearings in the calculation of B-10 life (the base-line calculation assumes 52100 material properties).

- Maximum DN value for ball thrust bearings is 1.7×10^6 mm-rpm (1.77×10^5 mm-rad/sec).

- Maximum DN value for roller bearings is 1.82×10^6 mm-rpm (1.91×10^5 mm-rad/sec).

- Seal rubbing speeds and sealing pressures will be within commercial engine limits.

The QE-3 bearings and seals meet these standards. The specific designs are discussed below.

a. Bearings

The size and speed of the shafts in the engine are the primary factors which must be taken into consideration in the design of the bearings. In addition, the Number 1 bearing must also be able to withstand the unbalanced load imposed by the loss of 10 percent of the fan blades, a load of 138,000 pounds (615,000 newtons). The bearing requirements imposed by the shafting are tabulated below:

Bearing No.	Bearing Type	Bore (mm)	Maximum Inner Race Speed (rpm)	Maximum Inner Race Speed (rad/sec)	DN (mm-rpm)	DN (mm-rad/sec)
1	Ball(Thrust)	165	3615	439	0.60×10^6	0.628×10^5
2	Ball(Thrust)	180	9455	989	1.70×10^6	1.78×10^5
3	Roller	190	9455	989	1.80×10^6	1.89×10^5
4	Roller	210	3615	439	0.74×10^6	0.775×10^5

Using the requirements shown above, the contractor used a five-step procedure to calculate the bearing design parameters. The five steps were: determination of the bearing's cross section by consideration of space limitations and the

criteria evolved from previous experience; optimization of the bearing's internal geometry; generation of life versus load curves, skid curves, and spring-rate curves; determination of the acceptable operating range; and justification of DN values and operating speeds. Table VIII describes the bearing designs arrived at for this phase of engine design, and Figures 50 and 51 show their predicted B-10 lives.

TABLE VIII
BEARING DESIGN

Bearing No.	Bearing No.	Bore (mm)	Outer Diameter (mm)	No. of Elements	Element Size (in)	Element Size (mm)	Allowable Thrust Range (lb)	Allowable Thrust Range (kN)
1	Ball	165	310	16	1.625	4.13	600–22,500	2.67–100
2	Ball	180	280	21	1.125	2.86	2150– 9,400	9.56–41.8
3	Roller	190	260	28	0.788 x 0.788	20 x 20	N/A	N/A
4	Roller	210	290	28	0.866 x 0.866	22 x 22	N/A	N/A

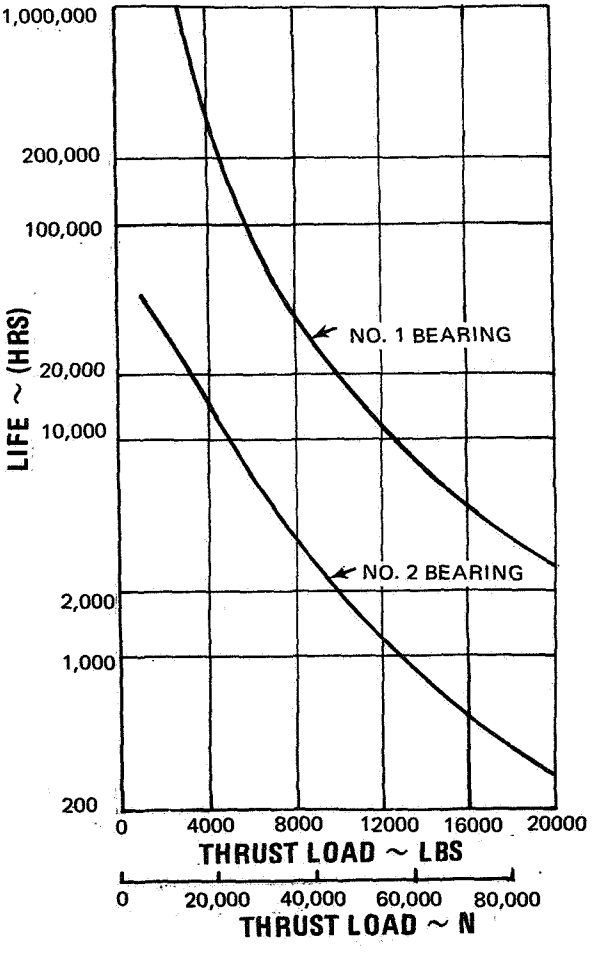

Figure 50 Estimated Lives of the QE-3 Thrust Bearings

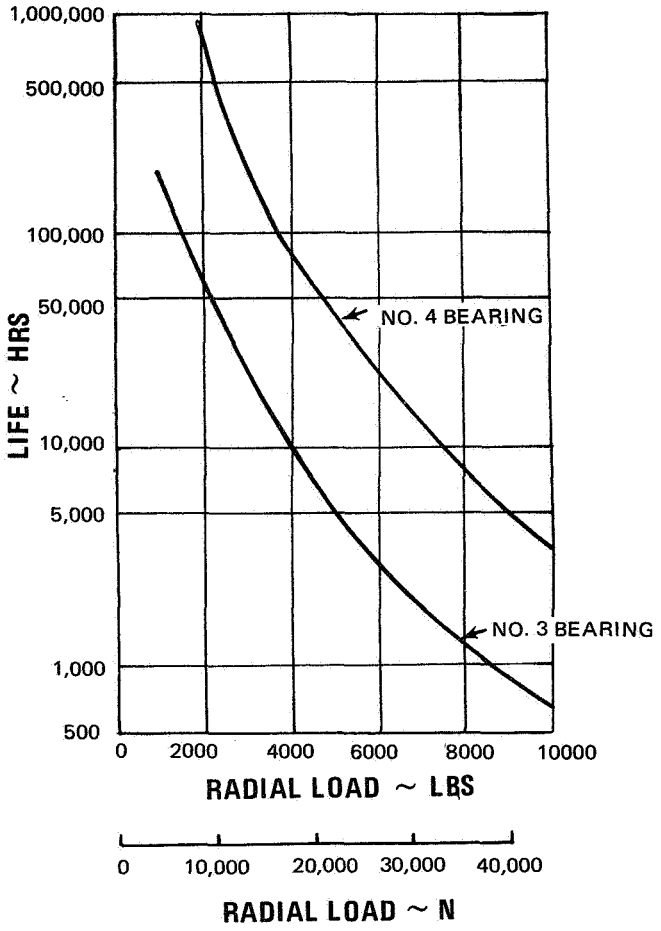

Figure 51 Estimated Lives of the QE-3 Roller Bearings

The DN values of the QE-3 bearings are within the limits which have been established by the current state of the art. Some of the internal speeds of the bearings are higher than those used in current commercial bearings, but these should not present significant problems.

- The absolute cage speed of the QE-3 Number 2 bearing is 10,100 ft/min (51.4 m/sec) and that of the Number 3 bearing is 9,950 ft/min (50.6 m/sec). The Number 3 cage speed is within previous experience, and the Number 2 cage speed exceeds previous experience by only 280 ft/min (1.24 m/sec). This slight excess is not of great consequence, since cage speed is a measure of cage stress, and Pratt & Whitney Aircraft cages have never been stress limited.

- The element speeds about their centers are measures of the relative velocity between the cage and the element. A slight excess over current commercial practice is present in both the Number 2 and 3 bearings but will not be difficult to account for if careful attention is paid to lubrication in this area.

- Although the relative velocity between the outer race and the cage is somewhat higher than current commercial practice in both the Number 2 and 3 bearings, this factor does not affect the bearing design, since both bearings have cages which ride on the inner lands.

- The cage speed relative to the inner race is 12,100 ft/min (61.5 m/sec) for the Number 2 bearing and 11,900 ft/min (60.4 m/sec) for the Number 3 bearing. While this is an important factor in the design of these bearings, its importance can be minimized by proper cage design and by careful design of the lubrication system, so that there is an oil film between the cage rail and the guiding lands. Rig testing has shown that with the proper introduction of oil into the area between the cage and the guiding land, bearings of the JT8D type can be routinely run with cage speeds relative to the inner race of 13,000 ft/min (66.2 m/sec). The cage speeds of both the Number 2 and 3 bearings are well within this range.

b. Seals

While a complete design of the mainshaft seals for the QE-3 was impossible during this phase of engine design, seal types and materials have been selected on the basis of known speeds and estimated air temperatures and pressure differentials. The remaining design parameters were not determined because the accuracy of the estimates of pressure drop did not warrant a refined analysis.

The seal selections are summarized in Table IX. Dry-face seals were chosen in locations where there was a low pressure drop and a relatively low rubbing velocity, while wet-face seals were chosen in locations where the rubbing velocity exceeded 380 ft/sec (116 m/sec).

While a ring seal would generally be more desirable for the Number 4 forward position because of the large differential growth, a dry-face seal was selected for this location because the seal diameter is excessive for a ring seal and because of mechanical assembly and disassembly problems. There should be no problem in designing a face seal to accommodate the differential growth in this area.

TABLE IX
SEAL DESIGN

Bearing No.	Seal Position Relative to Bearing	Rubbing Velocity (ft/sec)	Rubbing Velocity (m/sec)	Max. Est. Pressure Drop (psi)	Max. Est. Pressure Drop (N/cm^2)	Air Temp (F)	Air Temp (K)	Selected Seal Type
1	Forward	142	43.4	5.0	34.5	400	478	Dry Face
1	Rear	139	42.4	39.0	269	527	548	Dry Face
2	Forward	365	111	39.0	269	527	548	Wet Face
2	Rear	365	111	10.0	69	400	478	Wet Face
3	Forward	398	121	114.0	787	817	709	Wet Face
3	Rear	398	121	102.0	704	817	709	Wet Face
4	Forward	157	47.9	8.0	55.2	678	632	Dry Face

4. Maintainability

Maintainability has been a prime consideration in the design of recent engines. A concentrated effort was made during the design of the QE-3 to optimize maintainability by providing ready access to all sections of the engine. The design was reviewed by representatives of the Design Maintainability Group and features were incorporated in the design which would decrease the frequency of required maintenance and the time to perform the necessary maintenance actions.

The design of the diffuser section and annular combustion chamber provides the required burner performance in a shorter length than would be required of a can-type burner. Therefore, the length of both the high and low-pressure rotor systems has been minimized. The need for an intershaft bearing has been eliminated, removing associated lubrication and assembly problems. The shorter rotor construction also reduces the number of bearing compartments and support structures required. The result is a short compact, engine which achieves the high performance requirements with a smaller number of parts.

Specific design features have been incorporated which improve the maintainability in the following areas:

- Modular Assembly and Disassembly
- Inspection Techniques
- Combustion Section Design
- Rotor and Static Structure
- Bearing Compartment Design
- On-The-Wing Maintenance Capability

a. Modular Assembly and Disassembly

The QE-3 is composed of nine major units which may be replaced as sub-assemblies at dock-level maintenance facilities without the need for rebalancing. Through coordination with the airframe manufacturer, many of these units could be replaced with the engine installed in the aircraft. These "on-the-wing" maintenance capabilities are described in detail in section f.

The QE-3 engine has been designed to permit complete teardown and rebuild by either horizontal or vertical procedures. This capability will greatly reduce the time required for engine build and teardown.

The engine design permits independent replacement of either front or aft-end units with minimum disturbance to other units. All units forward of the high-pressure compressor are replaceable without removal of any aft-end units.

Similarly, all units aft of the high compressor are replaceable without removal of any front end units.

b. Inspection Techniques

It is anticipated that the engine inlet will be inspected daily. Inspection of this area has been improved by the elimination of the inlet case structure. Any ingestion damage will be readily visible and damaged first-stage fan blades will be accessible. Fan blades can be replaced without removing the fan disk.

The capability for extensive inspection of the interior sections of the engine has been incorporated in the QE-3 engine design. Ports have been provided for borescope inspection of all engine rotors and the combustion section. The location of several of these ports will be coordinated with the airframe manufacturer.

If inspection reveals a condition which requires a closer examination, the outer combustion case may be telescoped forward. The first turbine nozzle vanes may then be removed in two segments and individually inspected. Stretch measurement of the first-stage turbine blades may be accomplished through the space vacated by the first turbine vanes. The development of a new borescope with improved depth of field and increased lighting has permitted photographs to be taken through the borescope to further document engine conditions. Typical photographs taken through a borescope on a Pratt & Whitney Aircraft development engine are shown in Figure 52.

Bosses have been provided in the engine oil scavenge system to permit the use of chip detectors or collectors as a maintenance tool. One port has been provided in the angle gearbox, where any chips from the common scavenge of the front bearings compartment would tend to congregate. Ports have been provided in the scavenge lines from each of the two turbine area bearing compartments and in the accessory gearbox. All of these provisions will accommodate the standard commercial magnetic plugs and are designed to permit their removal without oil leakage.

Two mechanical signals may be attached to the main oil strainer housing; one to indicate when the filter requires cleaning; the other to indicate that the filter has been by-passed and the bearing compartments require flushing. These pressure-actuated signals will be visible at scheduled cowl checks. In addition, fittings are provided to permit measurement of the pressure drop across the main filter.

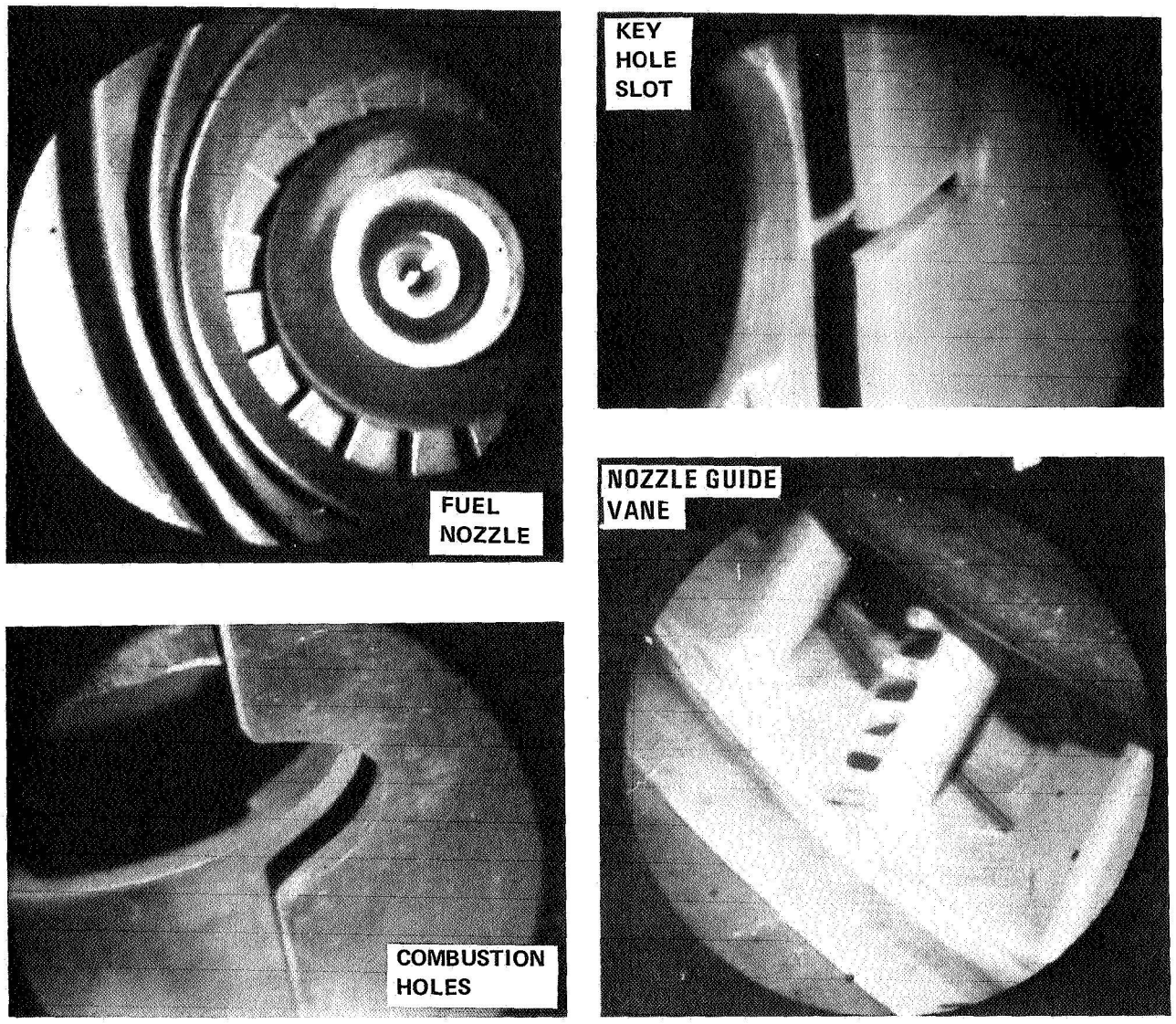

Figure 52 Borescope Pictures of Combustion Section (M-47388)

In addition to borescope inspection, the QE-3 engine design lends itself to radioisotopic inspection. The hollow low-speed shaft and a removable plate in the low-pressure turbine's rear hub permit positioning an isotope source in any axial plane in the engine. A film placed on the outside of the engine yields radiographs of the engine interior.

c. Combustion Section Design

Several features have been incorporated in the combustion section to reduce the frequency of maintenance and the manhours required to replace these critical parts. The use of an annular burner provides a more uniform temperature distribution throughout the combustion and turbine areas, reducing the possibility of distress due to thermal gradients. In addition, the need for crossover tubes and transition ducts, trouble areas associated with can-type burners, has been eliminated. These features will reduce the need for corrective maintenance in this area.

A sufficient number of borescope ports are provided in the combustion section to permit full inspection of the fuel nozzles by borescope. The fuel nozzles and the fuel manifold are mounted to the exterior of the diffuser case to permit replacement of individual fuel nozzles without removal of the fuel manifold or disturbance to the engine cases or combustion liners.

The combustion liners and first-stage turbine nozzle vanes and blades may be inspected with the engine installed in the aircraft. The use of modular construction permits replacement of the first-stage turbine disk and blade assembly with prior removal of only two basic units required.

The use of telescoping cases and split-ring structures in the first nozzle area permits removal of the vanes in two segments without removal of either turbine module. Subsequent replacement of individual vanes may then be easily accomplished.

The annular combustion liners have been designed to be replaceable without removal of the fuel nozzles or the attendant need for disconnecting joints in the fuel system, thus minimizing the check-out procedures required after liner replacement.

The final components of the combustion section, the spark igniters, are accessible from outside the engine. The continuity of the ignition system may be readily checked by disconnecting the electrical lead to one igniter and listening for the firing of the other as the system is energized. Faulty igniters are then individually replaceable without disassembly of engine cases.

d. Rotor and Static Structure

The engine design presents significant improvements in rotor balancing procedures. The rotors are balanced within their cases with the stator vanes in place. The resulting balanced compressor or turbine unit may be then assembled to the remainder of the engine without the need for rebalancing.

Moment-weight classified blades are used in the fan rotor. The blade retention in the fan rotor permits replacement of blades without removing the rotor. Fan and compressor blades are retained in their disks by shear devices or trapped flanges on the blade root.

Improved design of static structure in the QE-3 engine should reduce the frequency, expense and difficulty involved with repair of large cases. Integrally machined bosses, butt welding and large tapered flanges have been used to eliminate problems associated with fillet welds on other engines. Where feasible, parts subject to possible wear, such as knife edge seals and sliding surfaces, have been designed to be easily replaceable by means of riveted or bolted connections to the main structure.

e. Bearing Compartment Design

Due to the compact design of the engine only four mainshaft bearings are required; two on the low-pressure rotor and two on the high-pressure rotor. No intershaft bearing is required. The main rotor bearings and seals have been designed to be accessible with minimum engine disassembly. The low rotor thrust bearing and seal is accessible after the fan module has been removed. Separation of the intermediate case from the high compressor case then permits access to the high rotor thrust bearing and seal. The low rotor rear bearing and seal may be reached for inspection and replacement after removal of the bearing compartment rear cover. Access to the high rotor rear bearing compartment requires removal of both turbine units. The unit construction concept greatly facilitates these actions.

In addition to reducing the complexity of maintenance actions, attention was given during the design to reduce the frequency of bearing compartment maintenance. The mainshaft thrust bearings and accessory drive shaft bearings are located in the cool environment of the fan exit-intermediate case area. Because of the thermal environment in which the high rotor rear bearing compartment is located, cooling air is supplied around the entire compartment. Insulation blanketing and cooling air also isolate the turbine rear bearing compartment from its relatively high temperature environment. Under-race cooling of the mainshaft bearings and seal plates is used in all bearing compartments. Carbon face seals are used where feasible in preference to carbon seal rings. These features promote longer bearing and seal life and minimize the possibility of oil coking.

f. On-The-Wing Maintenance Capability

The ability to perform maintenance tasks with the engine installed in the aircraft was given prime consideration during design of the QE-3 engine. All of the scheduled inspections and many trouble-shooting inspections and unscheduled

parts replacement actions may be accomplished without removal of the engine from the aircraft. The extent to which this on-the-wing repair capability will be utilized will vary from one airline to another since it will depend upon the route structure and support concepts adopted. Provisions for mounting tracks or other ground support equipment to facilitate utilization of this maintenance concept should be incorporated in the airframe structure.

The design permits replacement of the fan, low rotor thrust bearing, and the fan case and stators, without disturbing either mount. Aft end units, such as the turbine exhaust case, low-pressure turbine, high-pressure turbine, and the annular combustion liner, may also be replaced on-the-wing after an alternate support for the aft end of the engine is installed.

5. Reliability

A major effort in the QE-3 program was directed at developing a highly reliable powerplant capable of operating without failure for long periods of time between repairs and overhauls.

a. Design Features

Relative to current turbofan and turbojet engines, the QE-3 configuration features a general reduction in over-all engine complexity. Important design features which give assurance of a greater engine reliability are as follows:

Instead of the sheet metal tablocks used in the past, fan and compressor blades are retained in their disks by either shear devices or trapped flanges on the blade root.

The interstage seals are designed such that excessive seal wear will not adversely affect rotor integrity.

Due to the compact design of the engine only two mainshaft bearings per rotor are required. The number of bearing support structures required has been reduced from four to three less complex structures. In addition, the QE-3 bearing configuration allows bearing support structures to be situated in relatively cool sections of the engine.

The use of single bearings is expected to eliminate the potential problem of skidding caused by unequal load distributions between duplex bearings at certain operating conditions. All four main bearings are oil cooled under the inner races. Thrust bearings are mounted on steel sleeves rather than directly on the torque carrying shafts to protect shaft integrity in the event of a bearing failure.

Thrust bearings have flanged outer races to eliminate outer race spinning. With this design the bearing outer race and outer race support is a single integral piece which is bolted into the bearing support structure to eliminate spinning.

The QE-3 diffuser case is a fusion butt welded structure. Weld joints between struts and diffuser walls have been located away from areas of high load or stress concentration. No thrust bearings are located in the diffuser area.

The overhung fan concept results in improved foreign object ingestion capability by eliminating the inlet guide vanes and consequently the possibility of trapping an object between the inlet guide vanes and the fan blades.

Maximum turbine metal temperatures are comparable to temperatures in current Pratt & Whitney production engines, and the most advanced materials and coating processes are being used.

An annular burner is used instead of the can-annular configuration of current engines. The annular burner produces lower circumferential temperature gradients, fewer hot spots, and has greater cylinder flexibility. This contributes to a reduced incidence of low cycle fatigue cracking and lowers the likelihood of pieces breaking out to cause downstream turbine damage. The elimination of the transition duct and crossover tubes as a result of the use of an annular burner is also expected to contribute to improved reliability.

b. Safety Considerations and Criteria

The following design approaches and criteria have been incorporated into the design of the QE-3 engine. These approaches and criteria have evolved as a result of Pratt & Whitney Aircraft's extensive experience with commercial aircraft jet engines.

A fail-safe design is provided to prevent turbine overspeed in the event of a shaft failure by the selection of axial clearances (between the rotating turbine blades and the stationary turbine vanes) which cause the blades to contact the vanes prior to any part contacting the disk.

The ability to contain blade failures is determined by an empirical "containment factor," which, basically, represents a measure of the relationship between the kinetic energy of the failed blade and the available energy absorption capability of the case.

Minimum material specifications and maximum load conditions are used to calculate the minimum case thickness, thereby providing a statistical factor of safety.

The low-speed rotor is prevented from uncoupling by a failsafe shaft system using a main thrust bearing sleeve arrangement. If a thrust bearing failure is experienced, resulting in severing the outer sleeve, the inner torque-carrying shaft remains intact.

The high-speed rotor is designed so that if shaft separation occurs, the axial spacing of the blades and disks is set so that the rotating airfoils will contact the stationary airfoils before any disk contact is made. This will prevent overspeed and/or subsequent rupture of any disk.

A redundant ignition system is used. The engine has two spark igniters and two ignition exciters, although only one of each is required for ignition.

6. Weight Analysis

The selected configurations of Task III were the result of a narrowing down process from the broad parametric studies of Task I through the four designs studied in Task II, to the single design and alternate studied in Task III. With each new task, the number of cycles or designs was reduced and the available informations became more detailed, allowing the weight analyses to become more detailed and accurate.

The method of analysis used in Task III was an extension of that used in past Pratt & Whitney Aircraft programs, and has been verified by comparing weights of manufactured engine with predicted weights. The procedure was similar to that used in Task II, except that the weight estimate for the fan rotor was more accurate because of the detailed design work performed on that component. The weight estimate for the fan rotor was made directly from the detailed design layout. For the other components, preliminary layouts were available which defined the over-all mechanical arrangement. A bill of material was established to ensure that all major items were considered. Component scaling was held to a minimum and strong emphasis was placed on the layout and bill of materials insofar as mechanical construction was concerned. Weights of rotating parts were obtained from a computer program which has been proven to provide accurate weight estimates with a minimum of input data.

The estimated weight of the QE-3 engine is 4950 pounds (2247 kilograms), while the QE-4 (offered as an alternate to the QE-3 and discussed in Section VII of this volume) has an estimated weight of 4750 pounds (2155 kilograms). The major reasons for the reduced weight are that the QE-4 has fan blades with higher aspect ratios, a reduced fan hub-to-tip ratio, and a higher turbine inlet temperature. Another major difference between the two configurations is the higher bypass ratio of the QE-4. A breakdown of weights by components is provided for both the QE-3 and QE-4 in Table X.

TABLE X
ESTIMATED WEIGHTS OF THE QE-3 AND QE-4

	QE-3 Weight (lb)	QE-4 Weight (lb)	QE-3 Weight (kg)	QE-4 Weight (kg)
Fan Section - Rotating Members (blades, disks, and attaching hub)	405	310	184	141
Fan Section - Static Members (outer case, stators, exit guide vanes, and acoustic liners)	380	300	172	136
Front Support Structure Section (rotor support structure, bearing compartments and seals, bearings and bearing supports, front engine mount ring, accessory drive shaft and gears, and remaining acoustic lining materials)	605	580	274	263
High-Pressure Compressor (blades, vanes, disks, attaching hubs, spacers, tiebolts, outer case, and inner seals)	660	660	300	300
Combustor (diffuser, combustion liners, inner and outer cases, fuel nozzles and fuel manifold, bearing compartments and seals, bearings and bearing supports)	420	420	191	191
High-Pressure Turbine (blades, disks, vanes, attaching hubs, spacers, tiebolts, outer case, and inner seals)	600	600	272	272
Low-Pressure Turbine (same as high-pressure turbine)	915	915	415	415
Turbine Exit (exit guide vanes, inner and outer cases, acoustic lining materials, rearmost bearing compartment, seals, bearing, and bearing support)	285	285	129	129
Shafting (total shafting for all rotors and shaft coupling - integral disk hubs are included in respective sections)	245	245	111	111
Accessories (accessory drive box, engine control system, fuel system, lubrication system, ignition system, and all associated plumbing)	435	435	197	197
TOTAL ENGINE WEIGHT	4950	4750	2247	2155

In addition to the standard equipment, the weight estimates include engine bleed valves and acoustic treatment within the engine. The weight of the fan outer case and front mount was estimated under the assumption that these parts would be designed to carry the loads imposed by a thrust reverser. The items included in the "Accessories"" heading of Table X are listed below:

- Full duty gearbox
- Fuel pump
- Fuel control system
- Ignition system without power source
- Pressurizing and dump valve
- Fuel, air, and oil plumbing
- Variable geometry actuation
- Two tachometers
- Fluid power pump
- Generator
- Starter
- Fireseals, installation, and miscellaneous

The items listed below are <u>not</u> included in the weight estimate:

- Nose spinner
- Exhaust nozzle
- Fan ducting
- Oil tank
- Fuel-oil cooler
- Fuel heater
- Handling brackets
- Thrust reverser

D. PERFORMANCE

An engine data book was prepared containing performance estimates covering a range of flight altitudes from sea level to 45,000 feet (13,700 meters), flight Mach numbers from 0. to 0.9, key dimensions, weight, center of gravity and external installation features. This data book, TDM-2157, "Preliminary Performance Estimates of the QE-3 Turbofan Engine" is enclosed as Volume V of this report.

The data in Volume V includes thrust settings representative of take-off, maximum continuous (climb), maximum cruise, and approach for the required range of altitudes and Mach numbers. The effect of ambient temperature variations on take-off, maximum climb, and maximum cruise ratings is included, as well as procedures to convert part-power settings to non-standard ambient temperature conditions. Correction factors to account for the effects of airbleed and power extraction on thrust and fuel consumption are included. In addition, thrust, thrust-specific fuel consumption, airflows, rotor speeds, and correction factors for inlet and exhaust duct pressure losses are included.

To generate the performance data, the contractor used standard equilibrium-matching computer programs. The component performance levels used in the computations were based on current component technology, and reflect the results of testing on current engines. A summary of component performance levels is given in Table XI.

TABLE XI
QE-3 COMPONENT PERFORMANCE ASSUMPTIONS
CRUISE DESIGN POINT

Fan Efficiency (%)	88.0
High-Pressure Compressor Efficiency (%)	84.5
High-Pressure Turbine Efficiency (%)	89.9
Low-Pressure Turbine Efficiency (%)	91.6
Turbine Cooling (%)	7.2 plus 0.3 overboard bleed
Burner Pressure Loss (%)	4.7
Primary and Duct Nozzle Velocity Coefficient	0.985*

* Adjusted to turbine discharge and fan discharge

Turbine temperature levels for the QE-3 were based on a compromise between thrust-to-weight ratio and jet and total noise. Turbine temperature levels are shown in Table XII and are lower than those of the JT9D-3 at any equivalent power setting.

TABLE XII
QE-3 RATED TURBINE TEMPERATURES

	°F	°K
Nominal Design Point, 35,000 ft (10,680 m), Mach 0.82	1740	1220
Sea-Level Take-Off, Standard Day	1920	1320
Sea-Level Take-Off, 84°F (302°K) Day	2077	1410
Maximum Cruise, Standard Day, 35,000 ft (10,680 m)	1788	1250
Maximum Cruise, Standard Day + 15K°	1931	1330
Maximum Continuous, Standard Day	1847	1280
Maximum Continuous, Standard Day + 15K°	1994	1360

SECTION V

QE-3 ENGINE NOISE

Acoustics work was performed in two areas: coordination of aerodynamic and mechanical design work with acoustical principles and computations of uninstalled engine noise. The purpose of this coordination was to determine features which minimize fan and engine noise generation. Engine noise levels were predicted during take-off and approach under standard conditions. For take-off, peak flyover total fan and jet noise levels were predicted for altitudes varying from 200 to 1700 feet (61 to 519 meters). For approach, peak flyover total fan and jet noise levels were predicted for an altitude of 325 feet (99 meters), for engine power variations from 20 percent to 40 percent of take-off thrust. Noise levels were predicted using the procedure developed for Task II studies. This procedure was based on empirical relationships developed from noise measurements of Pratt & Whitney Aircraft's current turbojet and turbofan engines.

This section of the report discusses the Quiet Engine noise reduction features, noise prediction results, and briefly discusses the prediction procedure, significant assumptions, and potential means of further reducing noise.

A. NOISE REDUCTION FEATURES

All known practical features which reduce fan and engine noise were incorporated in the design of the QE-3 engine. These features include low fan tip speeds, fan rotor to exit guide vane axial spacing, blade and vane number combinations as near optimum as possible within reasonable design contraints, the use of a single-stage fan, no inlet guide vanes, and acoustical treatment of the fan case aft of the rotor and acoustical treatment of the ducting leading to the high-pressure compressor. Relatively low levels of jet exhaust noise were achieved with the low jet exhaust velocities associated with the high bypass ratio.

The acoustical treatment of the fan case will serve to absorb some of the broadband and discrete-tone noise radiated rearward by the fan. Likewise, the acoustical treatment of the flowpath leading to the high-pressure compressor will serve to absorb some of the blade-vane interaction noise generated in the high-pressure compressor. Normally, this noise is considered to be of secondary importance, but with the noise-reduction features incorporated in the fan, noise generated in the high-pressure compressor may become significant.

Further suppression of fan noise might be obtained by acoustically treating the inlet and fan discharge ducts. Other programs funded by NASA are providing information in this area.

Some reduction in jet exhaust noise levels at take-off power might be obtained by mixing the primary and fan exhaust streams. At approach power, the primary and exhaust gas streams are of nearly equal velocities, so no significant improvements in noise level can be gained by mixing.

B. NOISE PREDICTIONS

Bare engine noise levels were predicted for four QE-3 engines at take-off and approach powers. These predictions are shown in Figures 53 and 54. The predictions represent the peak perceived noise levels on the ground as four QE-3 engines pass overhead at the given altitude. They do not, however, include installation effects such as shielding from the fuselage, nor do they include the effects of extra ground attenuation. Since both of these effects should tend to reduce perceived noise levels, the noise predictions can be considered to be conservative.

The noise prediction procedure used for this task was the same as that used in Task II. It includes the use of far-field noise measurements obtained from current Pratt & Whitney Aircraft engines. Briefly, the procedure required the separate calculation of jet exhaust noise, discrete fan noise, broadband fan noise, and combination tone noise. These four noise components were then combined to produce the estimate of over-all engine noise. The sequence of operations in the prediction system is summarized in Figure 55.

Central to any system of predicting engine noise are the assumptions on which the calculations are based. The assumptions used in the Task III predictions are discussed below.

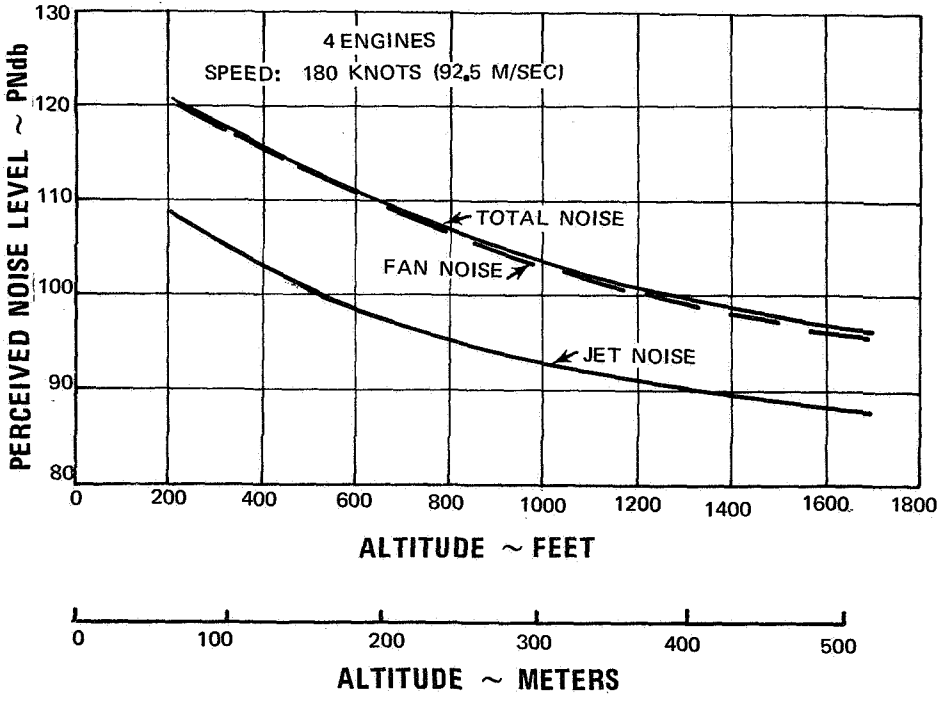

Figure 53 Estimated QE-3 Noise Levels at Take-Off Power

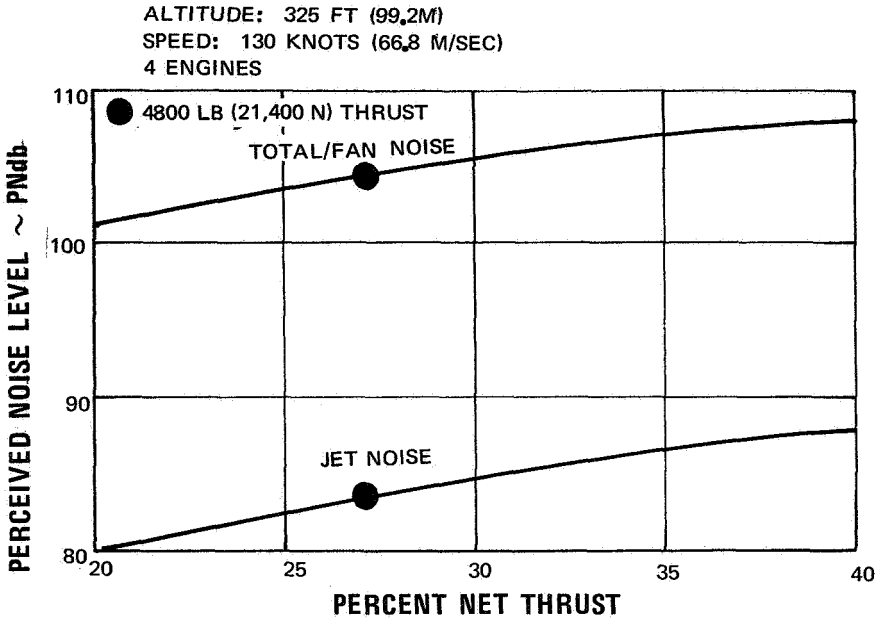

Figure 54 Estimated QE-3 Noise Levels on Approach

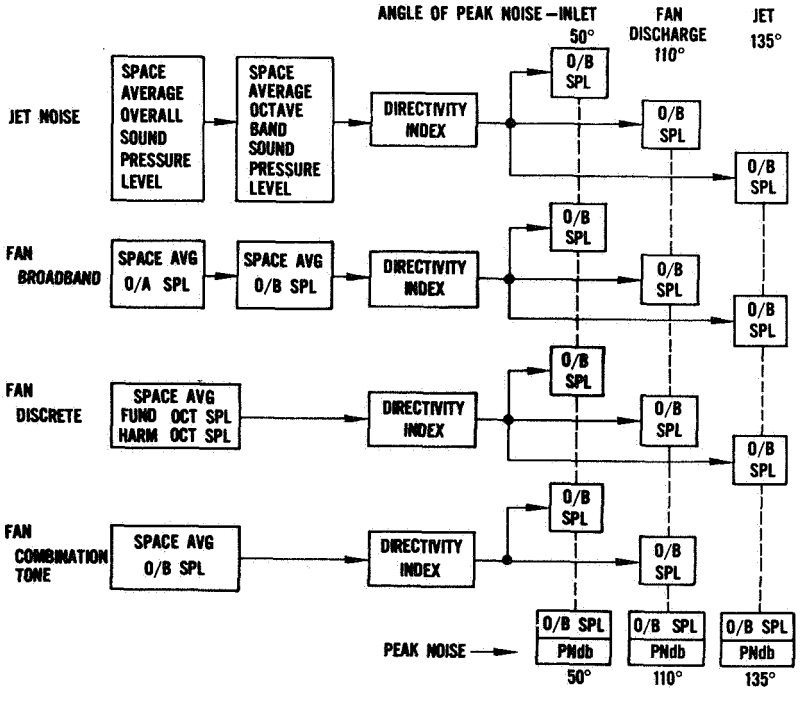

Figure 55 Noise Prediction Sequence (M-51248)

1. Jet Noise Assumptions

Jet noise was predicted on a straightforward basis using flow performance data and assuming conical nozzle characteristics. Basically, the procedure was the same as that described in SAE document AIR 876, "Jet Noise Predictions". One exception to that procedure was made necessary by the fact that the SAE relationships were valid only for jet exhaust velocities from 1000 to 2000 ft/sec (305 and 610 m/sec). Because the relative jet exhaust velocity for the QE-3 is less than 1000 ft/sec (305 m/sec) empirical relationships developed from noise measurements on current engines operating at low jet velocities were used.

2. Fan Noise Assumptions

Relative blade tip Mach number was assumed to be the major correlation parameter for fan noise. Noise data for existing engines indicate that basic relationships exist between noise level and relative blade tip Mach number. Such factors as stage pressure rise, rotor and stator aspect ratio, stage efficiency, airfoil camber and section shape, and fan duct length and geometry were neglected.

3. Turbine Noise Assumptions

Turbine noise was neglected in the calculation of over-all engine noise. Turbine noise has been identified in noise measurements from some current low-bypass turbofan engines with two-stage fans and high-bypass engines with single-stage fans, but in no instance has it been the dominant noise source. In low-bypass engines, it can only be identified at power settings below the normal operating range of the engine. In high-bypass engines it is somewhat more significant, but it still appears only at low power settings and is masked at higher settings.

4. Inflight Noise Assumptions

It was assumed that the nacelle would have no effect on perceived noise levels. Because the design features of the nacelle were unknown at the time the noise was predicted, the prediction was based on bare engine noise levels without acoustical treatment in inlet or fan ducts, an unchoked inlet, no inlet struts, and no other noise-suppressing or noise-generating device.

Forward airplane velocity was assumed to have no effect on noise generation. Inflight noise levels were calculated on the basis of inflight performance with inflight fan noise levels related to static noise data at the same relative blade tip Mach number and inflight jet exhaust noise were related to static data at the same relative jet velocity.

To extrapolate noise levels from the airplane to the ground, the contractor used the spherical divergence and standard-day extra air attenuation values given in SAE document ARP 866, "Standard Values of Atmospheric Absorption as a Function of Temperature and Humidity".

The Doppler shift was neglected. Changes in frequency as a result of Doppler shift were not considered, since they are not expected to have any significant effect on noise level.

Extra ground attenuation and shielding of engines by the fuselage were not considered in the noise predictions. When the airplane is at a large distance from the observer and, therefore, at a shallow angle relative to the ground, both of these effects may help to reduce the perceived noise level. Neglecting these effects tends to produce more conservative noise predictions.

C. NOISE REDUCTION SCHEMES

In addition to incorporating in the QE-3 design noise reduction features learned from recent full-scale turbofan engine and noise rig test experience, an attempt was made during the course of the program to explore new and novel ideas which might contribute to the achievement of a Quiet Engine. One idea did emerge which on the surface appeared promising enough to warrant at least a cursory evaluation.

The idea involved simultaneous slowing of the low rotor and reduction of the high velocity main engine exhaust stream by mixing with a portion of the lower velocity fan exhaust through a common exhaust nozzle. As a final result it was determined that some noise reduction can be achieved by this scheme. However, the amount of noise reduction was not large enough in comparison with the mechanical complexity involved to justify adopting it in the basic QE-3 design.

The system which would be employed to achieve a reduction in approach noise is shown in Figure 56. At approach power a portion of the fan duct flow would be bled from the outer ducts and around the gas generator, and injected into the Primary Exhaust flow upstream of the main engine exhaust nozzle. The conmixing of this portion of duct mass flow with the primary flow through the same nozzle will cause an engine rematch which reduces the fan rotor speed, hence rotor noise. This effect is the same as achieved by mechanically reducing exhaust nozzle area. In addition, the mixing of the cold fan air with the relatively hot primary gases will reduce the noise created by the high velocity primary jet exhaust. It should be noted here that complete mixing of the primary and duct bleed flow is not essential to achieve some suppression of the primary exhaust noise.

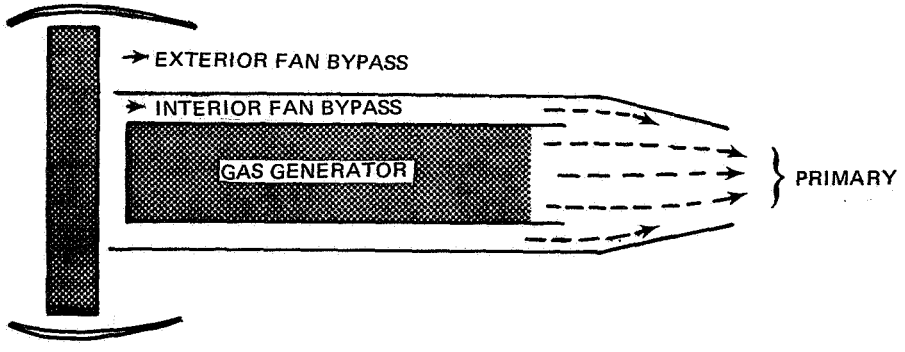

Figure 56 A Possible Noise Reduction Scheme

The results of the mixing scheme are compared in Figure 57 with those which could be obtained with the variable primary exhaust nozzle area method. The noise levels indicated in Figure 57 for the fan rotor, primary, duct exhaust, and total are not accurate in an absolute sense but do represent the relative changes in noise levels. Along with the noise levels, the amount of fan duct flow which must be bled as a percentage of the total fan duct flow is presented. This is an important criterion since large levels of bleed flow could present severe engine diameter problems along with significant weight penalties. An indication of the ratio of duct bleed flow pressure to the primary stream pressure is also shown in the top curve. As these pressures approach each other, turbine exhaust Mach number gets extremely high and the duct bleed flow Mach number is very low to prevent back-flow through the bleed system.

Figure 57 shows that the net reduction in noise from slowing the fan is approximately 2 PNdb with the variable bleed scheme, which is only about 1/2 PNdb superior to the variable exhaust nozzle scheme.

As a final consideration, significant reductions in primary exhaust noise could be achieved with the mixing scheme. If jet exhaust noise were to be a major problem, this scheme could prove extremely beneficial.

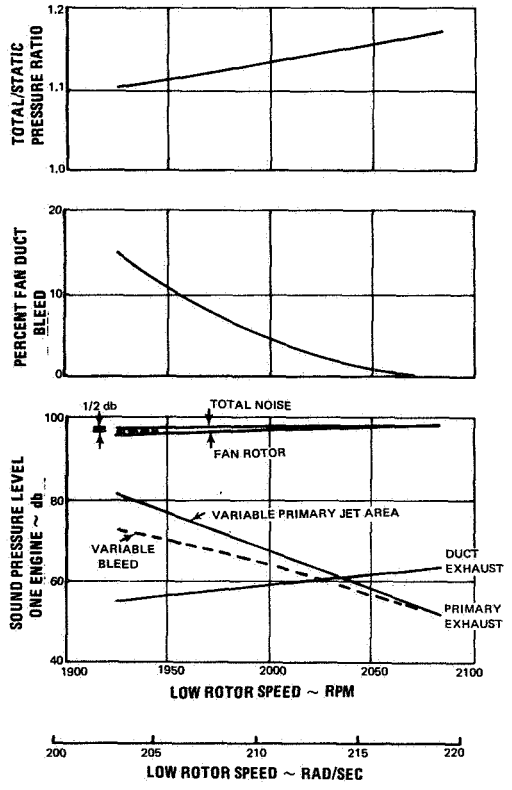

Figure 57 Effects of Noise Reduction Scheme

SECTION VI

FAN DESIGN

The aerodynamic and mechanical design of the QE-3 fan has been completed to the extent of defining flowpath contours, blade and vane shapes and the disk with attachments. Based on titanium as its selected material, a detailed aeroelastic analysis has verified that the fan will have satisfactory vibration characteristics and sufficient tolerance to bird ingestion. The fan can be ready for fabrication after detail drawings are prepared. The design features large spacing between the fan rotor and the duct exit guide vane as well as a carefully selected number of vanes to suppress discrete noise generation. It is capable of an average pressure ratio of 1.60 in the bypass portion and 1.45 in the gas generator portion.

A. AERODYNAMIC DESIGN

1. General Background

The final design of the QE-3 fan, shown in Figure 30 drew upon the original aerodynamic evaluation undertaken in the fan integration study, reported in Section III. In fact, it is quite similar to the QE-2 design studied in detail as part of the fan integration study. The basic design parameters for the QE-3 fan and the original QE-2 study fan are shown in Table XIII. Difference in bypass ratio and flowpath caused small changes in the aerodynamic loading levels throughout the fan stage. This meant that the QE-3 design could continue as a modification to the original study fan. The rotor was modified primarily by a change in the fan rotor tip slope which was required to prevent excessive diffusion along the duct outer wall. As shown in Figure 58, the peak D factor for the QE-3 fan rotor is about 3 percent higher than that for the study fan rotor. At the rotor tip, the D factor of the fan rotor is slightly lower at take-off conditions in the QE-3 fan than in the study fan, but it is slightly higher at design conditions. However, as shown in Figure 59, the loading increases slowly as the surge margin decreases, which permits a relatively high loading level with ample surge margin at design conditions. The surge margin at take-off conditions is about 8 percent, which should be adequate, although a higher margin would be desirable.

The completed airfoil design for the rotor and for the duct exit stator, both inner and outer portions, can be described by the dimensional data presented in Table XIV.

TABLE XIII

DESIGN PARAMETERS OF QE-3 FAN AND
FAN INTEGRATION STUDY FAN

	Study Fan	QE-3 Fan
Inlet Correct Flow Rate	965 lb/sec 43.6 kg/sec	850 lb/sec 38.5 kg/sec
Area Inlet Corrected Flow per Unit Annulus	41 lb/sec ft^2 200 kg/sec m^2	41 lb/sec ft^2 200 kg/sec m^2
Corrected Tip Speed	1120 ft/sec 342 m/sec	1090 ft/sec 333 m/sec
Tip Pressure Ratio	1.5	1.6
	1.45	1.45
	0.45	0.445

TABLE XIV

QE-3 FAN AIRFOIL DATA

	Rotor Blades	Outer (Bypass Portion) Stator Blades	Inner Stator Blades	Inner Exit Case Struts
Inlet Tip Diameter (in)	68.85	68.19	43.1	38.6
Inlet Tip Diameter (cm)	175	173	110	98.0
Inlet Root Diameter (in)	30.64	46.30	35.4	31.2
Inlet Root Diameter (cm)	77.4	118	90.0	79.3
Exit Tip Diameter (in)	66.46	68.68	42.6	31.75
Exit Tip Diameter (cm)	164	174	108	80.6
Exit Root Diameter (in)	34.12	49.10	35.1	20.88
Exit Root Diameter (cm)	86.6	125	89.2	53.1
Number of Blades	36	88	88	11 thin 1.10 in (2.79 cm) 1 thick 1.75 in (4.45 cm)
Airfoil Type	multiple circular arc	circular arc	circular arc	multiple circular arc
Max. Thickness/Chord Ratio	0.0525 0.018	0.06	0.05	thin 0.089-0.118 thick 0.142-0.118
	2.20	2.59	1.265	0.49
	2.685	2.59	1.265	0.37

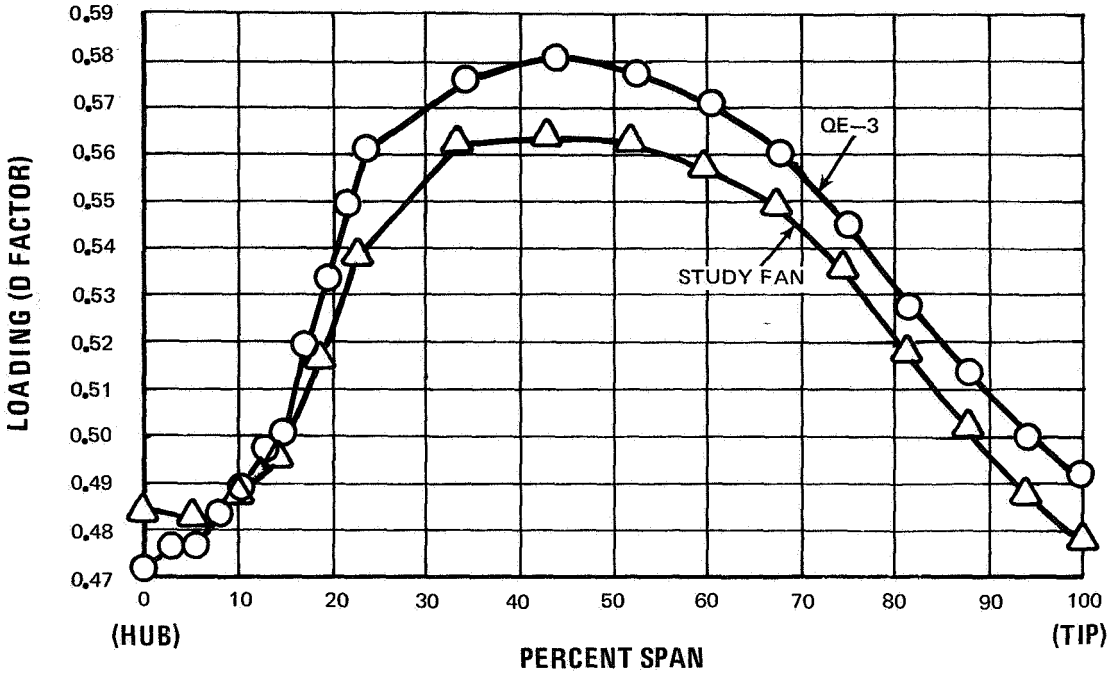

Figure 58 Spanwise D Factor Distribution for Study Fan and QE-3 Fan Blades

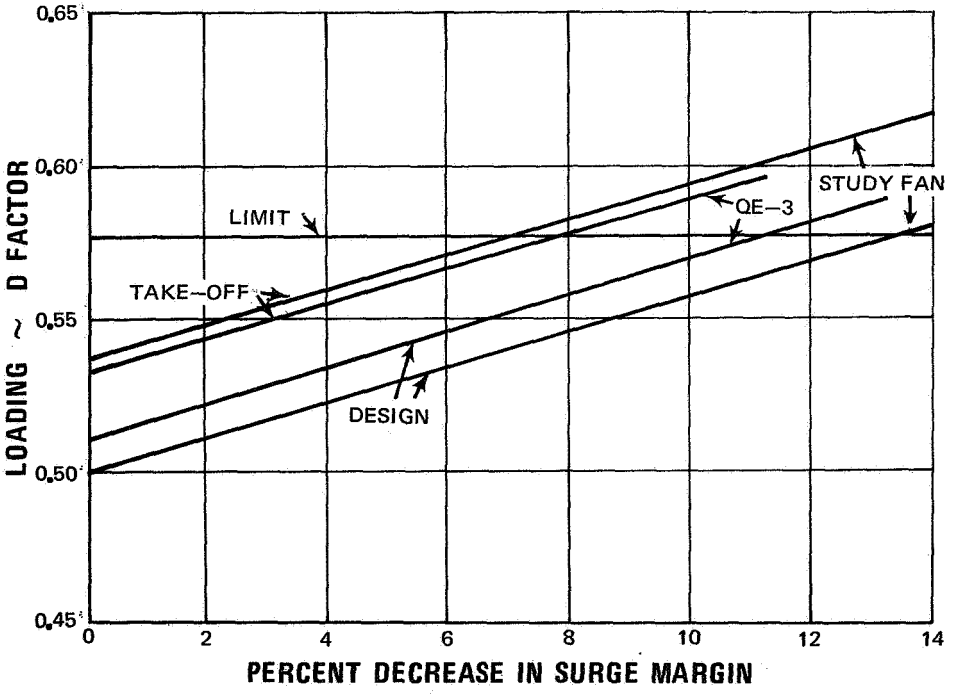

Figure 59 Effect of QE-3 Fan Tip Loading On Surge Margin

The fan integration study indicated that the loading at the root section of the rotor and at the duct exit stator vane would be very high. As shown in Figure 60, the duct exit vane for the study fan was expected to exceed the loading limit with a decrease in surge margin of less than 4 percent. Although excessive loading of the duct exit vane probably would not cause engine surge, it would result in excessive losses. Consequently, the loading was decreased by increasing the Mach number in the duct from 0.50 to 0.55 and by changing the duct contour to reduce the diffusion at the root of the vane. The result was a reduction in loading to the point where the duct exit vane will not exceed the loading limit.

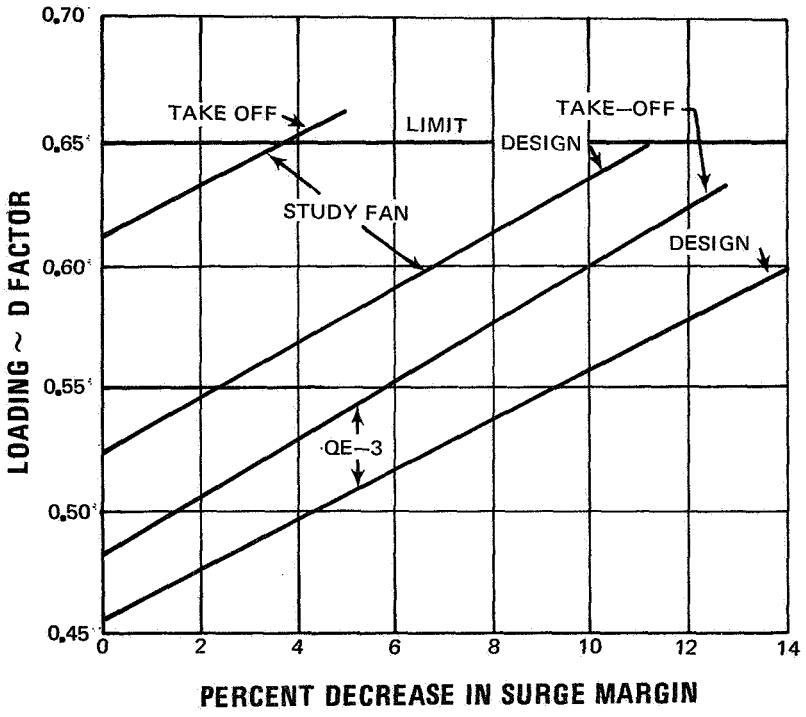

Figure 60 Effect of QE-3 Duct Exit Vane Root Loading On Surge Margin

The fan integration study also indicated that the loading of the fan stator would exceed the limit at which surge occurs at flight idle conditions. Accordingly, the amount of swirl removed by the stator was reduced in the QE-3 design from that in the study fan design to the level shown in Figure 61. The loading is still high, however, and it is recommended that a bleed be provided, at least for initial testing in this operating range. The swirl not removed by the stator will be removed by the cambered intermediate case struts. The loading level of the struts has been kept low with a D factor of only 0.21 at the ten percent span location since the struts are relatively thick and because the wall at the root has an adverse curvature.

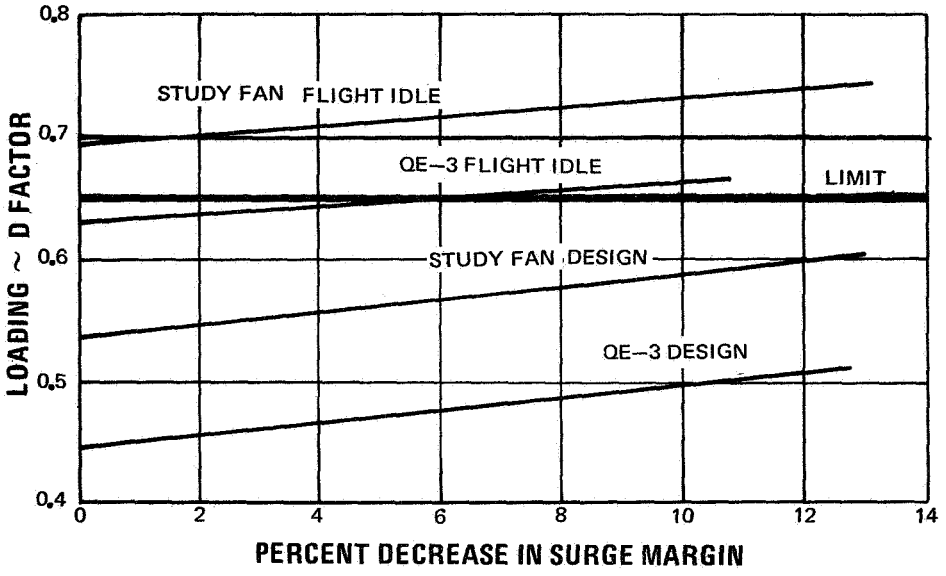

Figure 61 Effect of QE-3 Fan Stator Root Loading On Surge Margin

The overall design parameters of the QE-3 fan are shown in Table XV together with the corresponding parameters for the NASA low-tip-speed fan (Contract NAS3-10483). In general, the values for the QE-3 fan parameters fall between the values for the other designs. Internal contours are shown in Figure 62.

The predicted performance for the root and tip portions of the QE-3 fan is shown in Figure 63. Similar to the study fan, the original pressure ratio and flow rate goals for take-off conditions were not achieved. In the study fan, however, a new match point was established at the original pressure ratio goal but at a lower flow rate. As a result, the surge margin at the new match point was maintained at a higher level by permitting the decrease in flow rate to be accompanied by a decrease in pressure ratio. The design point efficiency is 88 percent.

TABLE XV

DESIGN PARAMETERS FOR QE-3 FAN AND
NASA LOW-TIP-SPEED FAN

	QE-3 Fan	NASA Low-Tip-Speed Fan
Pressure Ratio		
Root	1.45	1.5 (Stage)
Tip	1.60	No Splitter
Flow Per Unit Annulus Area	41 lb/sec ft^2 200 kg/sec m^2	42 lb/sec ft^2 205 kg/sec m^2
Bypass Ratio	5.4	No Splitter
Corrected Tip Speed	1090 ft/sec 333 m/sec	1000 ft/sec 305 m/sec
Aspect Ratio Relative to Tip Chord	2.2	1.572
Root Chord-to-Tip Chord Ratio	1.22	1.222
Hub-to-Tip Ratio	0.445	0.40
Work Coefficient		
10% Span	2.12	2.84
50% Span	1.52	1.56
90% Span	1.15	1.01

Note: Work coefficient equals total enthalpy rise divided by one-half the square of the tangential velocity at the specified span.

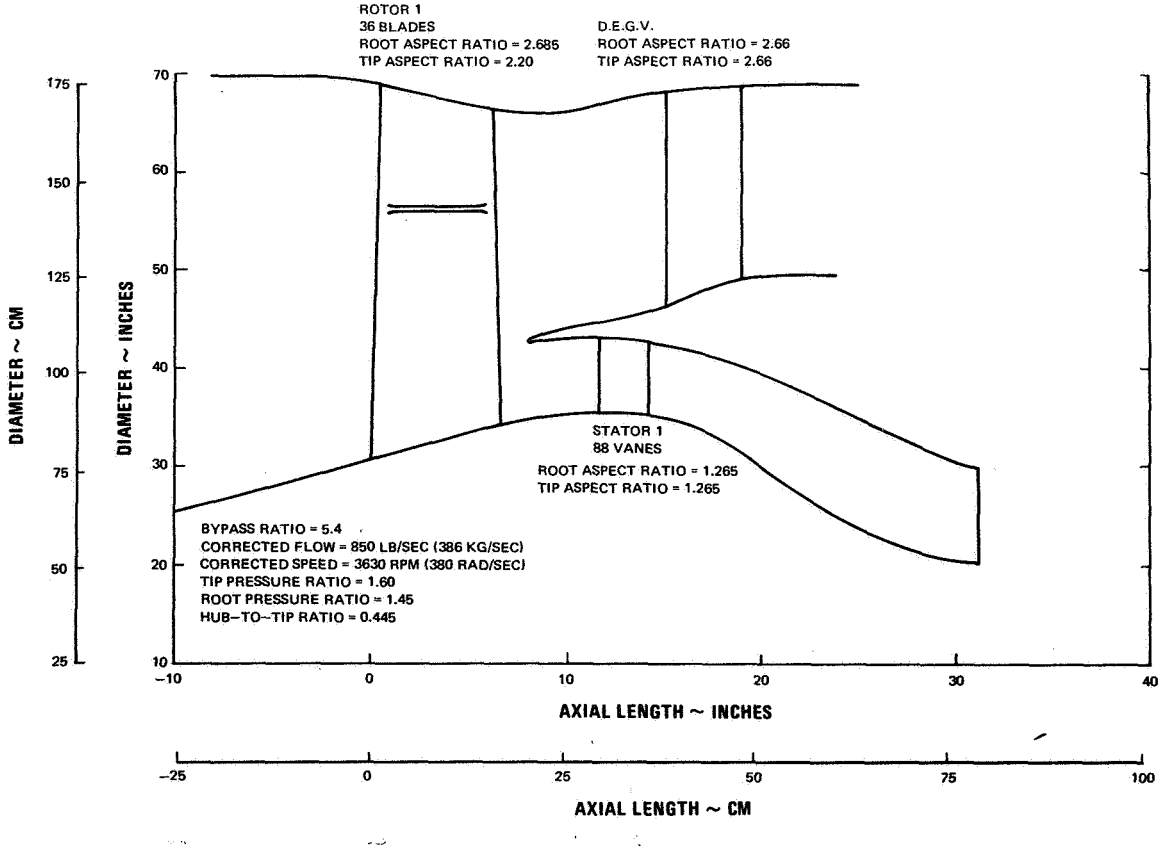

Figure 62 QE-3 Fan Internal Contours

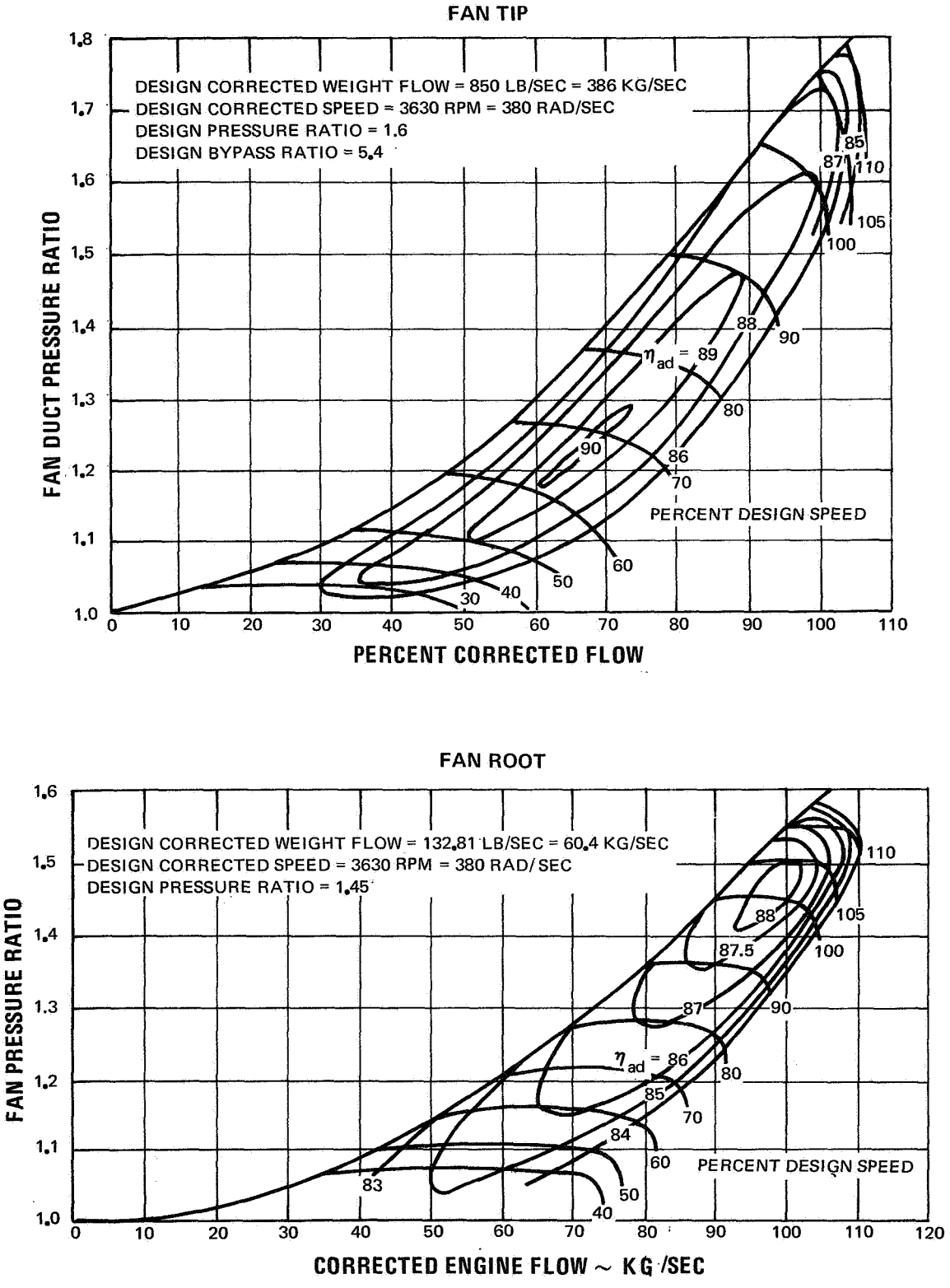

Figure 63 QE-3 Fan Predicted Performance Maps

2. Airfoil Design

The airfoil aerodynamic designs were performed by a computer program which included streamline and splitter effects in the radial equilibrium equation. Multiple-circular-arc airfoils were designed, and the airfoil sections were developed on conical surfaces which approximated streamlines. The mean camber line for this type of airfoil consists of two circular arcs with different radii of curvature but with a smooth contour at the transition point. This is achieved by joining the two curves at the point where the curves intersect a line connecting their centers. The transition point was positioned at the start of the portion of the airfoil which lies under the adjacent airfoil when the cascade is viewed along a line which is perpendicular to both the flow direction and to the blade span.

With multiple-circular-arc airfoils, the maximum thickness location can be positioned within wide limits anywhere along the blade chord length. For these airfoils, the maximum thickness was located just forward of the point where the thickness of the upstream portion of the blade could not longer decrease monotonically. This point is defined by the equation:

$$b_{tm} = 0.5\, b_{total} \left[1 + \left(\frac{S}{b_{total}}\right)^2\right]$$

where

b_{tm} = Most rearward maximum thickness location measured along the blade chord

b_{total} = Total chord length

S = Distance to the maximum thickness location measured along the mean chord line

The blade angles measured from the tangential direction along conical sections are shown in Figures 64 through 67.

For the subsonic portion of the blade, the blade throat area was set about 3 percent larger than the cross sectional area of the incoming flow. The throat area margin above the area at which choking occurs was decreased smoothly between the root and the 10-percent span location with a total reduction of about 40 percent at the root streamline. The reduction was required to account for viscous effects which were not included in the streamline calculation.

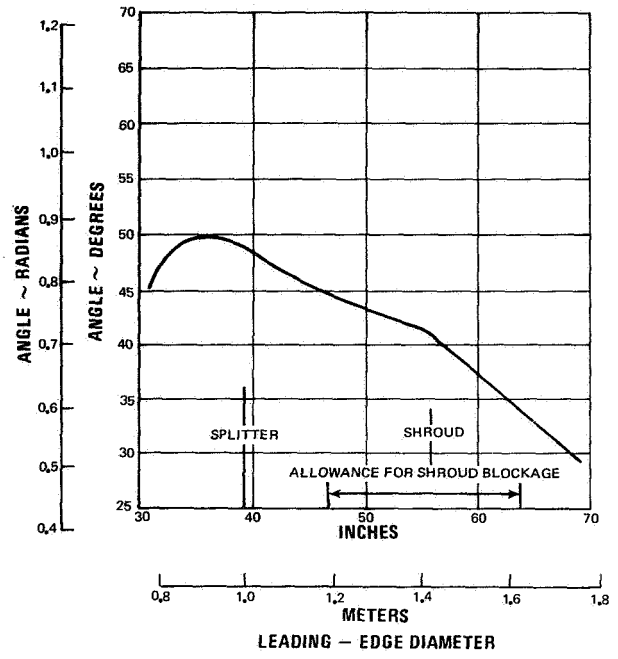

Figure 64 QE-3 Fan Conical Surface Inlet Metal Angles

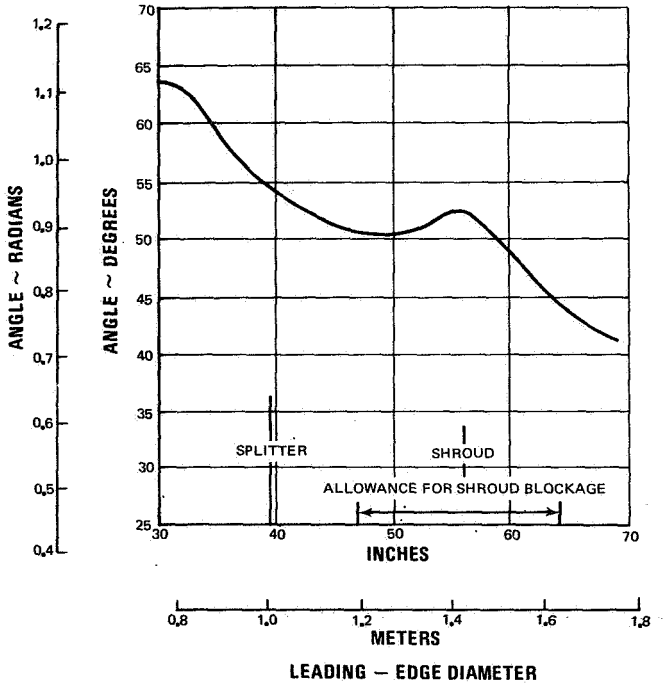

Figure 65 QE-3 Fan Conical Surface Transition Metal Angles

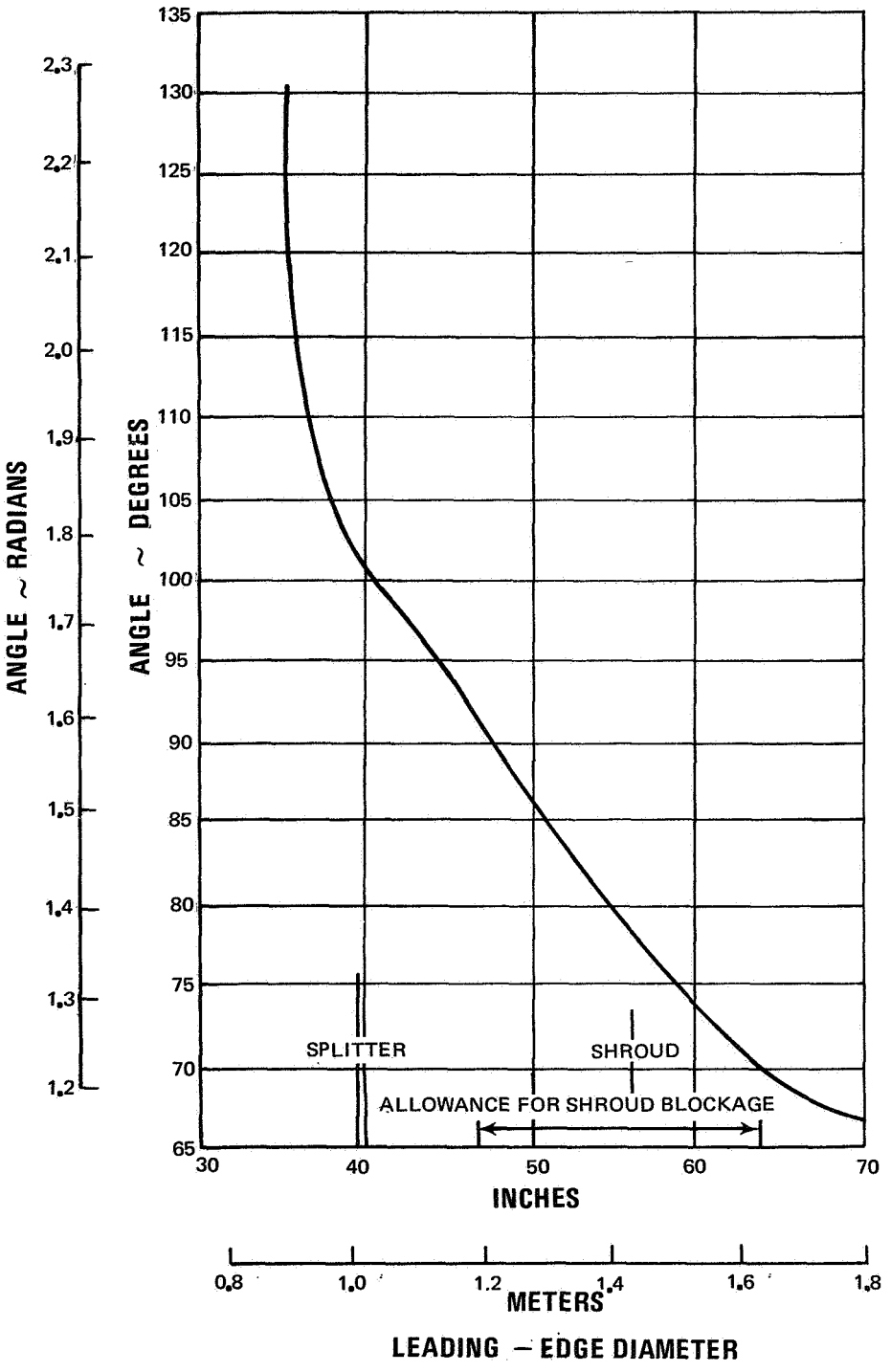

Figure 66 QE-3 Fan Conical Surface Exit Metal Angles

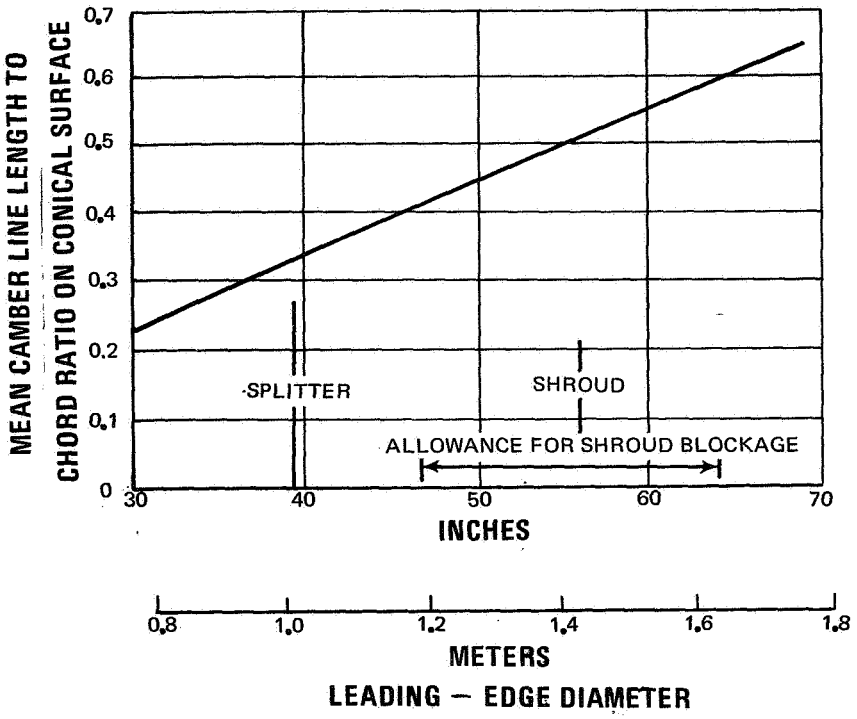

Figure 67 QE-3 Fan Mean Camber Length to Chord Ratio on Conical Surface

For the supersonic portion of the blade, the throat area was set to provide a 3 percent margin above the area that would produce choking. The losses in the blade passage increase as the area is increased, but some margin above the choking area is required to prevent choking as a result of nonuniformities in the flow or the build up of a boundary layer. Experience has indicated that a 3 percent margin is generally sufficient. Because of the area blockage produced by the shroud, it was necessary to increase the blade throat area over about 50 percent of the blade length in the vicinity of the shroud to maintain the 3-percent margin. The assumed distribution of the shroud blockage relative to the nominal streamline area is shown in Figure 68 (Each streamline in Figure 68 represents 10 percent of the total duct flow.) The resulting choke margin provided relative to the nominal flow area is plotted in Figure 69

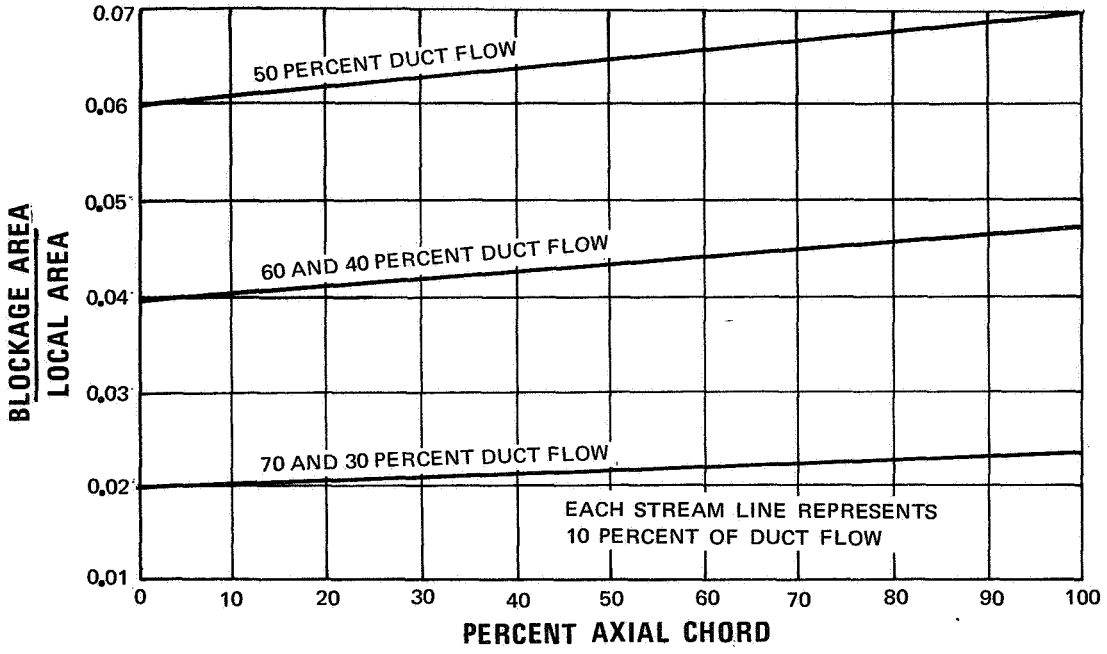

Figure 68 Relative Fan Blade Shroud Blockage Area Distribution

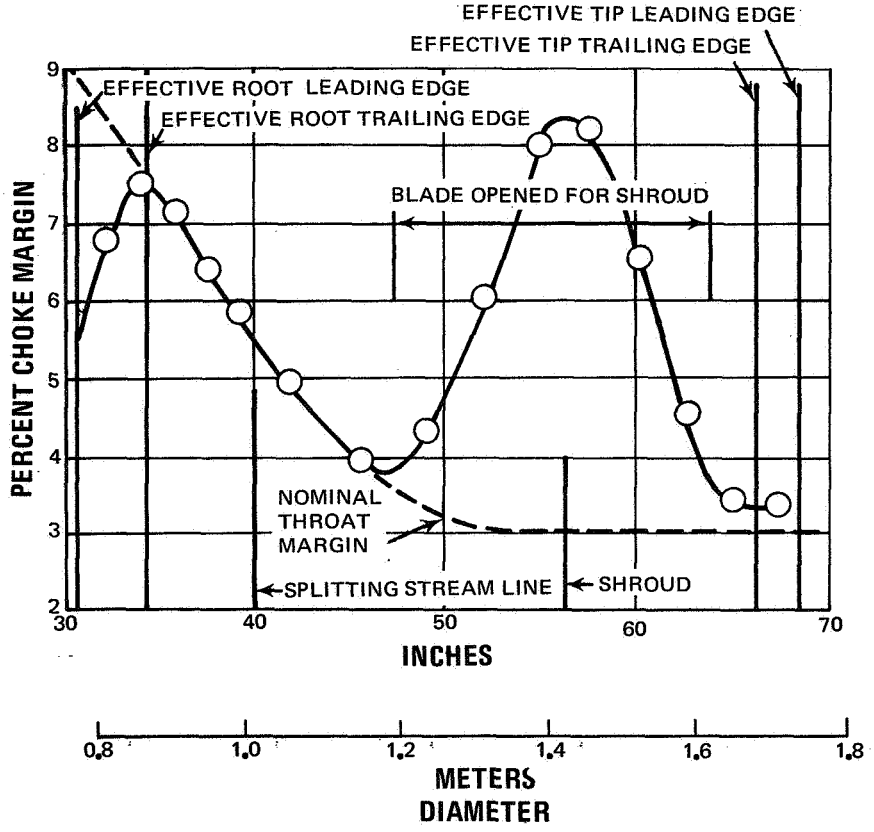

Figure 69 QE-3 Fan Blade Choke Margin Distribution

In the subsonic portion of the blade, the throat area is of greater importance than the blade incidence. Consequently, the incidence was set at a nominal value of 0.5 degree (0.0875 radian) relative to the suction surface at the leading edge. The incidence at the root was -9.5 degrees (-0.169 radian), however, to reduce the throat area, as discussed previously. In the supersonic region, the incidence to the suction surface was set at 1.5 degrees (0.026 radian) at a point half way between the leading edge and the intersection of the first contained Mach line with the suction surface.

The fan blade deviation was determined through the use of Carter's rule in the form:

$$\delta = m\theta^* / \sqrt{\sigma}$$

where

δ = Deviation

$m = 0.23(2a/b)^2 + 0.002$ $_2$

a = Chordal distance to the point of maximum camber

b = Blade chord

2 = Exit air angle measured from the axial direction

θ = Camber angle

σ = Solidity

The deviation given by Carter's rule was increased by about 3.3 degrees (0.058 radian) at the root and faired to the value given by the rule at the tip, as shown in Figure 70.

Both the duct exit guide vane and the fan stator were designed as circular-arc airfoils using the same criteria for incidence and throat area as for the subsonic portion of the fan blades. The incidence of the duct exit vane was decreased below the nominal value from the root out to about the 25-percent span location, and the incidence of the fan stator was decreased below the nominal value from the root out to about the 75-percent span location. Deviation values were selected on the basis of the standard United Aircraft Corporation turning correlation which is based on a large quantity of cascade test data and is similar to the correlation presented in NASA SP-36.

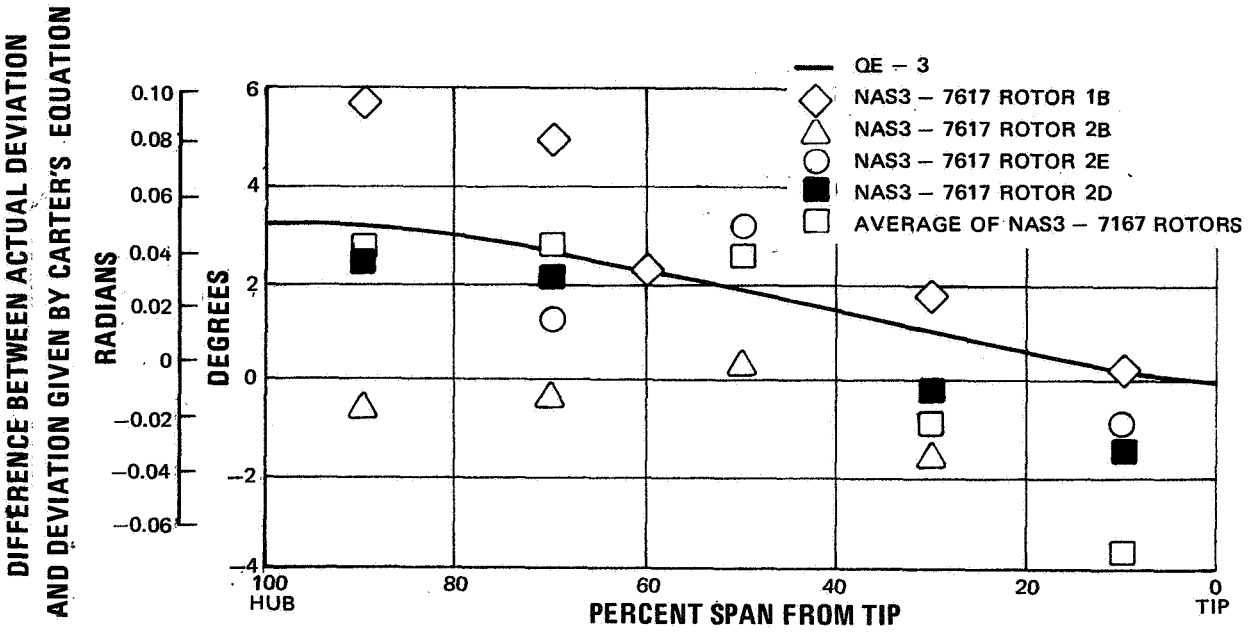

Figure 70 QE-3 Fan Blade Deviation Relative to Carter's Rule Deviation

The fan section includes twelve intermediate case struts which provide structural support, access for lubrication and cooling of the front bearings, and housing for the tower shaft, as well as removing some of the swirl in the flow when the fan stator loading was reduced. The struts are multiple-circular-arc airfoils with low turning (about 7 degrees or 0.12 radian) and low Mach number (about 0.54). The transition point was set at the location of maximum thickness on the basis of structural considerations in locating the tower shaft, and most of the turning occurs in the forward portion of the strut to reduce the rate of diffusion in the region where the root wall has adverse curvature. An additional consideration in the design of the struts was the additional blockage of the flow channel on either side of the strut which carries the tower shaft, since this strut is about 60 percent thicker than the others. The extent of the blockage along conical channels is shown in Figure 71. The channel areas were studied to verify that choking would not occur.

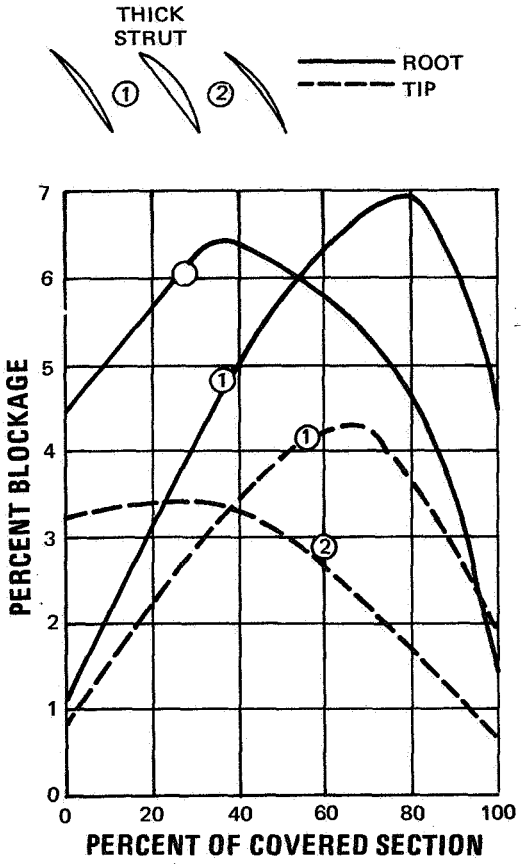

Figure 71 Flow Blockage Distribution From Intermediate Case Struts

B. AEROELASTIC ANALYSIS

The fan stage was subjected to a complete aeroelastic analysis including investigation of the resistance of the fan stage to bird ingestion. The results indicated that the vibration and flutter characteristics as well as the steady-state stress levels are acceptable.

The resonant diagram for the fan stage showing resonance margins for 2 and 6 nodal diameters at the fan red-line speed is shown in Figure 72. As shown, a 23.8 percent margin is available at the second-order vibration frequency, and a margin of 6.67 percent is available at the sixth-order vibration frequency. The diagram shown in Figure 72 was calculated on the basis of no hub restraint. The addition of hub restraint would be expected to increase the margin at the lower frequencies.

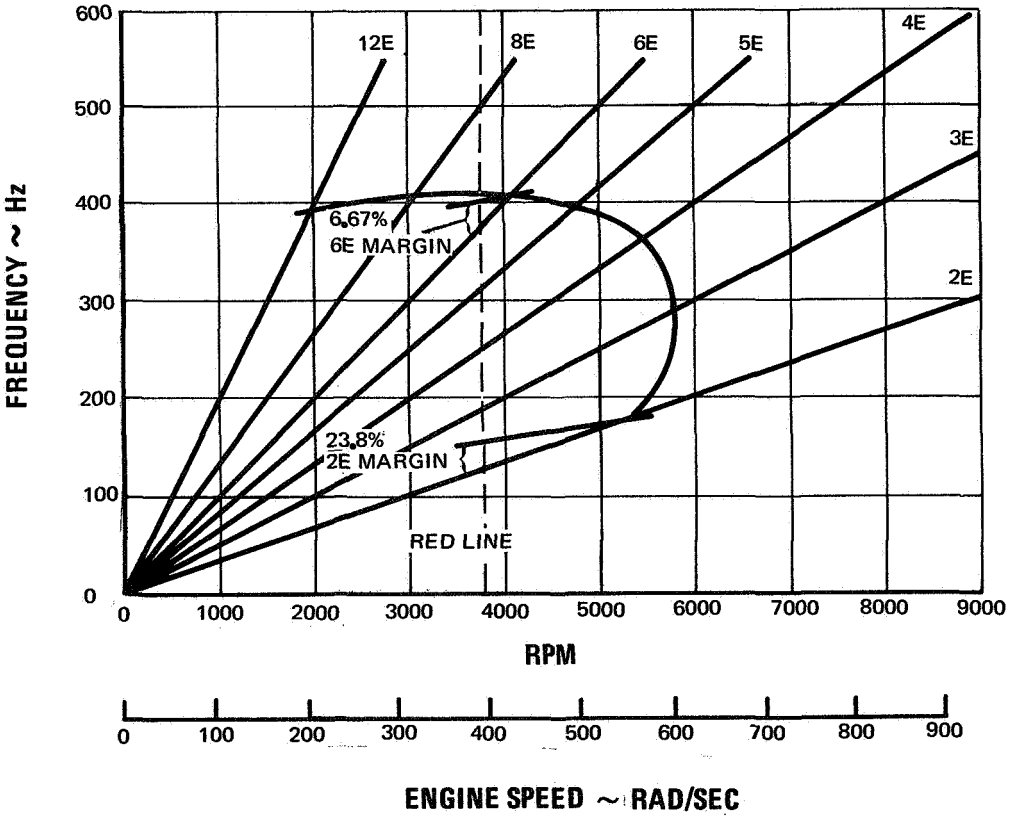

Figure 72 Resonance Frequency Diagram for QE-3 Fan Rotor

The flutter characteristics of the fan in the first coupled mode and in subsonic and supersonic torsional modes are shown in Figures 73, 74, and 75, respectively. For each flutter mode, the curves indicate that the QE-3 fan flutter parameter values are close to those of other successful fans and out of the region where flutter has been experienced. Consequently, the QE-3 fan can be expected to be free from flutter at all speeds up to 100 percent of the red-line speed. (The red line speed represents the mechanical speed of the engine at maximum operating conditions plus an allowance for variations in engine tolerances.)

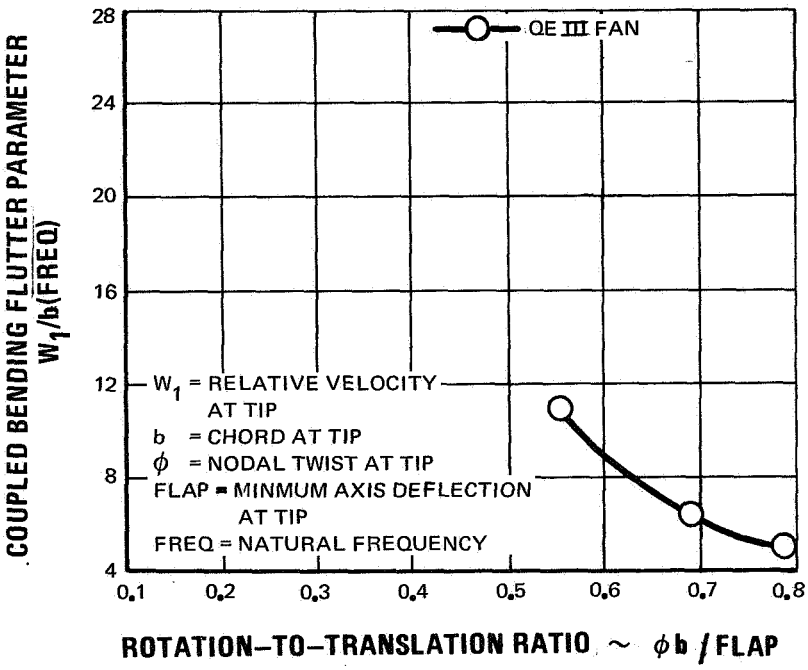

Figure 73 Coupled Bending Flutter Characteristics for QE-3 Fan Rotor

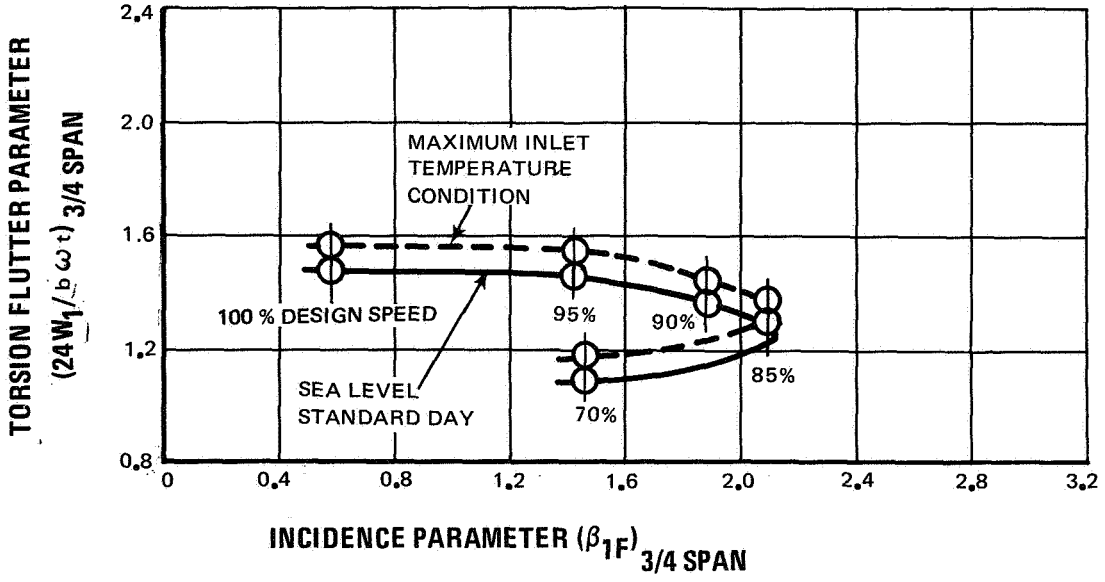

Figure 74 Subsonic Torsional Flutter Characteristics for QE-3 Fan Rotor

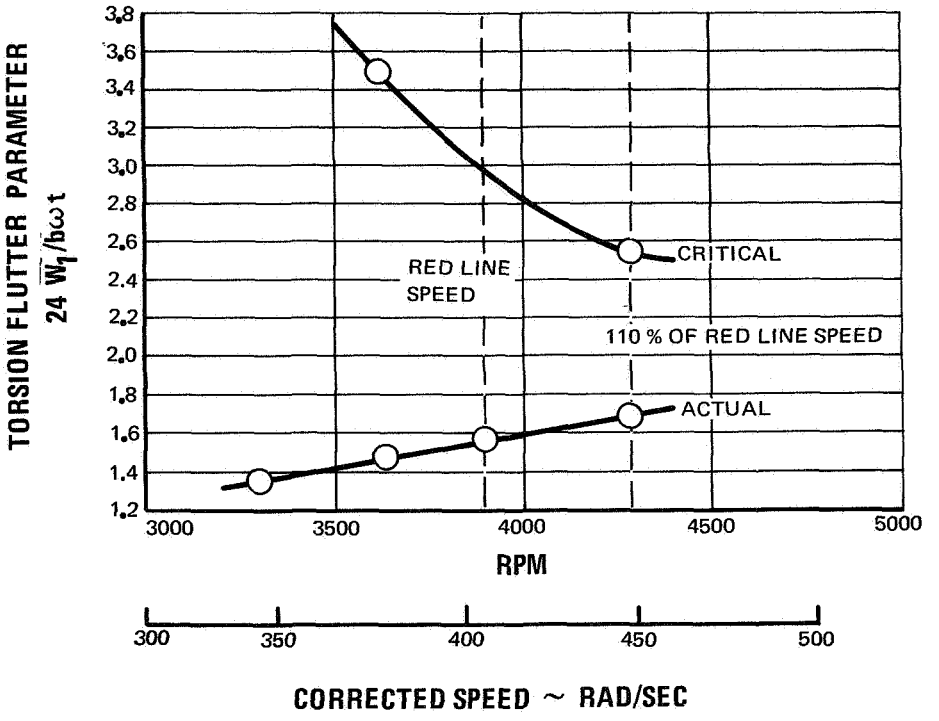

Figure 75 Supersonic Torsional Flutter Characteristics for QE-3 Fan Rotor

The bird-ingestion characteristics of the fan were evaluated by calculating the bird-ingestion parameter, which represents a normalized bending stress at a given span location associated with a unit load at the tip. Experience indicates that blade failure will not occur from bird ingestion if the value of this parameter is less than 1.7. For the QE-3 fan blade, the value of the parameter is 0.65 at the mid-span location and 0.32 at the root, representing a substantial margin below the critical value.

The ratio of the airfoil root stress to the attachment stress was calculated for various modes as a function of dynamic moment angle. The results, Figure 76 indicated that the ratio is greater than 2.0 for first coupled vibration modes with 2 through 8 nodal diameters, indicating adequate airfoil root characteristics.

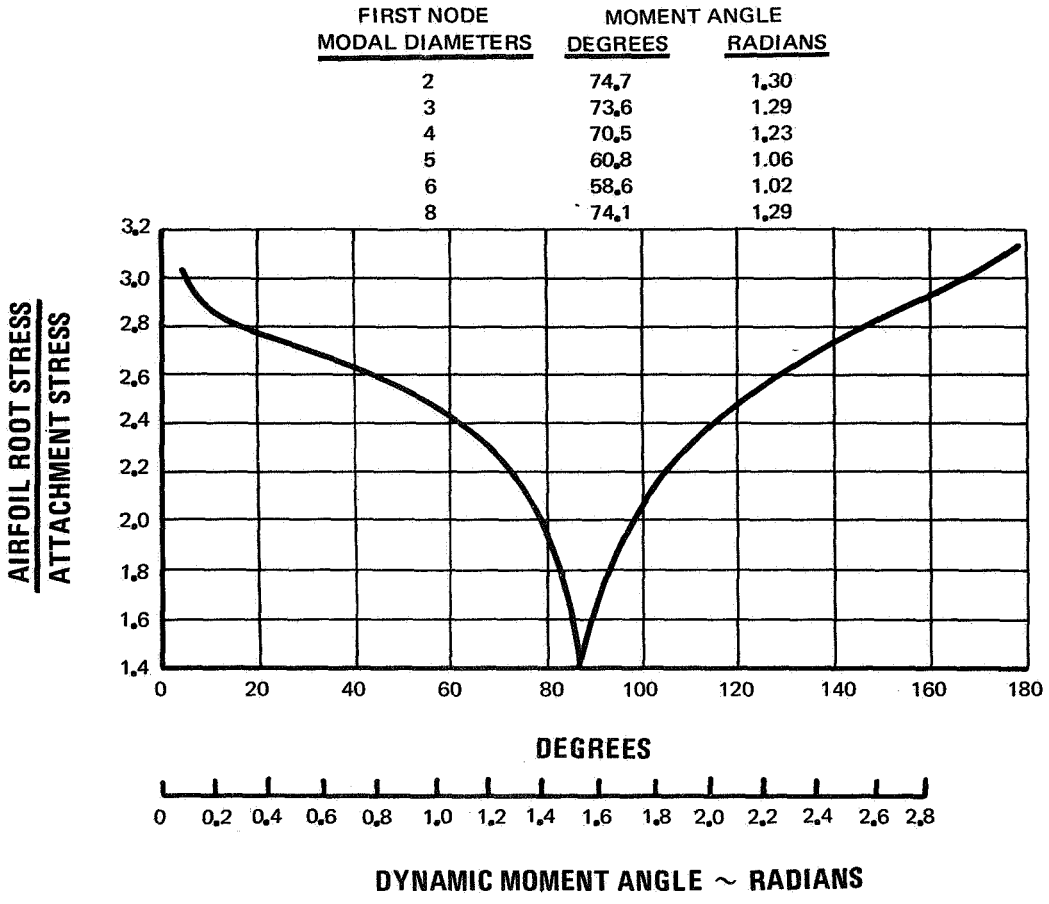

Figure 76 QE Fan Blade Attachment Stress Ratio for First Node QE-3 Fan Rotor Vibration with 2 Through 8 Nodal Diameters

C. MECHANICAL DESIGN

The layout designs of the fan blade, root attachment, and disk portion of the front hub have been completed and are ready for detailing. The fan stage consists of 36 part-span shrouded blades of AMS 4928 titanium alloy. These blades are mounted by conventional dovetail attachments in a disk which will also be fabricated from AMS 4928 titanium alloy. The dovetail attachment method used in conjunction with a blade retention plate represents the most efficient blade attachment method known and offers substantially lower weight and less interstage leakage than a pin-root attachment scheme.

The fan is coupled to a stub shaft by means of a face spline coupling, and the stub shaft is splined to the main drive shaft. The face spline was selected instead of a cylindrical spline to reduce weight, and a stub shaft is used to permit the fan stage to be removed without disturbing the rest of the rotor system.

SECTION VII

ALTERNATE ENGINES TO QE-3

Under Task III of this contract, a study was conducted to determine if alternate, lower fan tip pressure ratio versions of the QE-3 were feasible from a performance and structural viewpoint. The objectives were to maintain the same fan tip diameter and gas generator as the QE-3 engine.

To avoid undesirable increases in thrust specific fuel consumption which a lower fan pressure ratio would normally entail, the total airflow and therefore bypass ratio were increased by lowering fan hub-to-tip ratio. The decrease in fan hub-to-tip ratio also reduces the fan root pressure ratio and results in less actual flow through the gas generator.

The result of these changes is that a lower fan tip pressure ratio and hub-to-tip ratio require a higher turbine temperature to maintain constant cruise thrust. The lower hub-to-tip ratio versions do offer slight improvements in fuel consumption and take-off thrust for the same fan tip speed.

Figure 77 shows the design point cycles resulting from the hub-to-tip ratio and associated fan pressure ratio changes. Figure 78 shows turbine temperatures at maximum continuous and maximum cruise power settings. The 0.35 hub-to-tip ratio engine results in a turbine temperature about 35°F higher than the QE-3 engine at equivalent power settings.

Figure 78 also shows total corrected airflow thrust specific fuel consumption at the design point cruise condition. The 0.35 hub-to-tip ratio engine has about 0.5% better fuel consumption than the QE-3 engine.

Figure 79 shows take-off conditions for a constant fan tip speed of 1000 fps. The 0.35 hub-to-tip ratio engine has about 3 percent more static thrust than the QE-3, however, the turbine temperature is 30°F higher.

The engine with a fan hub-to-tip ratio of 0.35 has been designated the QE-4. A preliminary elevation of this engine is shown in Figure 80.

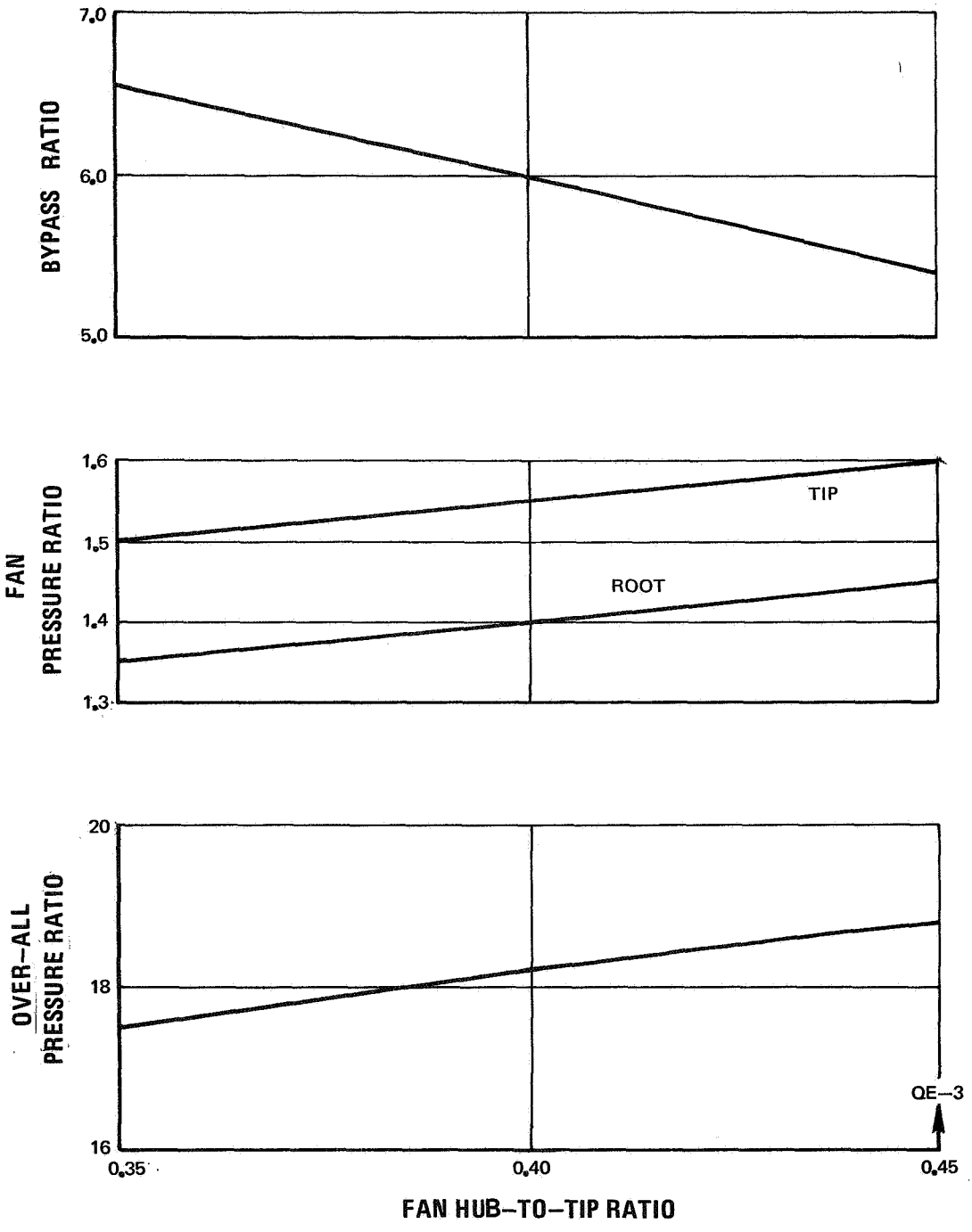

Figure 77 QE-4 Design-Point Cycles

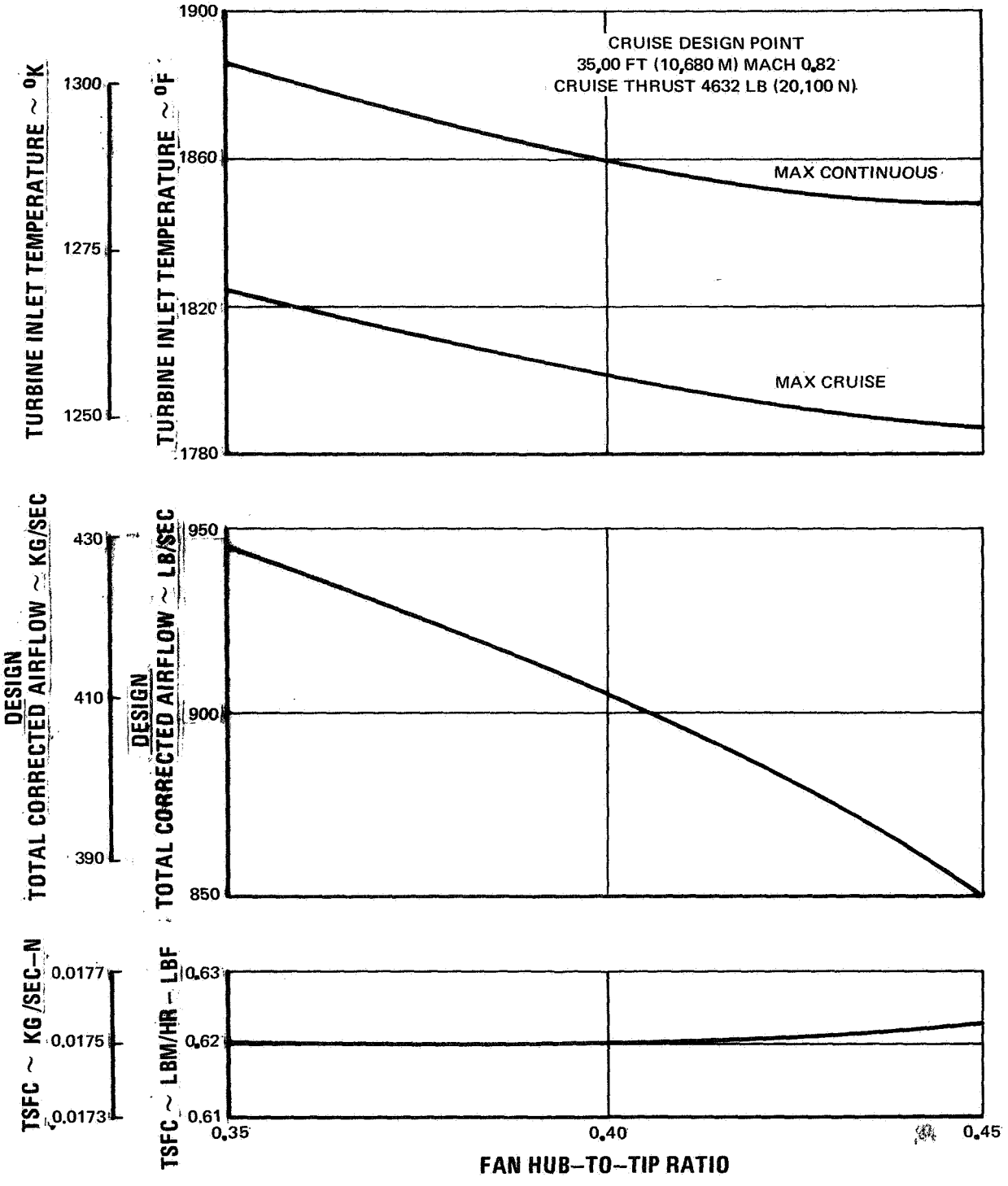

Figure 78 QE-4 Turbine Inlet Temperatures

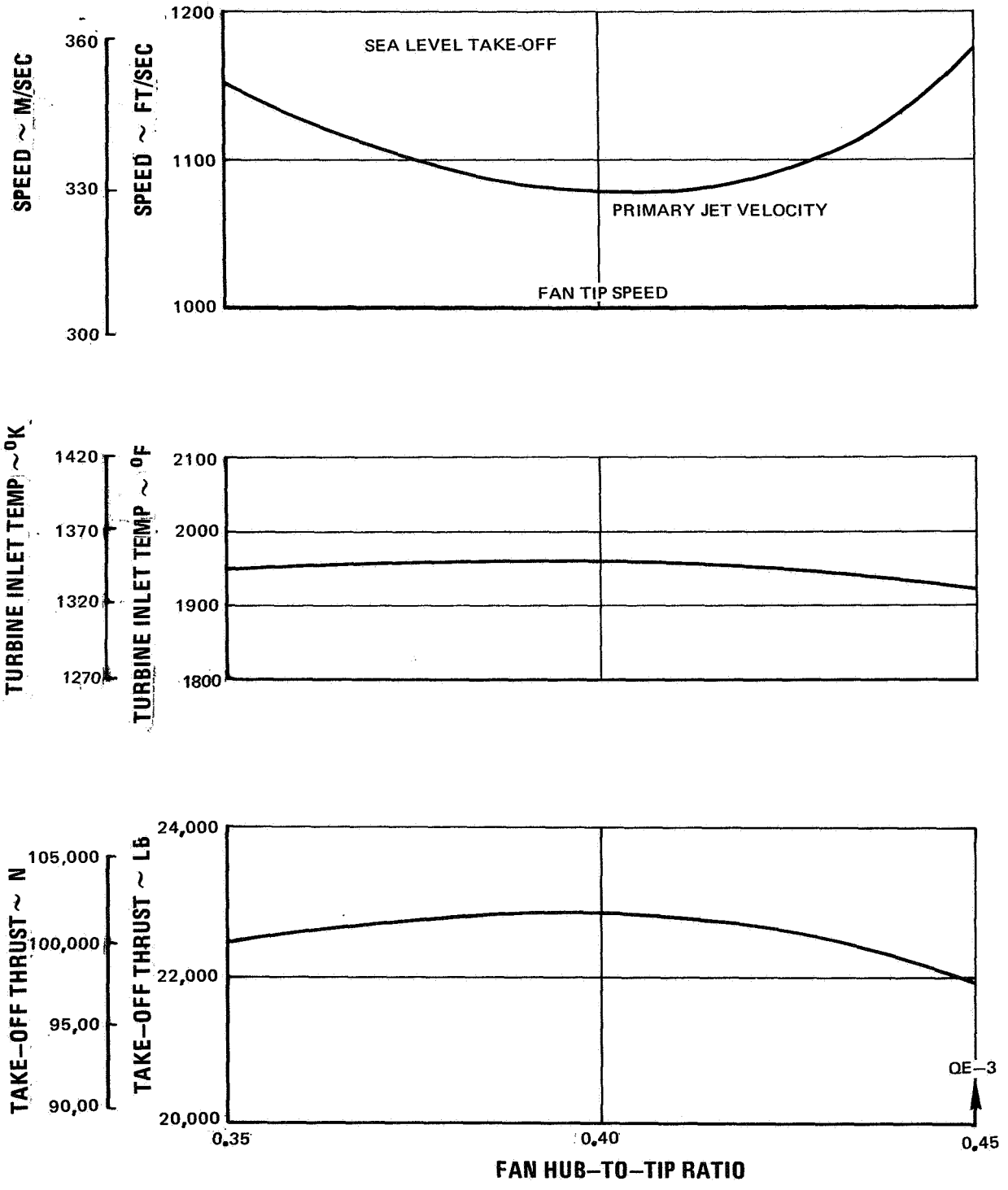

Figure 79 QE-4 Take-Off Conditions

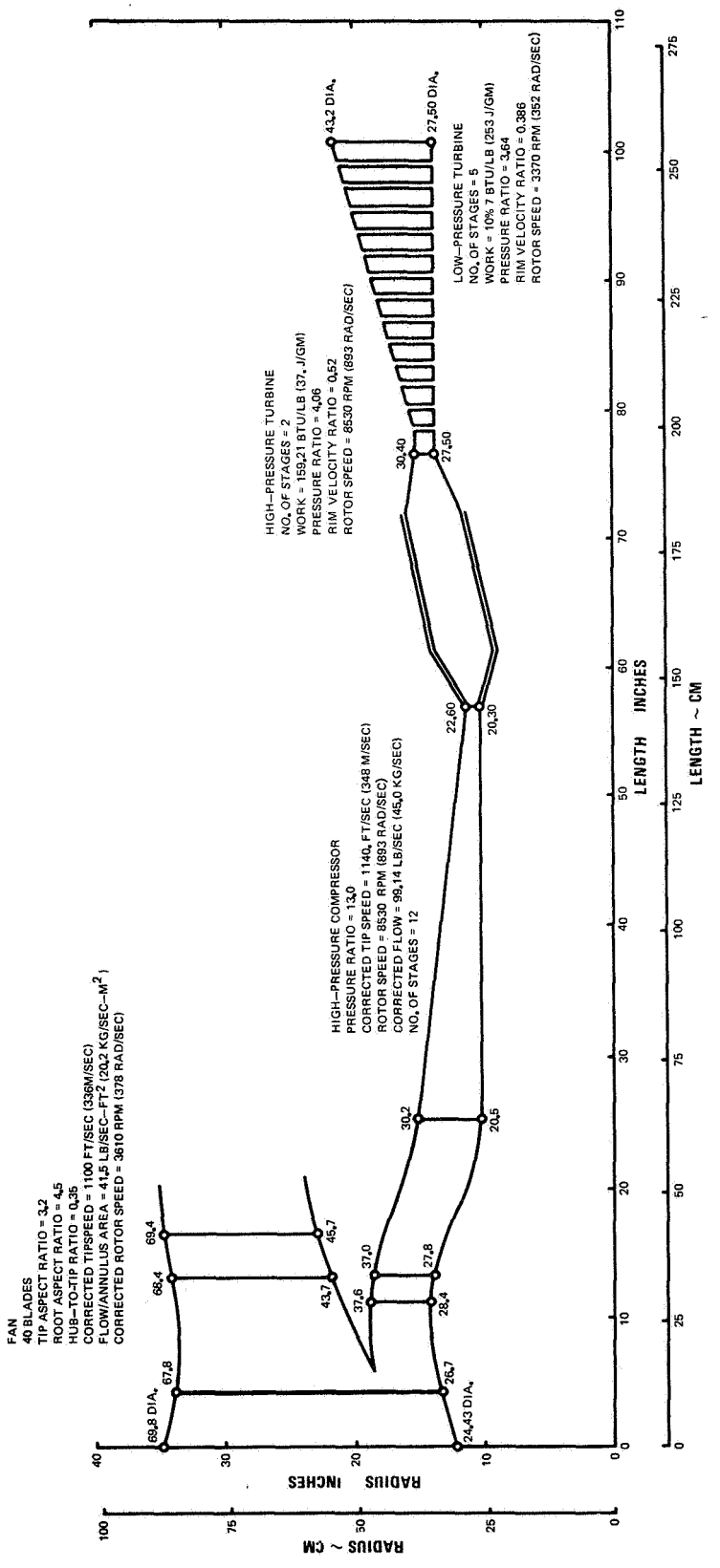

Figure 80 Flowpath for the QE-4

APPENDIX A
ENGINE SPECIFICATION

1 Introduction

The QE-3 is a 22,000 lb. (10,000 kg) thrust class two spool turbofan engine intended for use on subsonic commercial transport aircraft. Compared to the P&WA JT3D engine which is in the same thrust class, the QE-3 promises a substantial reduction in operating noise and in specific fuel consumption. These improvements result from the use of a low tip speed fan and a high bypass ratio cycle.

2 Scope

This specification presents preliminary performance, installation and operating data on the QE-3 engine. These data will be updated and expanded as the design study of the engine progresses.

3 Certification

The engine is designed and will be constructed for certification under Federal Aviation Regulation Part 33-Airworthiness Standards: Aircraft Engines (New).

4 Performance

a. Data

The estimated performance of the engine, including net thrust, specific fuel consumption, airflow, and installation correction factors for flight speeds and altitudes covering the entire operating envelope, is presented in Volume V of this report. The performance of the engine at several key flight conditions is summarized in Table XVI. Performance estimates are based on:

ICAO Standard Atmosphere
Fuel lower heating value of 18,400 BTU/lb (42,800 J/g)

100% ram recovery
P&WA Reference Exhaust System:
- Bypass stream-short ducts, convergent annular nozzle
- Gas generator-short conical nozzle

"Minimum" performance production engine

b. Operating Envelopes

The engine will function satisfactorily within the flight altitude and Mach number limits indicated by Figure 81, the ambient temperature limits indicated by Figure 82, and the following attitude limits:

TABLE XVI
QE-3 PERFORMANCE SUMMARY

Power Setting	Mach No	Pressure Altitude (ft)	Pressure Altitude (m)	Ambient Temp (°F)	Ambient Temp (°K)	Net Thrust (lb)	Net Thrust (kg)	TSFC (hr^{-1})
Max Continuous	0.82	35,000	10,680	-65.82	219	5,200	2,360	0.631
Max Continuous	0.82	35,000	10,680	-38.82	234	5,200	2,360	0.658
Max Continuous	0.82	35,000	10,680	-25.82	241	4,865	2,210	0.655
Max Cruise	0.82	35,000	10,680	-65.82	219	4,900	2,220	0.626
Max Cruise	0.82	35,000	10,680	-38.82	234	4,900	2,220	0.653
Max Cruise	0.82	35,000	10,680	-25.82	241	4,545	2,060	0.663
SLTO	0	0	0	59	288	21,900	9,940	0.337
SLTO	0	0	0	84	302	21,900	9,940	0.347
SLTO	0	0	0	120	322	18,740	8,510	0.351

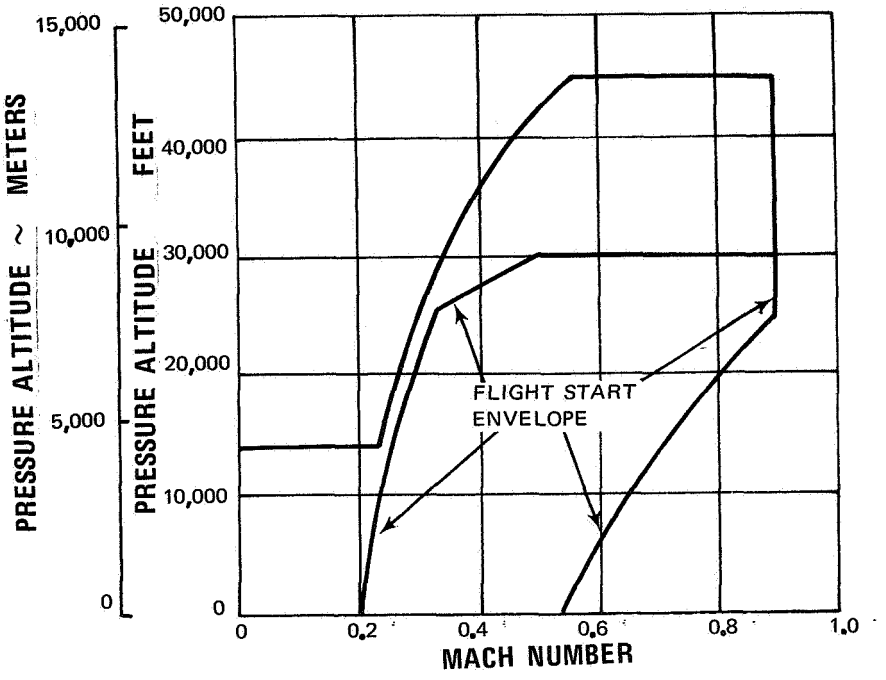

Figure 81 Estimated Operating Envelope for the QE-3 Engine

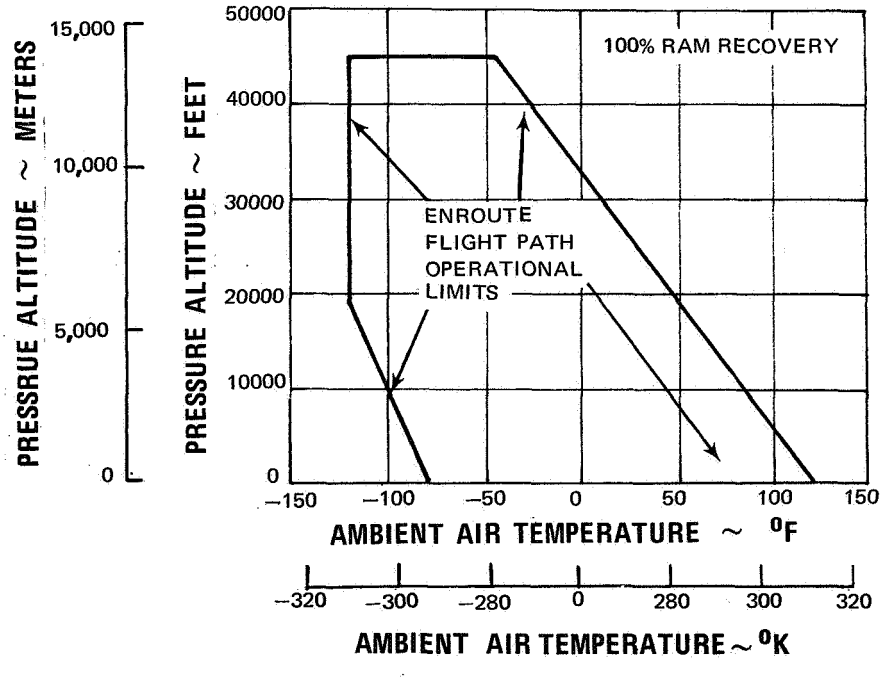

Figure 82 Preliminary Enroute Flight Path Operating Limits for the QE-3 Engine

- Level position (horizontal) with the engine rotated about the axial centerline 20 degrees (0.349 radian) to either side.
- 25 degrees (0.437 radian) nose up or 25 degrees (0.437 radian) nose down with the engine rotated about the axial centerline 10 degrees (0.1745 radian) to either side.

c. Idle

Under standard atmospheric conditions at altitudes up to 10,000 ft (3048 m) with the power lever in the idle position, engine thrust will not exceed 4 percent of the take-off thrust available at sea level static conditions.

d. Transients

The engine will be free from objectionable overspeed, compressor instability, combustion instability, or overtemperature during the selection of power lever positions in a normal flight sequence. The estimated acceleration and deceleration characteristics of the engine, based on power lever movements of one second or less, are shown on Figures 83 through 86.

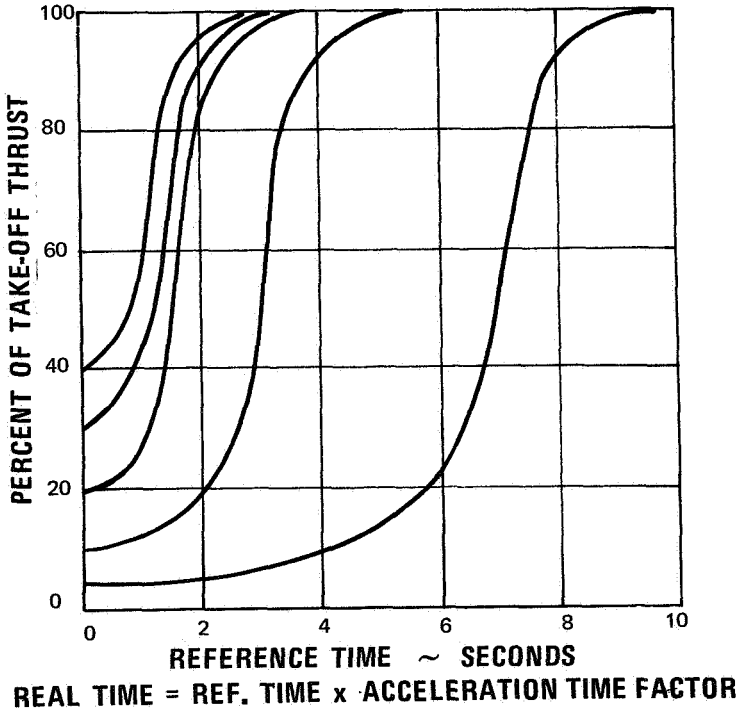

Figure 83 Estimated Acceleration Characteristics of the QE-3 Engine

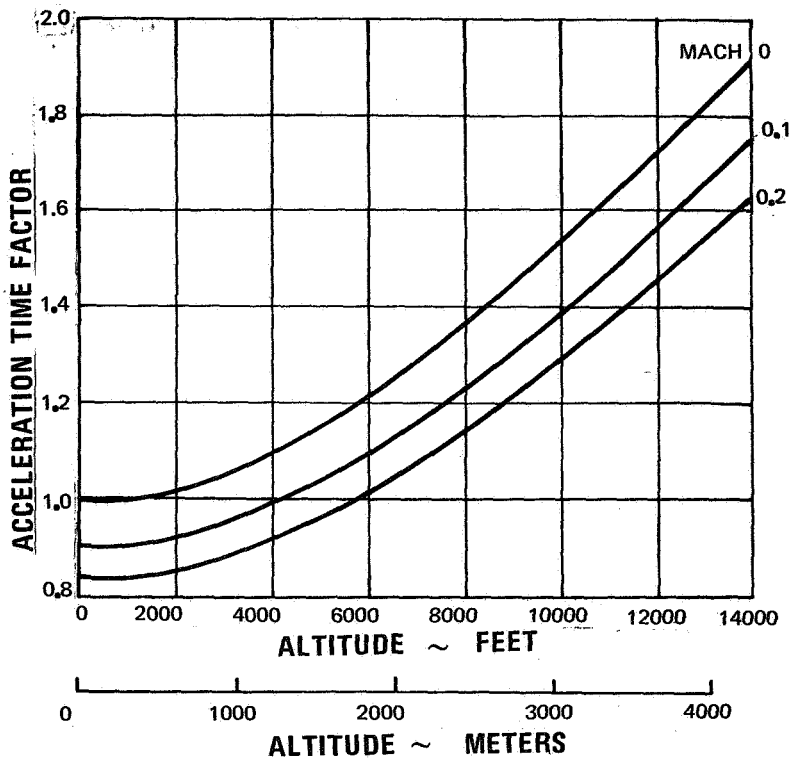

Figure 84 Preliminary Acceleration Time Factor for the QE-3 Engine

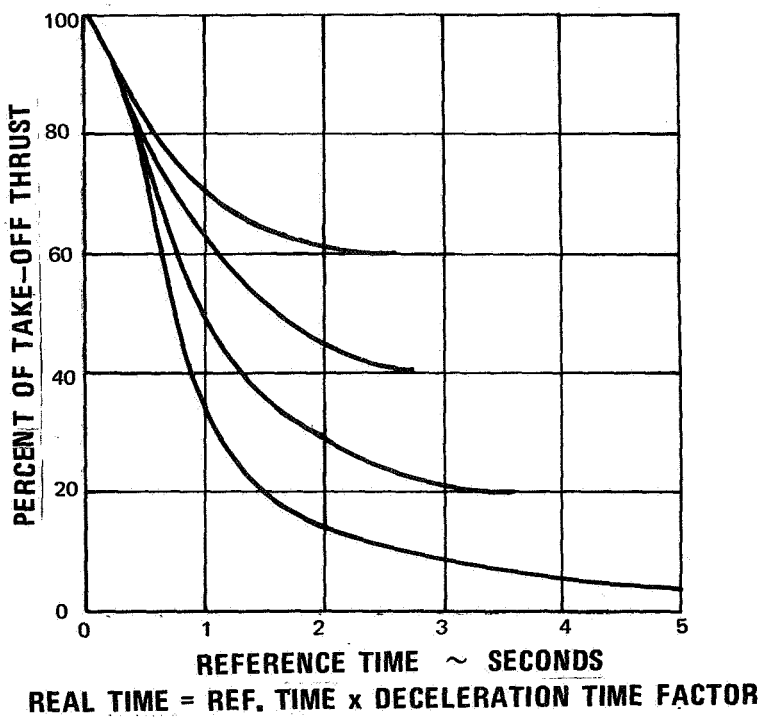

Figure 85 Estimated Thrust of the QE-3 Engine During Deceleration

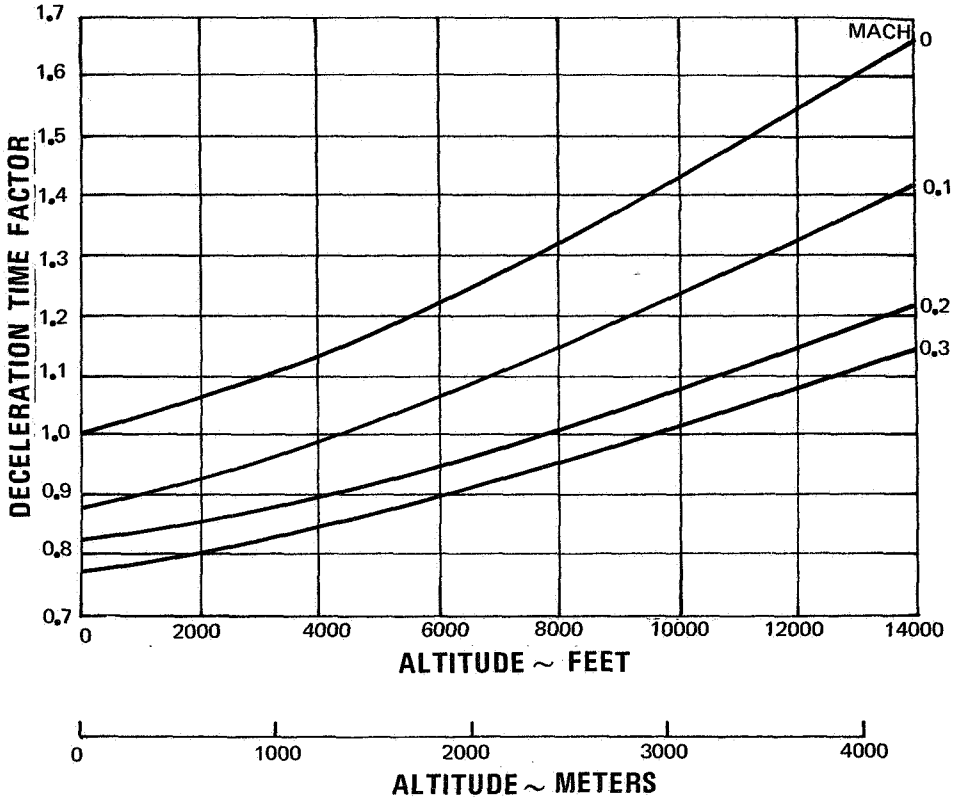

Figure 86 Preliminary Deceleration Time Factor for the QE-3 Engine

e. Windmilling

(1) Accessory Drive Power

The engine can be used to drive accessories during windmilling operation. The estimated power and RPM available are indicated as functions of flight speed and altitude on Figure 87.

(2) Drag

The estimated drag and airflow of the engine in windmilling operation are presented on Figures 88 and 89 respectively, as functions of flight speed.

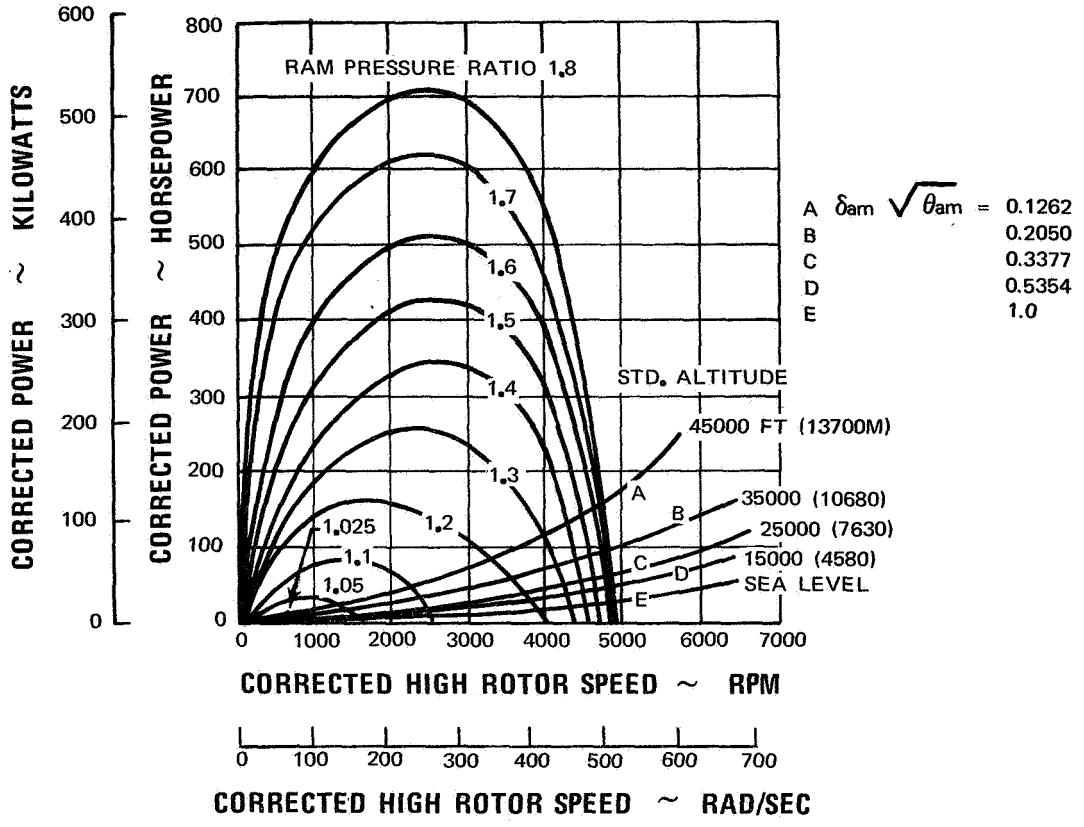

Figure 87 Estimated Power Available from the High-Pressure Rotor with the Engine Windmilling

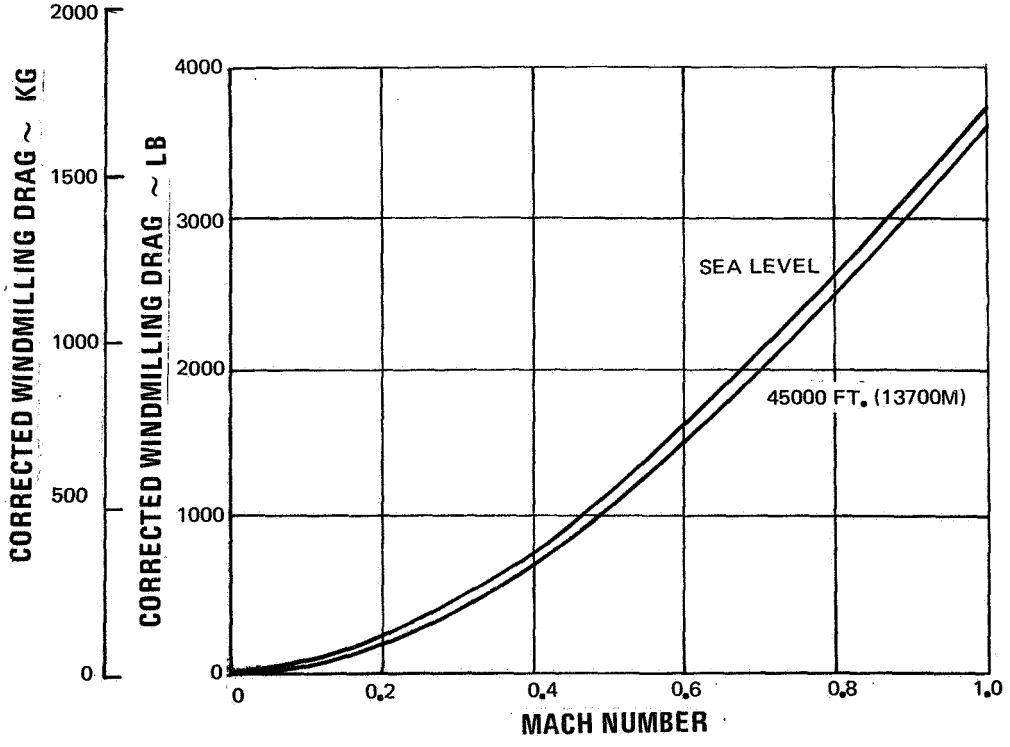

Figure 88 Estimated Corrected Windmilling Drag for the QE-3 Engine

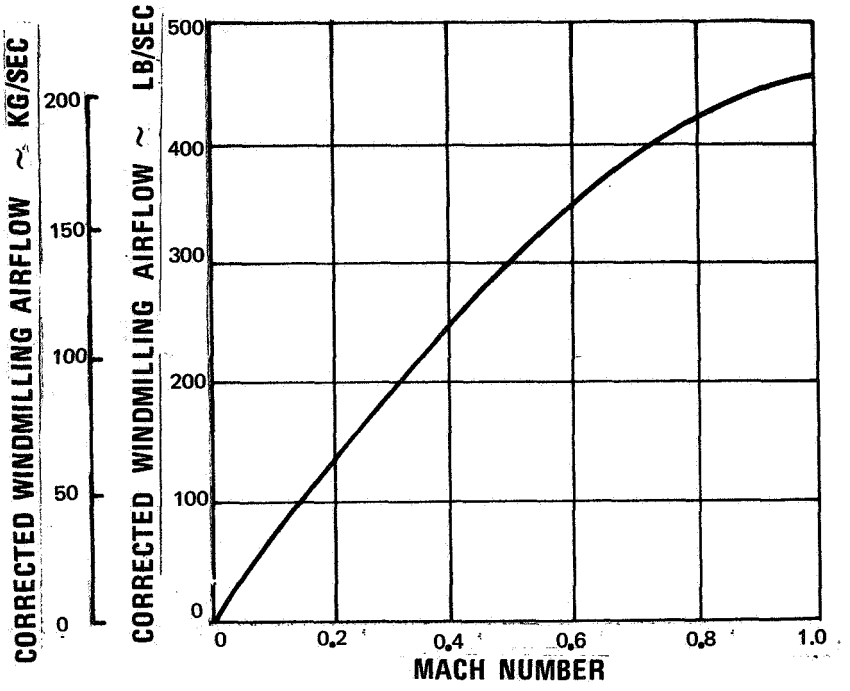

Figure 89 Estimated Corrected Windmilling Airflow for the QE-3 Engine

5 Installation

a. Weight

The estimated dry weight of the engine, including the items listed below, is 4950 pounds (2240 kg).

Basic engine
Fuel control system including fuel pump
Engine ignition system without power source
Acoustic treatment in fan case and fan to compressor transition duct
Gearbox with pads as indicated in Section 5h
Exhaust thermocouples and pressure probes
Compressor variable geometry actuation equipment
Provisions for attachment of ground handling equipment

b. Configuration

The external configuration of the engine is shown on Figure 90.

c. Mounting

The engine mounting provisions are shown on the Installation Drawing. The mounts shown are intended for use with a top center support arrangement with the rear mount taking thrust, vertical, side, and torque loads and the front mount taking vertical and side loads only.

d. Load Factors-Normal Operation

The engine and its mount points are designed to withstand without permanent deformation the flight, gust, and landing load factors shown in Figure 91. The ultimate load factor in each case is 1.5 times these limit loads.

e. Inlet

(1) Load Limits

The front flange of the engine is designed to withstand the loads indicated on Figure 90 to accommodate mounting of the inlet.

(2) Distortion Limits - (to be supplied)

(3) Performance Effects

The effect of inlet pressure losses on engine performance may be estimated using the correction factors and procedure in Volume V of this report.

f. Nozzles and Reversers

(1) Load Limits

The fan case rear flange and the turbine case rear flange are designed to withstand the loads indicated on Figure 90 to accommodate mounting of discharge ducts, nozzles and reversers.

(2) Distortion Limits - (to be supplied)

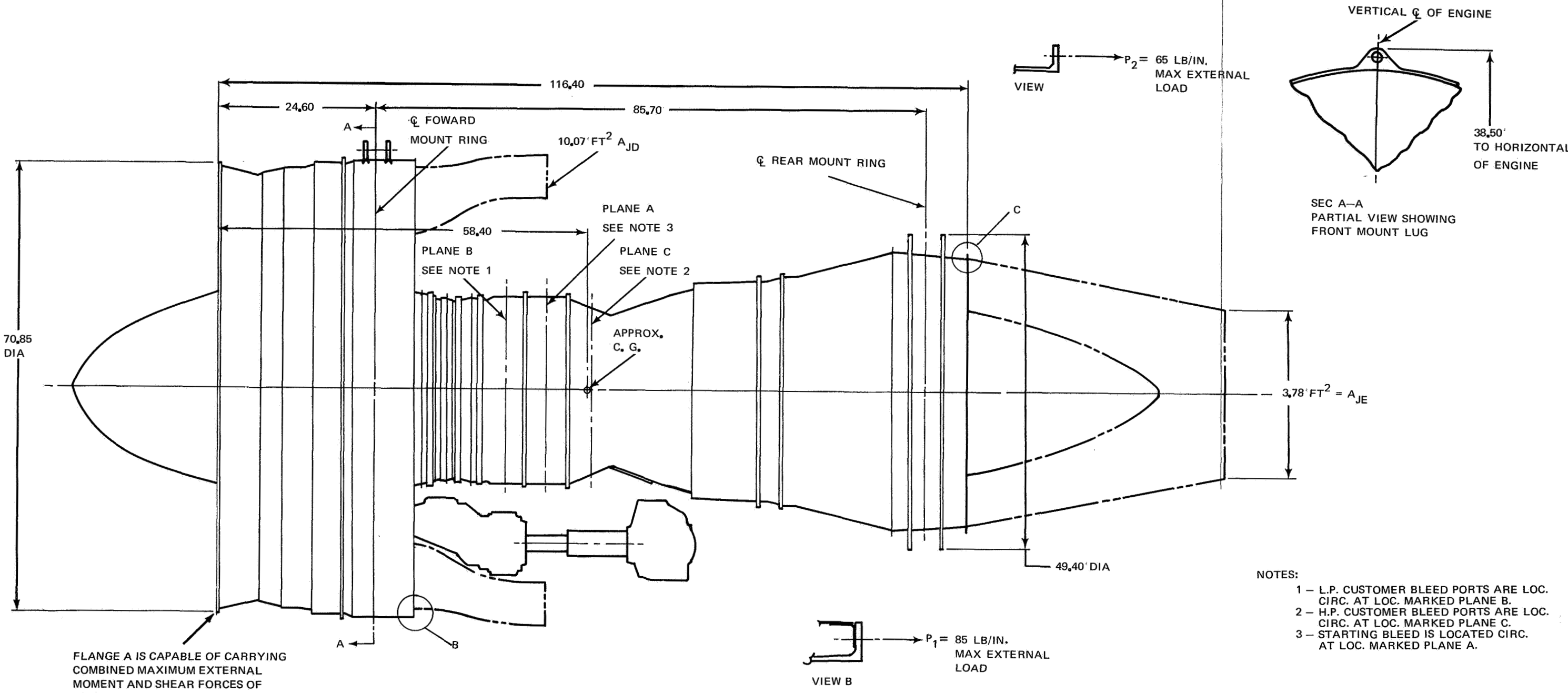

NOTES:

1 – L.P. CUSTOMER BLEED PORTS ARE LOC. CIRC. AT LOC. MARKED PLANE B.
2 – H.P. CUSTOMER BLEED PORTS ARE LOC. CIRC. AT LOC. MARKED PLANE C.
3 – STARTING BLEED IS LOCATED CIRC. AT LOC. MARKED PLANE A.

Figure 90 Installation Drawing of the QE-3 Engine

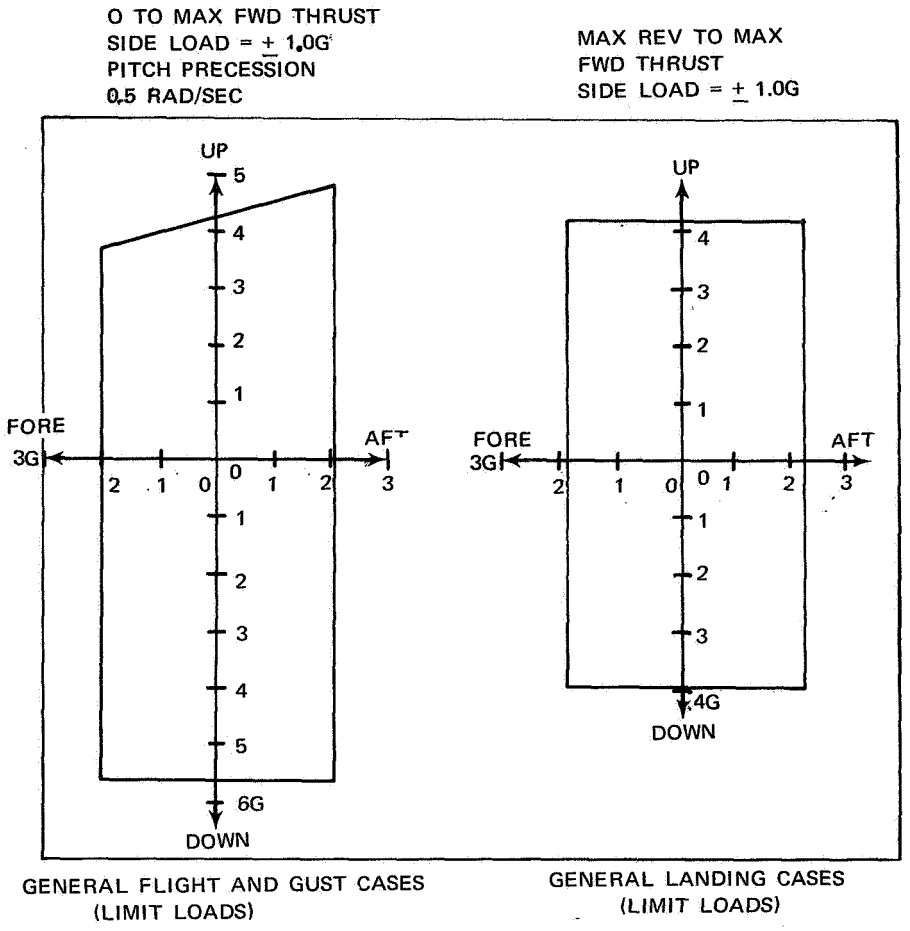

Figure 91 QE-3 Engine Flight and Landing Loads

g. Compressor Airbleed

(1) Starting Airbleed

Air is bled from ports located on Plane A (see Figure 90) during engine starting only. These ports are closed below idle RPM by valves supplied with the engine fuel control. The flow from the ports may be discharged at any convenient point, if the manifold pressure drop to ambient does not exceed 70 percent for the maximum corrected flow of 15 lb/sec (6.8 kg/sec) per port.

(2) Customer Airbleed

Air may be bled, within the limits established below, from ports located in Planes B and C (see Figure 90) for aircraft services such as cabin conditioning and anti-icing. Bleed ports may be located on Planes B and C to suit the customer's installation requirements. The ports deliver air taken through flush intakes on the compressor walls at the following locations:

Bleed Port Planes	Compressor Stage	Compressor Wall
B	Mid	OD
C	Discharge	OD & ID

The maximum airbleed flow that may be taken from the ports, either individually or in combination, is indicated below:

Bleed Port Plane	Power Setting	Maximum Bleed Flow (Percent of Primary Flow) Continuous	Intermittent
B	Maximum Cruise	3.2	4.0
C	Maximum Cruise	8.7	10.3

The ports are sized to choke at a flow below that which would damage the engine, in the event of a bleed manifold or valve failure. The pressure drop from the compressor wall to the port flanges is shown as a function of bleed flow on Figure 92. The pressures and temperatures of the air at the compressor wall are listed in Volume V of this report as a function of flight altitude, Mach number, and power setting. The effect of airbleed on engine performance may be estimated using the correction factors and procedures in Volume V.

(3) Contamination

Contamination of the bleed air by engine fuels, lubricants or other engine materials is minimal. The gaseous substances contributed by the engine will not exceed those listed below. Solid particles contributed by engine operation will not exceed 5 milligrams/cubic meter for particles below one micron in size.

Substance	Parts per Million
Carbon Dioxide	5000.0
Carbon Monoxide	50.0
Ethanol	1000.0
Fluorine (as HF)	0.1
Hydrogen Peroxide	1.0
Aviation Fuels	250.0
Methyl Alcohol	200.0
Methyl Bromide	20.0
Nitrogen Oxides	5.0
Oil Breakdown Products (e.g., acrolein, aldehydes)	1.0
Ozone	0.1

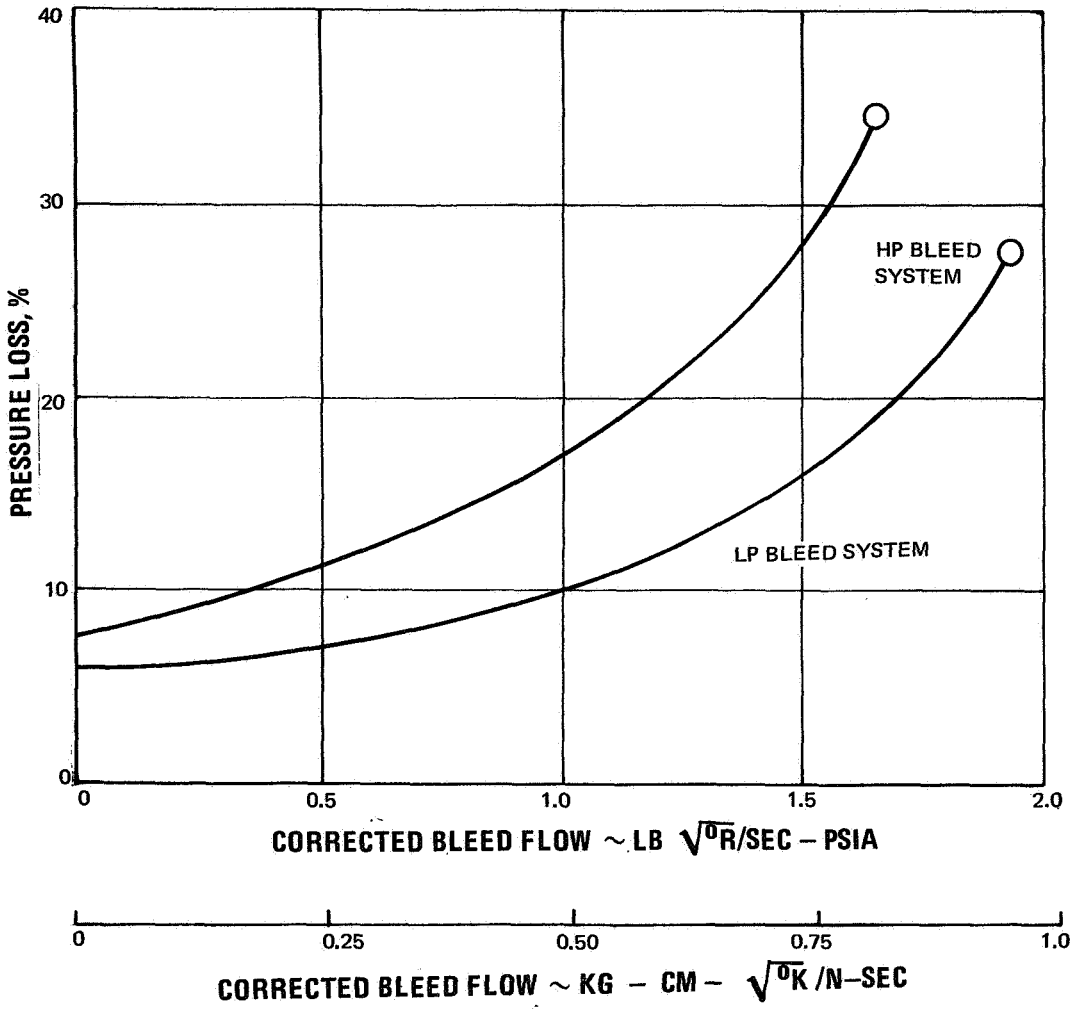

Figure 92 Estimated Bleed System Pressure Loss for the QE-3

h. Accessory Drives

Drive	AND Type	Mount Pad Stud Configuration	Torque Rating	Rotating Facing Pad
Tach L.P.R.	XVB AND 20005	1.875"	T_S = 50 lb-in	CW
Starter	XII-S AND 20002	5.000" B.C.	T_S = 685 lb-in	CW
Tach H.P.R.	XVB AND 20005	1.875"	T_S = 50 lb-in	CW
Generator	XVI-C AND 20006	10.000" B.C.	T_S = 11,000 lb-in	CW

Fluid Power Pump	XII-K AND 20002	5.000 B.C.	T_S = 4,400 lb-in	CW

(1) Performance Effects

The effect of power extraction on engine performance may be estimated by using the correction factors and procedures in Volume V of this report.

i. Starter

The torque required to motor the engine at constant speed is indicated on Figure 93 . The minimum torque required from the starter to provide satisfactory engine starting is also indicated. Higher starter torques, up to the limit indicated, may be used to obtain shorter starting times.

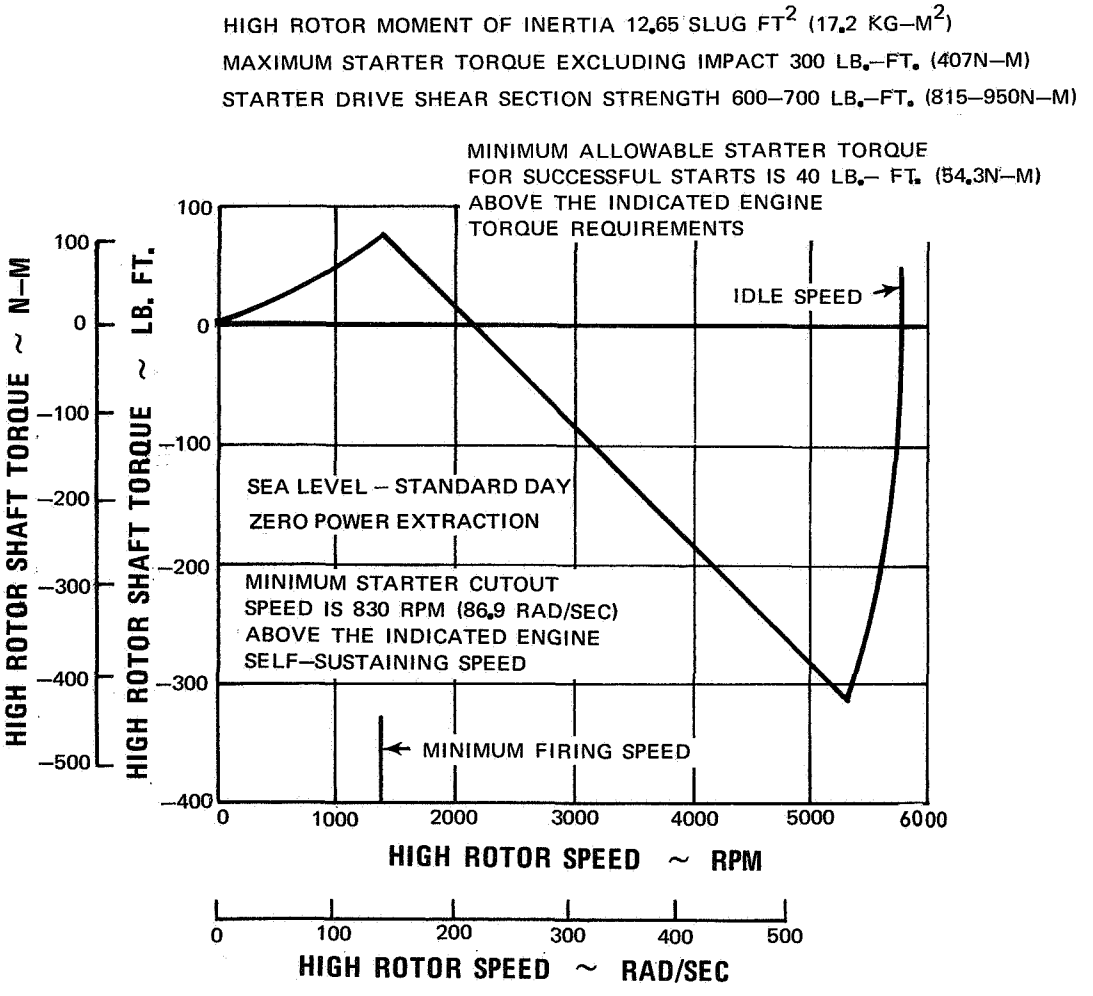

Figure 93 Estimated Starting Torque Characteristics of the QE-3 Engine at Sea Level on a Standard Day with Zero Power Extraction

j. Instrumentation

The following instrumentation is recommended for the engine in service use:

1. Engine inlet air total temperature (T_{T2})
2. Engine inlet air total pressure (P_{T2})
3. Fan rotor speed (N_1)
4. High compressor rotor speed (N_2)
5. Turbine discharge total temperature (T_{T7})
6. Turbine discharge total pressure (P_{T7})
7. Engine oil inlet temperature
8. Engine oil pressure
9. Pressure drop across the engine main oil strainer
10. Fuel flow
11. Fuel pump inlet temperature
12. Fuel pump inlet pressure
13. Vibration pickups
14. Fuel de-icing air shutoff valve position indicator
15. Fuel filter pressure differential

6 Operation

a. Starting

(1) Ground

The engine is designed to permit starting in 30 seconds on a standard day at sea level if sufficient starter torque is applied. The minimum time between starting attempts is 30 seconds.

(2) Flight

The engine can be started in flight without starter assist within the envelope indicated on Figure 94.

b. Thrust Control

The engine fuel control is designed to maintain rated thrust over the flight speed and altitude range of the engine without manipulation of the power lever, if the rate of change of ambient temperature with altitude is standard. If the rate of change of temperature is not standard, such as in a temperature inversion condition, minor adjustments of the power lever are required.

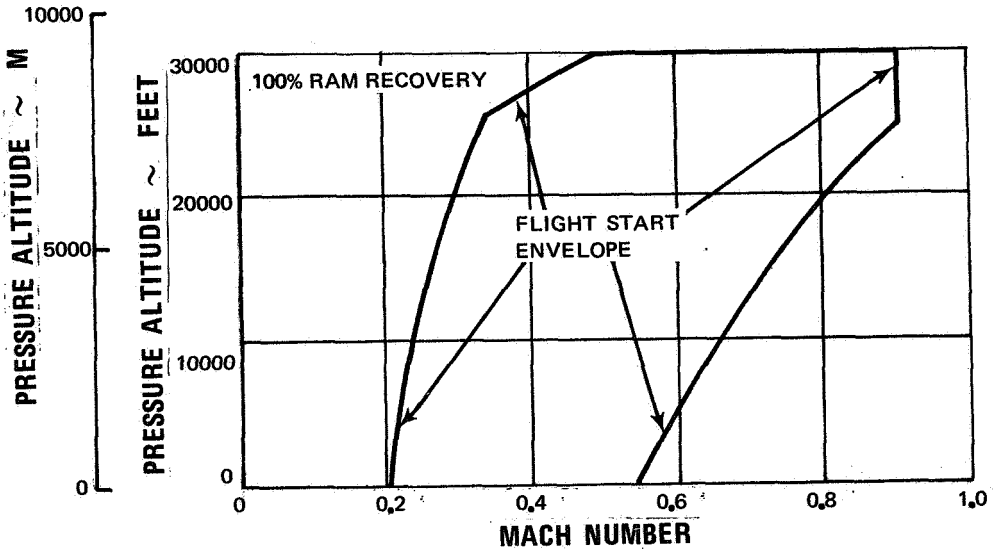

Figure 94 Starting Envelope for the QE-3 Engine (Assuming 100 Percent Ram Recovery)

c. Thrust Indication

The primary indication of engine thrust is engine pressure ratio (EPR), with tailpipe temperature (T_{T7}) and high rotor RPM (N_2) used as engine condition monitors. The values of these parameters for each thrust rating will be presented as functions of inlet total temperature and flight altitude for use by the flight crew.

d. Fuel

Acceptable limits governing fuel characteristics and elements are contained in Specification PWA 522.

e. Oil

Definition of the synthetic oil required for the engine is contained in Specification PWA 521. The maximum oil consumption averaged over a 10 hour flight will not exceed 0.25 gal/hr (0.945×10^{-3} m^3/hr).

f. Smoke

The engine shall be designed to limit the smoke emitted from the gas generator to a Von Brand continuous filtering smoke meter density reading of 25 percent at any usable level of power from ground idle to take-off at flight speeds from 0 to 0.6 Mach number and altitudes from sea level to 5000 feet (1520 meters).

g. Noise

The estimated maximum perceived noise levels from the engine are indicated below, based on:

Sea level, static, standard day conditions with 70 percent relative humidity.

P&WA standard bellmouth inlet

P&WA Reference Exhaust System

Peak PNdb along a 200-foot (61-meter) offset line parallel to the engine centerline.

Engine Operating Condition	Maximum Perceived Noise Level
Take-off Power	121.
Approach Power	109.

h. Foreign Object Ingestion

As required by FAR Part 33, the engine is designed so that ingestion of foreign objects such as birds, ice and hail will be unlikely to produce flame-outs, lengthy power recovery time, or severe sustained power losses, although some damage to engine parts may occur.

i. Blade Loss

The rotor and bearing supports are designed to withstand the equivalent unbalance load of 10 percent loss of the blades in any stage at maximum shaft overspeed.

j. Vibration

The engine is designed to avoid the generation of excessive vibration stress in any portion of the engine under normal operating conditions. The engine balance will not result in more than ±3 mils (0.0762 mm) displacement of the engine cases.

k. Useful Life

The major engine parts are designed for the following levels of useful life:

- Major structural components — 30,000 hours
- Low Cycle Fatigue Limited Parts — 8,000 LCF cycles
- Creep-limited parts (1%) — 5,000 hours